BNL-65926

Proceedings of RIKEN BNL Research Center Workshop Volume 10

PHYSICS OF POLARIMETRY AT RHIC

August 4–7, 1998

Organizers

Ken Imai and Doug Fields

RIKEN BNL Research Center

Building 510, Brookhaven National Laboratory, Upton, NY 11973, USA

Other RIKEN BNL Research Center Proceedings Volumes:

Volume 9 - High Density Matter in AGS, SPS and RHIC Collisions - BNL-65762
July 11, 1998 - Organizers: Klaus Kinder-Geiger and Yang Pang

Volume 8 - Fermion Frontiers in Vector
Lattice Gauge Theories - BNL-65634
May 6-9, 1998 - Organizers: Robert Mawhinney and Shigemi Ohta

Volume 7 - RHIC Spin Physics - BNL-65615
April 27-29, 1998 - Organizers: Gerry Bunce,
Yousef Makdisi, Naohito Saito, Mike Tannenbaum and Aki Yokosawa

Volume 6 - Quarks and Gluons in the Nucleon - BNL-65234
November 28-29, 1997, Saitama, Japan
Organizers: Tashiaki Shibata and Koichi Yazaki

Volume 5 - Color Superconductivity, Instantons and Parity (Non?)-Conservation at
High Baryon Density - BNL-65105
November 11, 1997 - Organizer - Miklos Gyulassy

Volume 4 - Inauguration Ceremony, September 22 and
Non-Equilibrium Many Body Dynamics - BNL- 64912
September 23-25, 1997 - Organizer - Miklos Gyulassy

Volume 3 - Hadron Spin-Flip at RHIC Energies - BNL-64724
July 21 - August 22, 1997 - Organizers: T.L. Trueman and Elliot Leader

Volume 2 - Perturbative QCD as a Probe of Hadron Structure - BNL-64723
July 14-25, 1997 - Organizers: Robert Jaffe and George Sterman

Volume 1 - Open Standards for Cascade Models for RHIC - BNL-64722
June 23-27, 1997 - Organizer - Miklos Gyulassy

Preface to the Series

The RIKEN BNL Research Center was established this April at Brookhaven National Laboratory. It is funded by the "Rikagaku Kenkysho" (Institute of Physical and Chemical Research) of Japan. The Center is dedicated to the study of strong interactions, including hard QCD/spin physics, lattice QCD and RHIC physics through nurturing of a new generation of young physicists.

For the first year, the Center will have only a Theory Group, with an Experimental Group to be structured later. The Theory Group will consist of about 12-15 Postdocs and Fellows, and plans to have an active Visiting Scientist program. A 0.6 teraflop parallel processor will be completed at the Center by the end of this year. In addition, the Center organizes workshops centered on specific problems in strong interactions.

Each workshop speaker is encouraged to select a few of the most important transparencies from his or her presentation, accompanied by a page of explanation. This material is collected at the end of the workshop by the organizer to form a proceedings, which can therefore be available within a short time.

T.D. Lee
July 4, 1997

CONTENTS

Preface to the Series i

Some RHIC Polarimeter Issues
G. Bunce 1

Polarimeter Options Overview
Y.I. Makdisi 8

Status of Accelerator Progress
M. Syphers 16

CNI Theoretical Status
T.L. Trueman 24

Simulations for RHIC CNI Polarimeter
D. Fields 33

MCP Test Experiment @ Kyoto
J. Tojo 40

Toward RHIC CNI Polarimeter
K. Imai 46

The Polarimeter for RHIC Based on the Elastic (pe)-Scattering
S.B. Nurushev 52

Results from AGS-E925
A. Yokosawa 57

Test of the Coulomb-Nuclear-Interference-Polarimeter with the Extracted Polarized Proton Beam of AGS at 23 GeV/c
S.B. Nurushev 63

Note on Calculation of Pion Production from Carbon Target
D. Underwood 71

RHIC Proton Beam Polarimeter Based on Primakoff Effect
S.B. Nurushev 73

The Inclusive Neutral Pion Polarimeter for High Energy Accelerators/Colliders
S.B. Nurushev 77

Summary of Working Group on PP2PP and RHIC Polarimetry
W. Guryn 83

Current Design of Polarimeter Area
H. Huang 92

E880 Status
M. Bai 98

Summary of the Workshop
K. Imai 107

List of Participants 109
Workshop Agenda 110

G. Bunce
4 August 1998

Some RHIC Polarimetry Issues

We discussed a number of polarimeter concerns for RHIC.

1. Experiments use the polarization information to normalize their raw asymmetry, obtaining the "physics" asymmetry. The value of the polarization scales the result. Therefore, if we know our polarization to 10% of itself, we know the physics asymmetry to 10% of itself, ignoring the statistical error. This would be for a single polarized beam asymmetry. For the polarization uncertainty to become comparable to the statistical uncertainty, the statistics for the raw asymmetry would need to be at a 10 sigma level. For two beam asymmetries, A_{LL} or A_{NN} where both beams are polarized, a 10% polarization uncertainty leads to a 20% uncertainty on the physics asymmetry, ignoring the statistical error.

Therefore, the goal of a 5% polarization uncertainty only becomes important if we see a 20 sigma asymmetry, for one polarized beam asymmetries, such as the parity violating asymmetry A_L. For A_{LL} a 5% uncertainty in the polarization leads to a 10% uncertainty in the physics result, equivalent to a 10 sigma effect.

5% polarization uncertainty is a noble goal.

2. We often use a figure of merit to evaluate a method of polarimetry, NA^2. A represents the analyzing power of a reaction, and N the cross section. This figure of merit considers only the statistical significance of the measurement. If A is small, a systematic error could become important. We discussed this. Dave Underwood showed that for the AGS internal polarimeter, at 23 GeV, *AP=0.004+/-0.00038*, for a typical measurement that took 10 minutes. This is 10 sigma, without a noticable systematic error (the points being quite repeatable).

3. Experiments at RHIC will collide different sets of bunches, and these sets will be a subset of the bunches in each ring. This is due to the abort gaps in each ring, 6 missing bunches (I believe). If we can

monitor the polarization for each bunch, then each experiment can calculate a weighted average of their polarization for each beam, weighted by the luminosity for each crossing measured at the experiment.

4. Sergei Nurushev brought up another point: we have had no plan to measure longitudinal polarization at Phenix or Star. Our only approach was to verify the vertical component of the stable spin direction at the location of the polarimeter for various settings of the spin rotators. We then discussed the possibility of using a pi^0 polarimeter observing over 360° in phi at Phenix or Star, set for large x_F and p_T=.7 GeV/c. The pi^0 would pass through the DX magnet within the beam pipe, and an em calorimeter could observe it at the location of the Zero degree calorimeter. We could then demonstrate the absence of transverse polarization.

August, 1998
G. Bunce

Some RHIC Polarimetry Issues

1. Beam polarization <u>normalizes</u> measured asymmetry:

$$A_{LL} = \frac{A_{raw}}{P^2}, \quad A_{raw} = \frac{N_{++} - N_{+-}}{N_{++} + N_{+-}}$$

$\Rightarrow$ changes scale of result

How well do we need to know P?

2. Measurement of polarization uses analyzing power:

$$P = \frac{A_{raw}}{A_N}, \quad A_{raw} = \frac{N_L - N_R}{N_L + N_R}$$

If A_N is small, systematic error in A_{raw} can dominate. We should discuss this.

3. Experiments collide different sets of bunches. Average polarization of a ring (given by polarimeter) is not average of bunches used by an experiment.

4. Q: (Sergei Nurushev) How do we know beam is longitudinally polarized at an experiment?

A: Only by verifying spin motion of spin rotators at the location of the polarimeters (12 o'clock).

We should discuss ways to measure P_L at experiment(s).

ep is one way.

1. How well do we need to know P?

$$A_{LL} = \frac{A_{raw}}{P^2} \qquad A_{raw} = \frac{N_{++} - N_{+-}}{N}$$

(N_{++}, N_{+-} are normalized by luminosity)

$$\left(\frac{\Delta A_{LL}}{A_{LL}}\right)^2 = \left(2\frac{\Delta P}{P}\right)^2 + \frac{1 - A_{raw}^2}{A^2 N}$$

if $\frac{\Delta P}{P} = .1$, contribution to $\frac{\Delta A_{LL}}{A_{LL}} = .2$ $\Rightarrow$ important only for a measurement with $\frac{\Delta A_{LL}}{A_{LL}} \lesssim .2$ (or 5σ statistics.)

- <u>Goal</u> of $\Delta P/P = 0.05$ is important only for $\underbrace{\frac{\Delta u}{u}(x > .2)}$ and if $\frac{\Delta g}{g}$ is very large.

$\rightarrow$ for A_L, $\left.\frac{\Delta A_L}{A_L}\right|_P = \frac{\Delta P}{P}$ and for

$\frac{\Delta P}{P} = .05 \Rightarrow 20\sigma$ equivalent

Spin Discussion

6/29/98

G. Bunce

Spin and Luminosity at RHIC

$$A_L = \frac{\sigma_+ - \sigma_-}{\sigma_+ + \sigma_-}$$

Beam is not 100% polarized. We measure a combination of σ_+ and σ_-:

Counts (for 100% acceptance): also use $L^+ = L^- = L$

$$C^+ = L_+^+ \sigma_+ + L_-^+ \sigma_- \qquad (L = \int L' dt)$$

– for beam polarized in + direction

$$C^- = L_+^- \sigma_+ + L_-^- \sigma_-$$

– beam pol. in – direction

... algebra

$$\boxed{A_L = \frac{1}{P_{avg}} \frac{C^+ - C^-}{(C^+ + C^-) - (C^+ - C^-)\frac{P_{dif}}{P_{avg}}}}$$

$$P_{dif} = \frac{P^+ - P^-}{2}$$

$$P_{avg} = \frac{P^+ + P^-}{2}$$

$$P^+ = \frac{L_+^+ - L_-^+}{L_+^+ + L_-^+} \qquad P^- = \frac{L_-^- - L_+^-}{L_-^- + L_+^-}$$

P^+ and P^- can be calculated from the polarization of individual bunches:

$$P^+ = \frac{B_+^+ - B_-^+}{B_+^+ + B_-^+}$$

B_+^+ = number of beam protons with pol = + for a + pol. sign bunch; $L_+^+ = \text{const.} \times B_+^+$

$$= \frac{\sum (B_{+i}^+ - B_{-i}^+)}{\sum (B_{+j}^+ + B_{-j}^+)}$$

sums over crossings for + polarized bunches

$$= \frac{\sum B_i P_i^+}{\sum B_i} \qquad P_i^+ = \frac{B_{+i}^+ - B_{-i}^+}{B_{+i}^+ + B_{-i}^+}$$

$$\boxed{P^+ = \frac{\sum L_i^+ P_i^+}{\sum L_i^+}}$$

$$\boxed{P^- = \frac{\sum L_i^- P_i^-}{\sum L_i^-}}$$

P^+ and P^- are the weighted avg.s of the bunch polarizations, weighted by the luminosity of the crossings.

Polarimeter Options Overview

Y. I. Makdisi

Workshop on Polarimetry at RHIC

August 4-7, 1998

(Abstract)

Measurement of the proton beam polarization at RHIC has been the focus of attention for the last several years. A RHIC Polarization Measurement Working Group searched for a polarimeter that satisfies two goals. One being fast enough to provide a relative measurement in a short time scale for machine tuning and diagnostics, and the other an absolute beam polarization calibration with a 5% accuracy for physics over the entire energy range of RHIC from 23 GeV to 250 GeV.

Several candidate processes were studied from the perspective of large analyzing power, large cross sections, susceptibility to background, and competing mechanisms. These included pp and pC elastic scattering in the CNI region and pe elastic scattering processes that are calculable in principle, Primakoff production in the Coherent Coulomb region, and inclusive pion production at large x_f.

The consensus is to build an inclusive charged pion production polarimeter based on data from experiments with production from hydrogen at 12 GeV/c at the Argonne ZGS and 200 GeV/c at Fermilab. The polarimeter will employ a carbon target and is expected to serve as the day-1 instrument to provide a 10% measurement of the beam polarization. The plan calls for installing this polarimeter in one ring along with a pair of low energy spectrometers viewing the same target to measure pC scattering in the CNI region. In this arrangement, the pion polarimeter will calibrate the CNI polarimeter and, if successful, another CNI polarimeter will be installed in the second ring.

In preparation for this task, we are measuring the analyzing power of inclusive pion production from a carbon target at RHIC injection energy (AGS experiment E925) to compare with that from hydrogen. Parallel studies are underway at IUCF and Kyoto University to develop the pC apparatus to be installed in the AGS as a precursor to a RHIC polarimeter.

The 5% goal will be achieved by using a polarized hydrogen jet target. The target polarization can be absolutely determined to better than 5%. This will be used to measure the analyzing power in pp elastic scattering in the CNI region at any energy. The latter measurement will then be used to provide the absolute beam polarization. This is required as RHIC reaches its design luminosity.

The Boundary Conditions

- The polarimeter has to cover the full energy range:

  23 GeV to 250 GeV

- The polarimeter should provide an absolute accuracy:

  better than 5%

- Cost effective:

  Construction and operating (limited resources)

- This spawned the RHIC Polarization Measurement Working Group.

The Problem

- We are into the high energy domain where there are:

  A limited number of experiments w/polarized beams
  mostly w/polarized targets
  The available data are marginal

  Common wisdom ⇒ low polarization effects but !!
  there are always some surprises.

Candidate Processes

- p-p Elastic scattering
  The AGS internal polarimeter, the analyzing power is proportional to 1/p. Experimental data good to 10%.

- Primakoff Production in the Coherent Coulomb region (E704)
  $p + Z \rightarrow \Delta / N^* + Z \rightarrow \pi^o + p + Z$
  $(\gamma + p \rightarrow p + \pi^o)$ at $t < 0.001$
  A large analyzing power of -0.57 +/- 0.12 +/- .20
  Large background.
  D. Carey et al Phys. Rev. Lett. **64,** 357 (1990)

- p-e elastic scattering
  Calculable process with large analyzing power A_{NN}, A_{LL} in the forward direction of the electron and drops dramatically with large angles at few mr. A_{SL} possible at RHIC.

  I. V. Glavanakov et al. Proceedings of Spin 96.

- e-p Deep inelastic scattering, G. Igo (from SMC and SLAC)

- p-p elastic scattering in the CNI region using the PP2PP

- Inclusive Pion production,
  (ZGS & E704 from H_2) and (E925 from Carbon and H_2)

- P Carbon CNI (tests at Kyoto, IUCF, AGS)

- Charge exchange polarimeter p n $\rightarrow$ n p at large u

i.e. Glauber ... SL Elastic pe scattering
use for target 2) Permendur wire 2 Gas jet or e+ beam

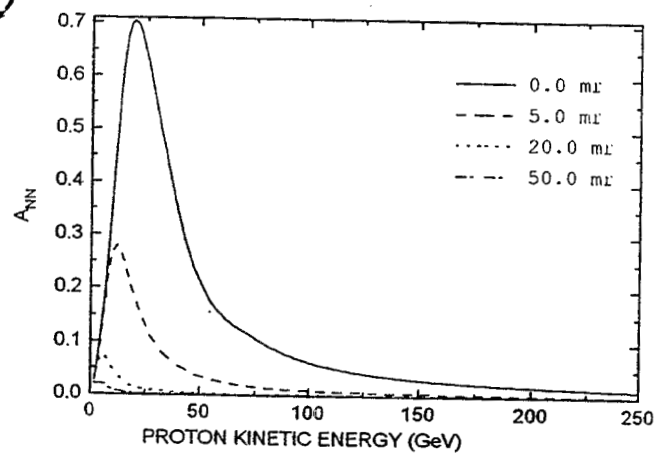

Figure 1: The energy dependence of the spin correlation parameter A_{NN} for the elastic scattering of the transversely polarized protons on the transversely polarized rest electrons for different angles.

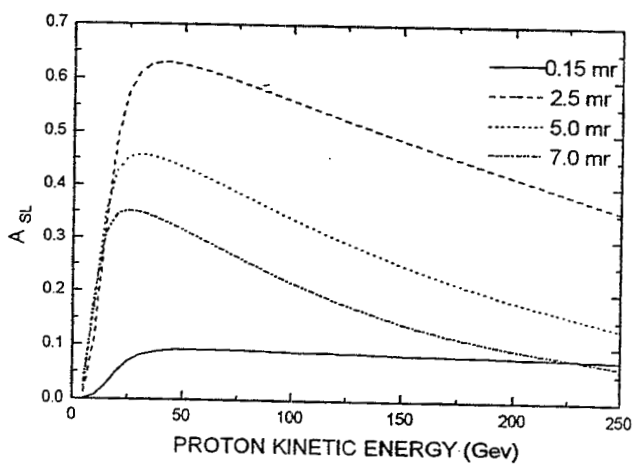

Figure 2: The energy dependence of the spin correlation parameter A_{SL} for the elastic scattering of the transversely polarized protons on the longitudinally polarized rest electrons for different angles.

$p^{\uparrow}p$ – CNI using PP2PP experiment ✓

⇒ statistical accuracy ✓

⇒ A_N ~ Energy independent ✓

? Spinflip hadronic amplitude !!

$p^{\uparrow}$carbon CNI

⇒ Simple detectors (Si, MCP) ✓

⇒ detect Carbon recoil (200keV–1MeV) ✓

? What is the effective analyzing pow

? How do we deal w/ N^*, Δ production

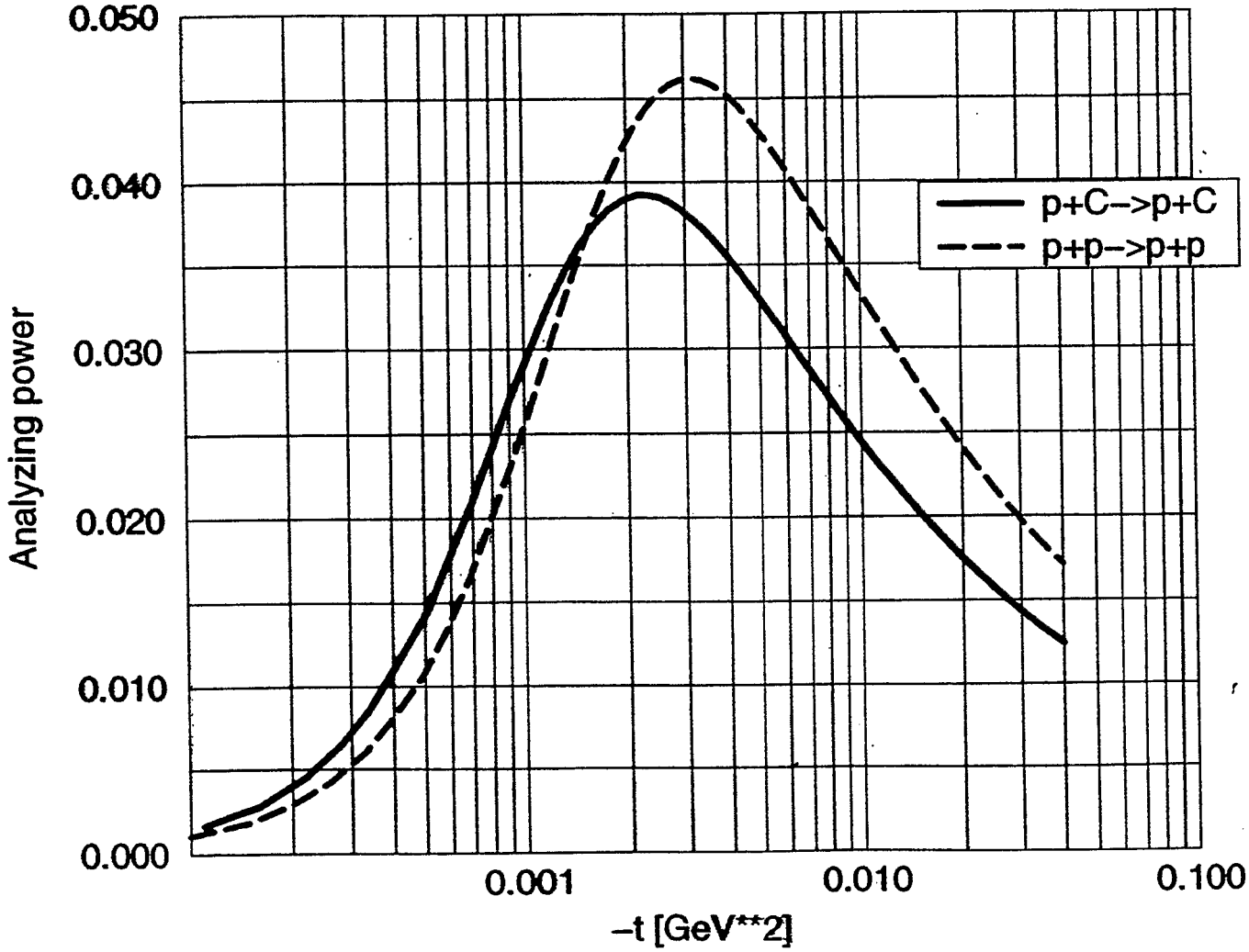

The Original Plan:

- A Polarization Measurement Working Group selected the asymmetry in Inclusive pion production as the choice for a day-1 polarimeter with an estimated accuracy of 10%.

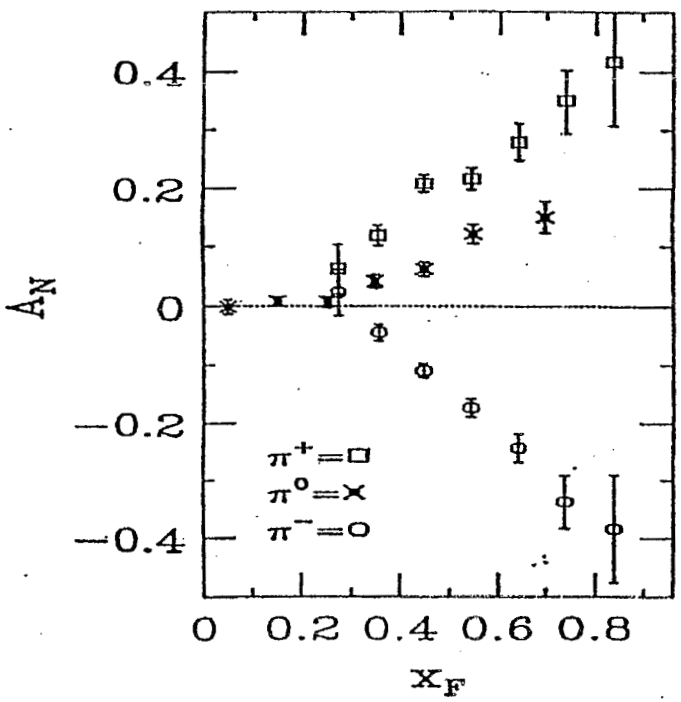

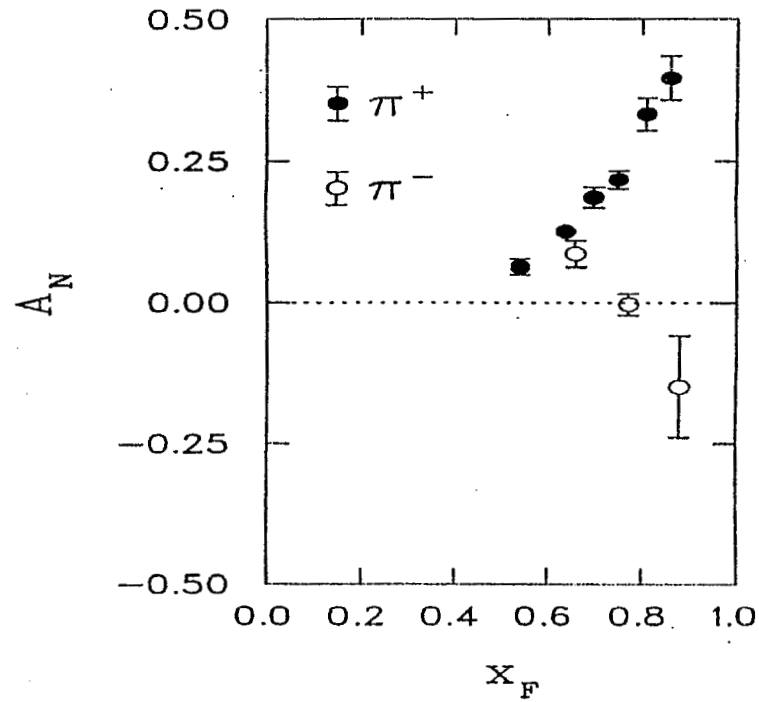

Fermilab @ 200 GeV/c

ZGS @ 12.75 GeV/c

D.L. Adams et al. Phys Lett B264, 462(91)

Dragoset et al Phys Rev D18, 3939 ('78)

- We developed a design for a two-arm polarimeter based on the toroid magnet design using a 5 um carbon target.
  (Inclusive pion polarimeter)
- A cost estimate of $1.5 M + forced us to scale back.

- The choice required further investigation that:

  1. The asymmetry is large over the entire RHIC energy range especially at injection.

  2. The use of the nuclear target does not dilute the asymmetry.

  3. The π^- asymmetries exhibit the same behavior as π^+. They are easier to detect with lower background.

The 5% Solution and Long Range Plan

- Install a polarized hydrogen Jet Target,
- Measure the Jet target polarization to less than 5%,
- Measure the beam polarization,
- Calibrate analyzing power of the polarimeter to better than 5%,
- Use the calibrated polarimeter to measure the absolute beam polarization. This process could be done at any desired energy.

pn → np charge exchange
E. Stephenson et al. (IUCF)

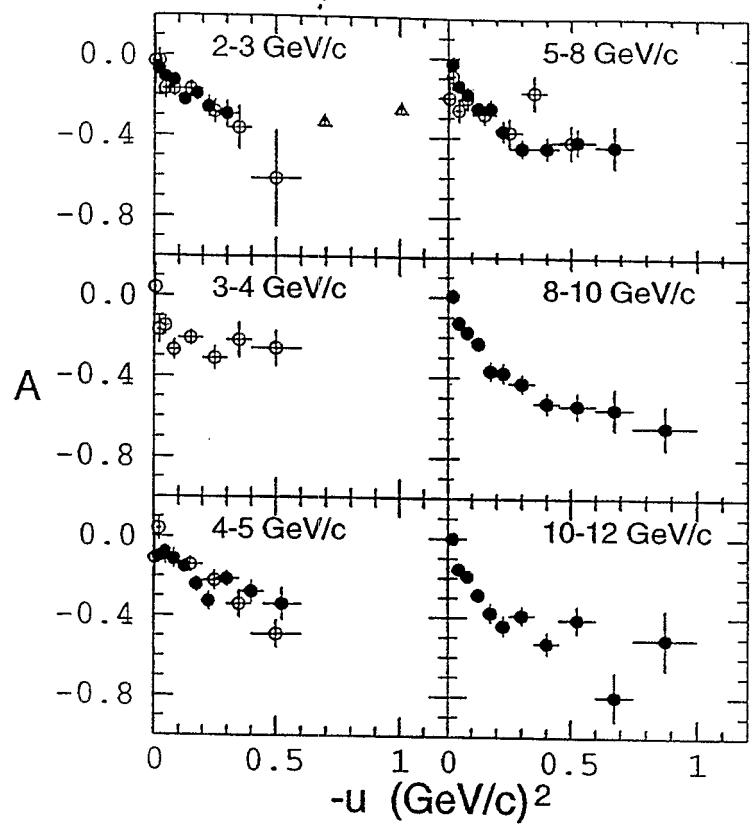

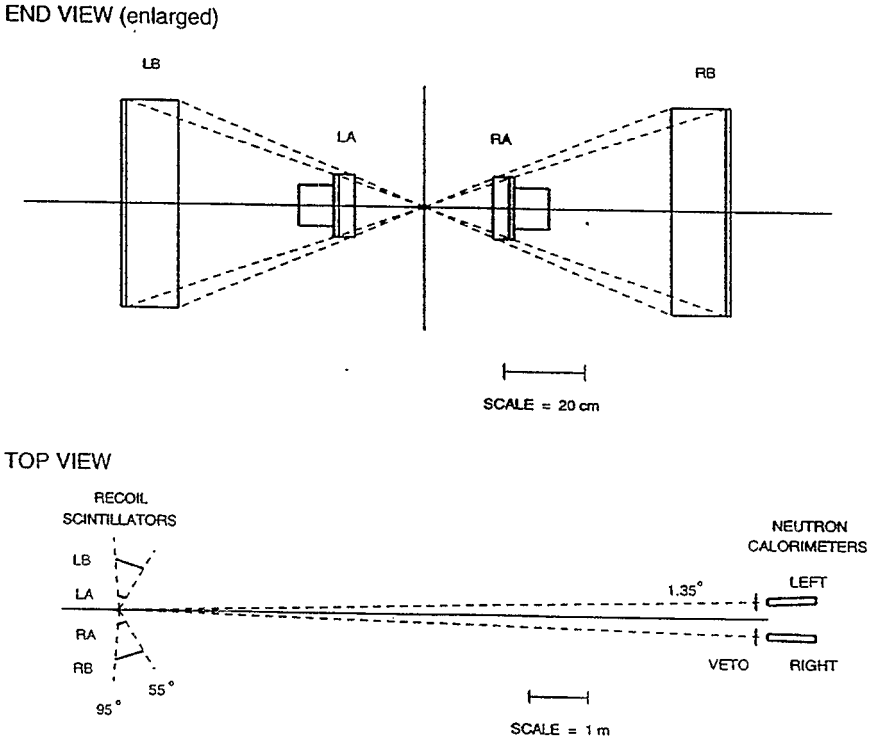

Figure 4. End and top views of a nominal polarimeter setup for 23 $(\mathrm{GeV/c})^2$. Detectors are shown with thick lines, the limits of scattered protons or the average path for neutrons with dashed lines. In the top panel, the front acceptance of the neutron calorimeters is partially shadowed by the left and right "A" recoil detectors.

STATUS of ACCELERATOR PROGRESS

MIKE SYPHERS
BNL
pC Polarimetry Workshop
8/4/98

- Overview of Spin Dynamics
- Siberian Snakes and Helical Dipoles
- RHIC Program -- Requirements & Status

Spin Dynamics

Particle trajectory governed by Lorentz force:

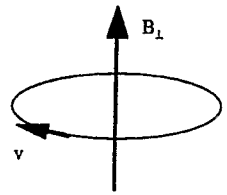

$$\frac{d(\gamma m\vec{v})}{dt} = e\left\{\vec{E} + \vec{v}\times\vec{B}\right\}$$

$$\frac{d\vec{v}}{dt} = -\frac{e}{m\gamma}\left\{\vec{B}\times\vec{v}\right\} \qquad (for\ \vec{E}=0)$$

$$= -\left[\frac{e\vec{B}_\perp}{m\gamma}\right]\times\vec{v}$$

$$= -\vec{\Omega}_{rev}\times\vec{v}$$

(assuming γ changing slowly)

In a frame rotating with the particle velocity vector, the equation for spin precession is:

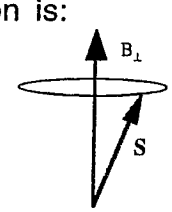

$$\frac{d\vec{S}}{dt} = -\frac{e}{m\gamma}\left\{G\gamma\vec{B} - (\gamma-1)G\frac{(\vec{v}\cdot\vec{B})\vec{v}}{v^2} + \gamma\left(G - \frac{1}{\gamma^2-1}\right)\frac{\vec{E}\times\vec{v}}{c^2}\right\}\times\vec{S}$$

$$= -\frac{e}{m\gamma}\left\{G\gamma\vec{B}_\perp + G\vec{B}_\parallel\right\}\times\vec{S} \qquad (for\ \vec{E}=0)$$

$$= -\left[\frac{e\vec{B}_\perp}{m\gamma}G\gamma\right]\times\vec{S} \qquad (for\ \vec{E}=0,\ \ \vec{B}_\parallel=0)$$

$$= -G\gamma\vec{\Omega}_{rev}\times\vec{S}$$

Here, the fields are those in the lab frame, whereas the spin vector is in the particle's rest frame.

For a pure vertical guide field in a circular accelerator, the spin precesses $G\gamma$ times per revolution. Thus, the "spin tune" is $\nu_s = G\gamma$.

Depolarizing Spin Resonances

Field perturbations cause undesired precession, and when resonance conditions hold can generate depolarization...

- Imperfection Resonances
  - ◊ arise from sampling of error fields, fields due to closed orbit errors, etc.
  - ◊ $G\gamma$ = *integer*
- Intrinsic Resonances
  - ◊ arise from sampling of focusing fields due to finite beam emittance
  - ◊ $G\gamma \pm \nu_y$ = *integer*;

    ν_y = vertical betatron tune

These resonance conditions can be avoided through the use of "Siberian Snakes."

Some examples of crossing a resonance of strength $\varepsilon = 0.015$ ($\varepsilon^2 = 2.25\times10^{-4}$) at various speeds...

$\alpha = 0.53\times10^{-4}$

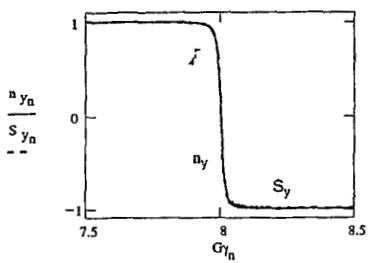

$\alpha = 1.6\times10^{-4}$

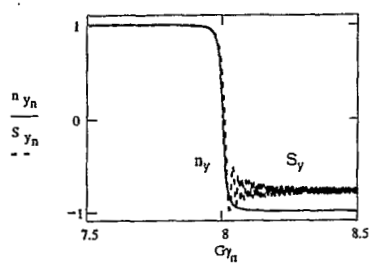

$\alpha = 5.3\times10^{-4}$

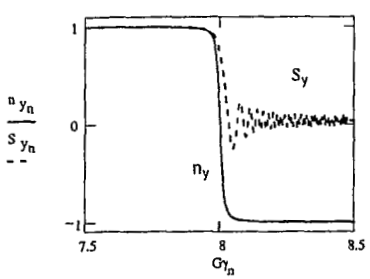

$\alpha = 16\times10^{-4}$

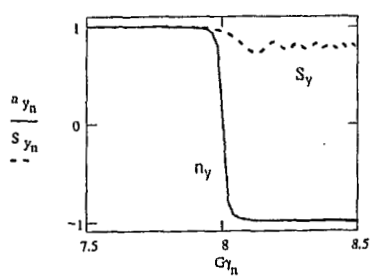

MJS, BNL

Siberian Snakes and Partial Siberian Snakes...

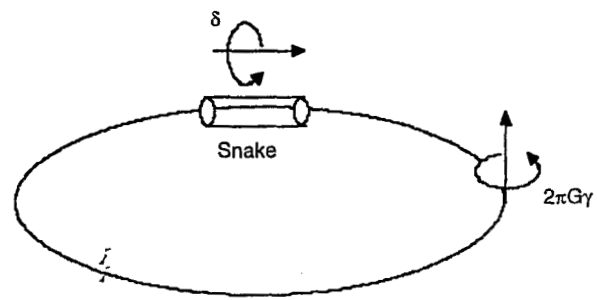

Intentionally introduce a strong horizontal field to produce large spin rotation --

$$\begin{pmatrix} S_x \\ S_y \\ S_z \end{pmatrix}_{n+1} = \begin{pmatrix} \cos\delta & \sin\delta & 0 \\ -\sin\delta & \cos\delta & 0 \\ 0 & 0 & 1 \end{pmatrix} \begin{pmatrix} \cos 2\pi G\gamma & 0 & \sin 2\pi G\gamma \\ 0 & 1 & 0 \\ -\sin 2\pi G\gamma & 0 & \cos 2\pi G\gamma \end{pmatrix} \begin{pmatrix} S_x \\ S_y \\ S_z \end{pmatrix}_n = M \begin{pmatrix} S_x \\ S_y \\ S_z \end{pmatrix}_n$$

$$\cos\pi\nu_s = \cos(\delta/2)\,\cos\pi G\gamma$$

So, if $\delta = \pi$ (Full Siberian Snake), then $\nu_s = 1/2$,
if $\delta = 0$ (No Snake!), then $\nu_s = G\gamma$,
and otherwise (Partial Snake) , then
ν_s cannot be an integer!

Crossing Intrinsic Resonance using RF Dipole

Adiabatically generate a Coherent Betatron Oscillation to increase the resonance strength seen by every particle; thus, all will flip spin

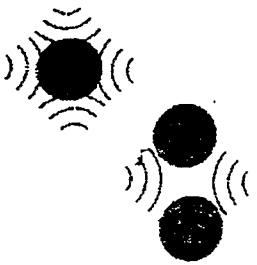

In frame rotating at the RF dipole frequency:

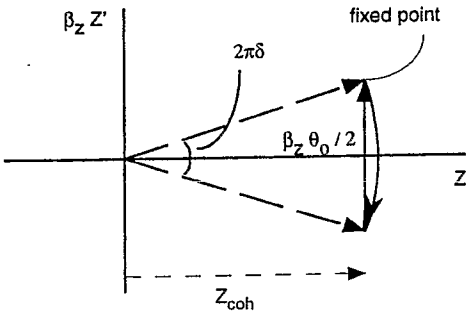

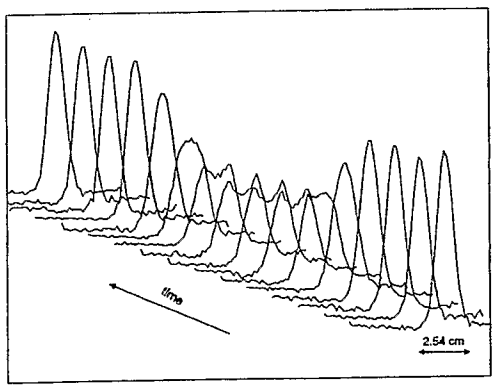

$$Z_{coh} = \beta_z \theta_0 / 4\pi\delta$$

$$\delta = \nu_{rf} - \nu_\beta$$

Emittance is preserved throughout the process

Crossing of intrinsic resonance in AGS using RF dipole magnet...

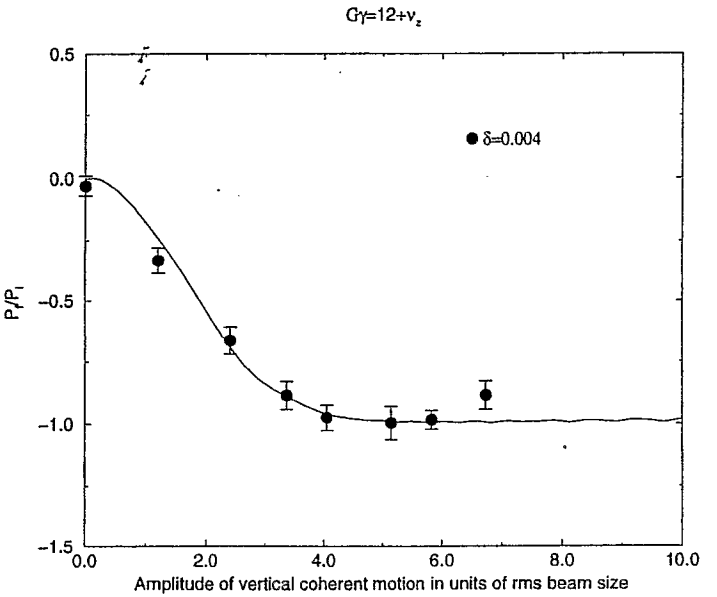

Total Spin Flip is generated

The RF dipole modulation tune was separated from the betatron tune by 0.004

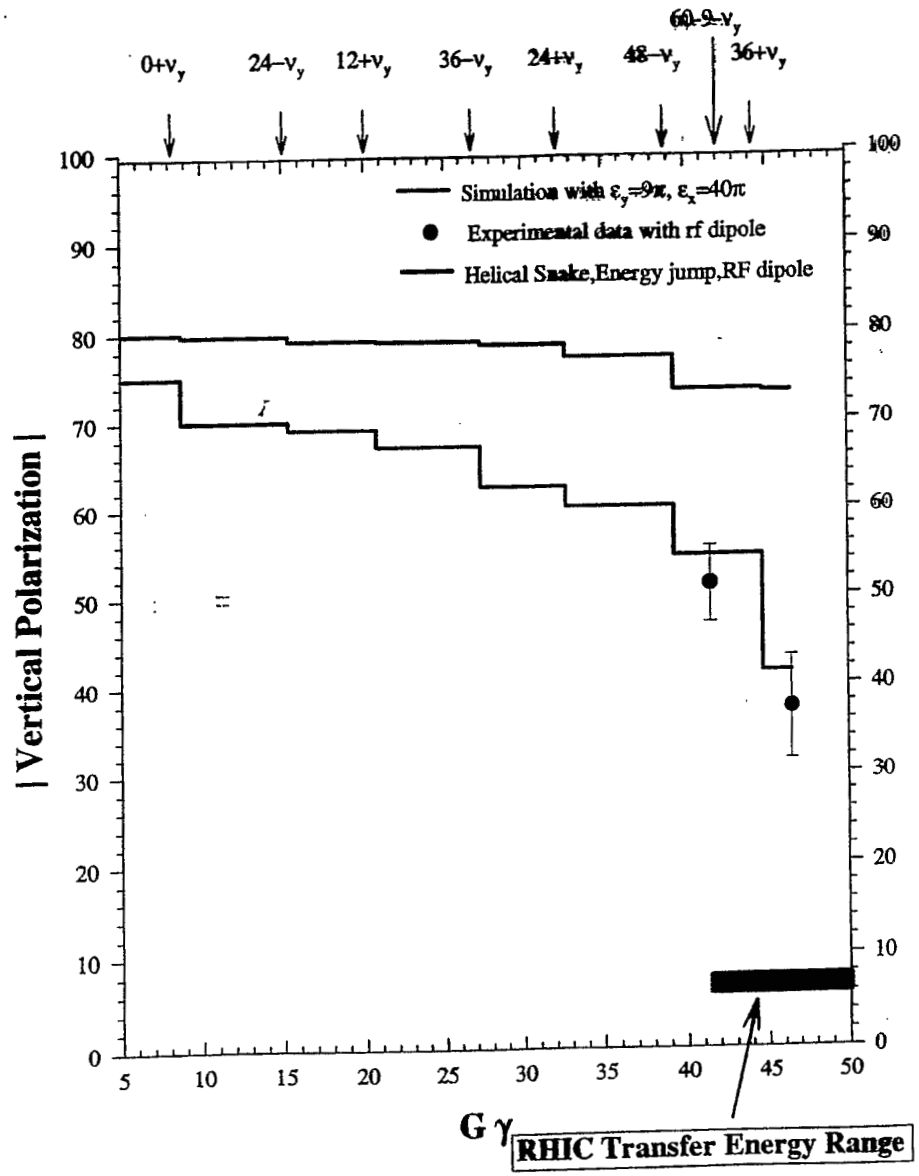

AGS Status:

- Recent polarized proton runs, using AC Dipole
  - * Successfully crossed strong intrinsic resonances using AC dipole to generate sustained coherent betatron oscillations
  - * Record polarization (50%) at high energy in AGS
  - * Improvement to 70% needed, and plans exist
    - ⇒ Improvements to orbit/feed-down effects, emittance
    - ⇒ Improvements to coupling
- Main issue will be control of both horizontal and vertical emittances in the AGS
- New optically pumped polarized ion source (OPPIS) in collaboration with KEK, RIKEN, and TRIUMF; presently being assembled at TRIUMF for testing; scheduled to arrive at BNL 1999; designed to reach intensity goals of RHIC
- Improve transverse coupling in AGS using

♦ Helical Partial Siberian Snake

Superconducting Magnet System Requirements

For the Siberian Snakes and Spin Rotators in RHIC:

- Works for 250 GeV Protons with reasonable field strengths
- Large aperture, for necessary orbit distortions, ...
  ... yet high field to keep orbit distortions small and local
- Low current (low heat-leak through power leads) and tunable
- Fits in available space in RHIC ring
- Minimize number of different components to be built

Nice solution for Snakes and Rotators proposed by Ptitsin and Shatunov (BINP), and refined at BNL over past few years, using helical dipole magnets...

- high field superconducting helical dipole magnets keep orbit distortions small and allow for the spin manipulations to be performed in a compact region
- four helical dipoles fit within standard RHIC straight section, keeping the assembly between already cold superconducting quadrupoles Q7 and Q8
- Rotators located in "warm" regions (which must be modified slightly), but modular design allows Snake and Rotator hardware to be as similar as possible
- low current, many-turn magnet designs being considered

Solutions for Siberian Snakes in RHIC:

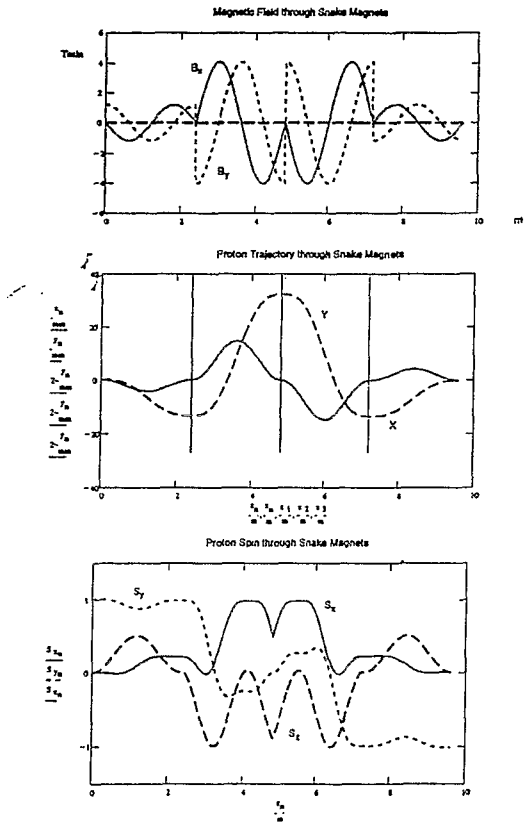

MJS, BNL

A schematic layout of RHIC showing the placement of Snakes as well as Spin Rotators (to make local longitudinal polarization). The designations "L" and "R" denote the "handedness" of the helical dipole magnets.

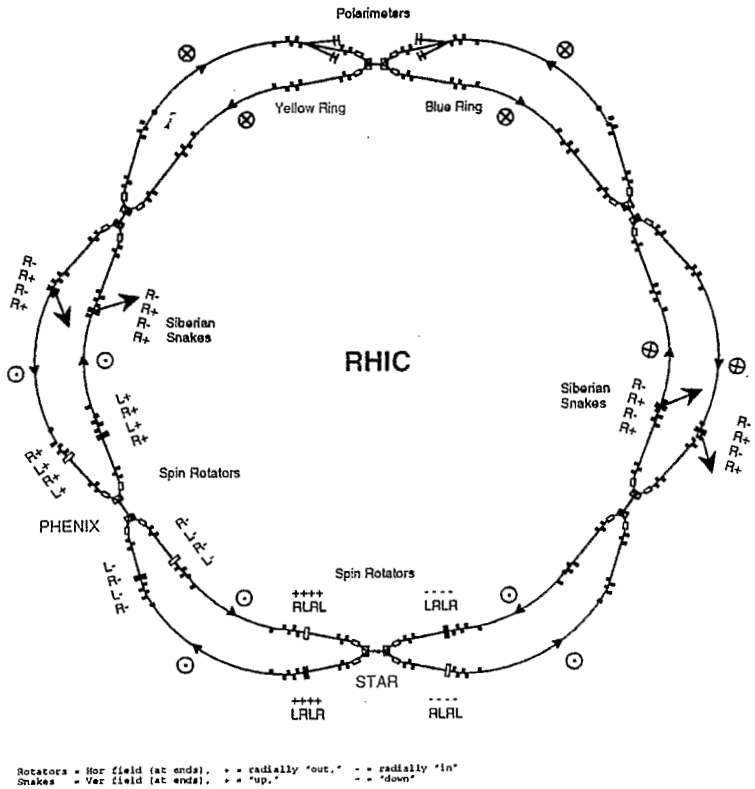

MJS, BNL

Construction of the helical dipoles is presently taking place in the RHIC Magnet Group at BNL. The winding machine shown below is being used to place superconducting cable into helical grooves machined into aluminum cylinders. Two concentric cylinders surrounded by iron laminations are used to produce the central field of 4 Tesla.

MJS, BNL

Present Project Status:

Accelerator Physics:

- Spin tracking studies concentrating on closed orbit correction schemes, crossing of strongest intrinsic resonances.

Magnets:

- Magnet R&D: success with both methods in making 4 Tesla helical dipole magnets! Slotted magnet more robust, chosen as design. >80% of Mechanical/Electrical drawings complete; most of remaining work is in cryostat assembly.
- Tooling (winding machine) is complete; most operational issues have been worked out. (Will still be learning things as we build first magnet.) Lamination stacking fixture complete.
- Procurement of long-lead-time items (aluminum tubes, iron yoke laminations, superconductor) in good shape.
- First full-length production magnet was to begin in January; delays, primarily in tube machining. First full-length tube now mounted on winding machine and winding has begun.

Polarimeter:

- Toroid double-arm polarimeters are too expensive for our "actual" budget. Building scaled-down, "day one" system.
- Developing CNI system as second "day one" polarimeter, and considering future systems such as jets.

Important Dates and Schedule

RHIC Spin Collaboration (RSC) Proposal	**September 1992**
1. Review of Pol. Proton Accel., Feasibility	**February 1993**
AGS Partial Snake Test (E–880)	**April/ Dec. 1994**
2. Review of Pol. Proton Accel., Progress	**March 1995**
RHIC Spin Physics Review	**June 1995**
RIKEN/BNL MoU signed	Sept. 25, 1995
RIKEN Japan Funding for Accel. (10M$) and PHENIX Detector (10M$)	**1995 – 1999**
Final Report of Polarization Measurement Working Group	**July 31, 1996**
First Helical Dipole Prototype Complete	**October 1996**
Second Helical Dipole Prototype Complete	**January 1997**
3. Review of Pol. Proton Accel., Progress	**February 1997**
First Full Helical Dipole Complete	**May 1998**
RHIC Completion	**June 1999**
2 Snakes and one Polarimeter Installed	**September 1999**
First Polarized Beam in RHIC	**> October 1999**
All Spin Rot./Snakes and Polarimeters Inst.	**September 2000**
First Spin Physics Run in RHIC	> October 2000

CNI Theoretical Status

height of CNI peak in A_N proportional to

$$(\mu - 1 - 2\tau)$$

$$\tau = \frac{\text{flip}}{\sqrt{-\frac{t}{m^2}}\ \text{non-flip}}$$

10% measurement requires

$\tau \lesssim 0.1$

or known ± 0.1

704 – $\tau = 0 \pm 0.05$

Resse fit to $\pi^{\pm} p$ A_N for 6 - 14 GeV/c

$\tau \leq 0.03 \pm 0.003$

(Kopeikovich - tentative)

models - many & varied; "average" ~ 0.05

educated guess (Low, Landshoff, ...)

$$\frac{\mu_p - 1 + \mu_n}{2} = \frac{1.79 - 1.91}{2} = -0.06$$

CNI for proton on nucleus

- same shape in very small-t region

$$A_N = \sqrt{\frac{8\pi Z\alpha}{m^2 \sigma_{tot}^{pA}}} \frac{y^{3/2}}{1+y^2} (\mu - 1 - 2\tau_A)$$

$$y = -\frac{\sigma_{tot}^{pA} t}{8\pi\alpha Z}$$

- for slightly higher t form factors F_H, F_c important

$$A_N = 2 A_N(y=1) \frac{y^{3/2} F_H(t) F_c(t)}{F_c^2(t) + y^2 F_H^2(t)}$$

(neglecting real parts of nuclear amplitudes)

$$F_c(q^2) = \frac{1}{A} \int d^2b \, e^{i\vec{q}\cdot\vec{b}} \, T(b)$$

$$F_H(q^2) = \frac{1}{2\sigma_{tot}^{pA}} \int d^2b \, e^{i\vec{q}\cdot\vec{b}} \left[1 - e^{-\frac{1}{2}\sigma_{tot}^{pN} T(b)}\right]$$

$$T(b) = \int_{-\infty}^{\infty} dz \, \rho_A(b,z) = \text{"nuclear thickness"}$$

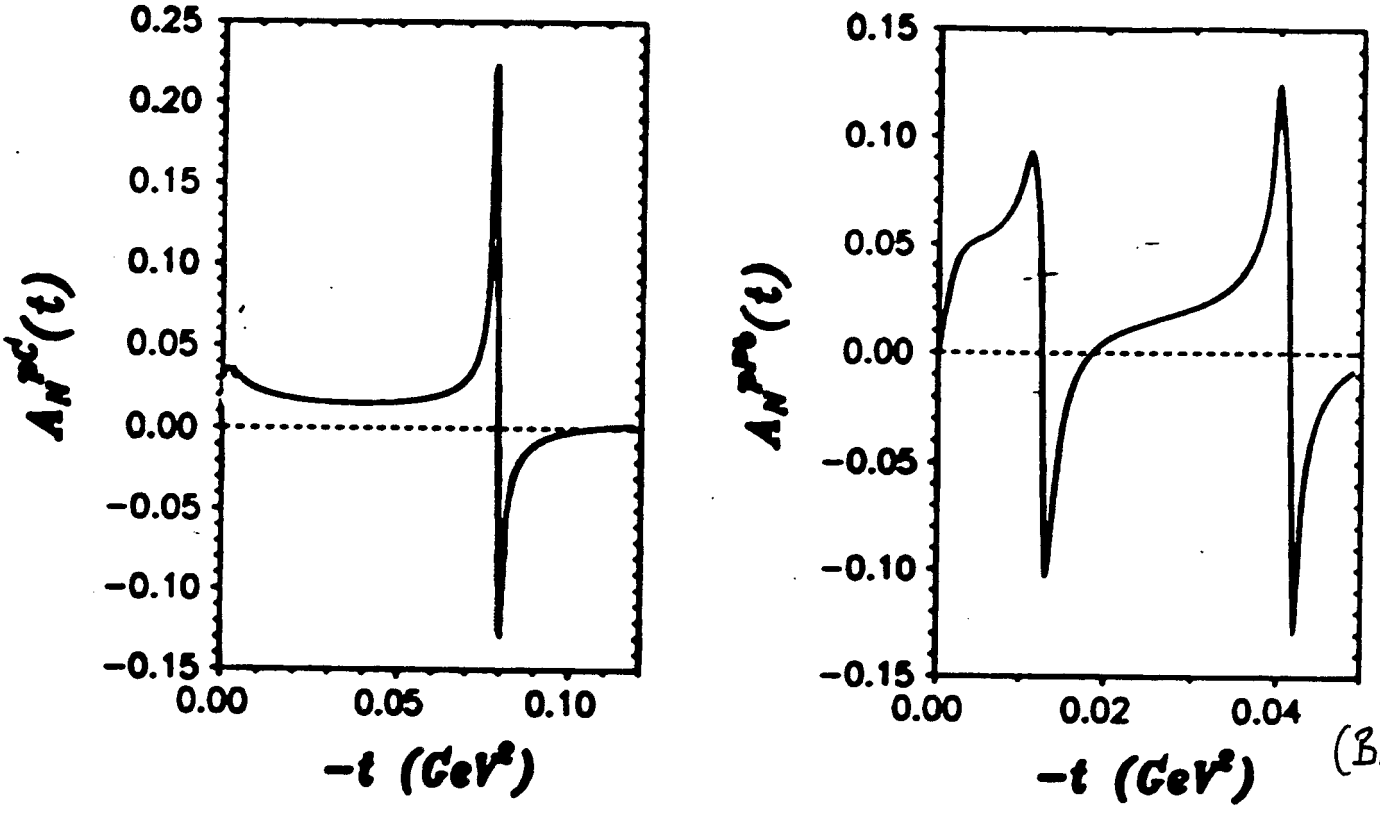

(B.K.)

Figure 3: ***Asymmetry in polarised proton scattering on carbon and lead, calculated using (12).*** pure CNI

If $\tau_A \neq$ scale shifts thenshown by factor

$$\left(1 - \frac{2\tau_A}{\mu - 1}\right)$$

Sadly, the argument is wrong!

Optical model, spin zero nucleus, neglect spin of unpolarized nucleons and assume scattering on p and n the same

$$f(\vec{q}) = f_0(\vec{q}) + i\,\vec{\sigma}\cdot\frac{\vec{k}\times\vec{k}'}{|\vec{k}\times\vec{k}'|}\, f_s(\vec{q}^{\,2})$$

small angle, high energy

$\vec{k}-\vec{k}' = \vec{q}$ transverse to beam

Write down eikonal ($\vec{b}$ impact parameter)

$$\chi(\vec{b}) = i\int d^2\vec{u}\; \tilde{f}(\vec{b}-\vec{u})\, T(\vec{u})$$

$$T(\vec{b}) = \int_{-\infty}^{\infty} dz\; \rho(\vec{b}, z)$$

Shift to

$$\chi(\vec{b}) = i\int d^2 l\; \left[\tilde{f}_0(l) + i\,\vec{\sigma}\cdot(\vec{l}\times\hat{k})\,\tilde{f}_s(l)\right] \times T(b-l)$$

Standard non-flip: neglect variation of T over range ℓ so

$$\chi_0(b) = T(b) \cdot \int d^2\ell \, \hat{f}_0(\ell)$$

$$= \frac{2\pi}{k} T(b) f(0)$$

"Spin-orbit" coupling $\vec{\sigma} \cdot \vec{\ell} \times \vec{k}$ gives cancellation of paths with same $|\vec{\ell}|$ but opposite signs so no flip unless path length is non-uniform. To lowest order

$$T(b-\ell) = T(b) - \vec{\ell} \cdot \vec{\nabla}_b T(b) + \cdots$$

Giving

$$\chi_s(b) = -\frac{1}{2} \int d^2\ell \; \ell f_s(\ell) \, \vec{\sigma} \cdot (\hat{k} \times \nabla_b) T(b)$$

$$= \underbrace{\left.\frac{\partial f_s(q)}{\partial q}\right|_{q=0}} \left(\vec{\sigma} \cdot \hat{k} \times \vec{\nabla}_b \, T(b) \right)$$

and from $f_s(q) = \frac{q}{m} \tau f_0(q)$: $= \frac{\tau}{m} f_0(0)$

so

$$\mathcal{A}_{opt} = \frac{2\pi}{k} f_0(\sigma)\left(1 - i\frac{\tau}{m}\vec{\sigma}\cdot\hat{k}\times\vec{\nabla}_b\right)T(b)$$

$\Rightarrow$ inelastic amplitudes in optical approx.

$$F_0(q) = -i\int d^2b\, e^{i\vec{q}\cdot\vec{b}}\left(e^{\frac{2\pi i f(0)T(b)}{k}} - 1\right)$$

and, to lowest order in τ,

$$F_s(q) = +\frac{2\pi i\,\tau f_0}{km}\int d^2b\, e^{i\vec{q}\cdot\vec{b}}\,\hat{q}\cdot\vec{\nabla}_b T(b)\, e^{\frac{2\pi i f(0)T(b)}{k}}$$

$$= +\frac{\tau}{m}\int d^2b\, e^{i\vec{q}\cdot\vec{b}}\,\hat{q}\cdot\nabla_b\left(e^{\frac{2\pi i f(0)T(b)}{k}}\right)$$

(integrate by parts)

$$= -\frac{\tau}{m}\,\hat{q}\cdot\int d^2b\,\nabla_b e^{i\vec{q}\cdot\vec{b}}\left(\quad\right)$$

$$= -i\frac{\tau}{m}\,q\int d^2b\left(e^{2\pi i f(0)T(b)/k} - 1\right)e^{i\vec{q}\cdot\vec{b}}$$

$$= \frac{\tau}{m}\,q\,F_0(q) \qquad !\ !$$

Generalization with different assumptions –

optical model result depends only on ratio f_s/f_0 at $t=0$, not on shape but depends on assumptions about nuclear structure and correlations

Following result depends on eikonal and assumed ratio independent of t but does not depend on nuclear details:

easy integration by parts exercise to show that

$$f_s(q) = \frac{q}{m}\tau f_0(q) \Rightarrow$$

$$\tilde{f}_s(b) = \frac{\tau}{m}\frac{d}{db}\tilde{f}_0(b)$$

(this form true for a vector field interaction with τ the "anomalous magnetic moment")

General eikonal form to lowest order in spin-flip

$$F_0(\vec{q}) = \frac{k}{2\pi i} \int e^{i\vec{q}\cdot\vec{b}} d^2b \int \prod dx_i \, |u_i(x_1 \cdots x_N)|^2$$

$$\cdot \left(\prod_{i=1}^{N} (1 - f_0(\vec{b} - \vec{x}_{i\perp})) - 1 \right)$$

$$F_s(q) = -\frac{k}{2\pi i} \int e^{i\vec{q}\cdot\vec{b}} d^2b \int \prod dx_i \, |u_1(x_1 \cdots x_N)|^2$$

$$\sum_k \prod_{i \neq k}^{N} (1 - f_0(\vec{b} - \vec{x}_{i\perp}))$$

$$\times f_s \, \hat{q} \cdot \frac{\vec{b} - \vec{x}_{k\perp}}{|\vec{b} - \vec{x}_{k\perp}|} \qquad (\vec{q} \text{ in } x\text{-dir.})$$

$$= -\frac{k}{2\pi} \frac{\tau}{m} \int e^{i\vec{q}\cdot\vec{b}} d^2b \frac{d}{db_x} \int \left(\prod_{i=1}^{N} (1 - f_0(b - x_i)) - 1 \right) |u|^2$$

$$= \frac{\tau}{m} q \, F_0(q) \qquad \text{as before}$$

(same result also from factorization)

so $\tau_A = \tau$ robust result

Precise calculation requires improvements:

- better nuclear wave functions; inelasticity
- allow different (τ) t-dependence for flip & non-flip
- off-shellness of protons between collisions

Simulations For RHIC CNI Polarimeter

by Doug Fields

Contents

Introduction
Geometry
Run Conditions
Analysis
Conclusions

Introduction

For the purposes of keeping progress towards a RHIC CNI polarimeter, it is necessary to have a good idea of what environment the recoil detectors will be living in. It was decided that we need a GEANT simulation of this environment at the very least. What is presented below is the work of Doug Fields and he is solely responsible for the mistakes which it is likely to contain. Please forward all comments to him so that he can incorporate them into the MC.

Geometry

I have created as simple a geometry as I thought I could get away with. This geometry can now be detailed as suggestions for possible background sources come to me.

Volumes:

Beam Pipe:

The beam pipe is made of aluminum and is 8 cm in diameter with a 2 mm thick wall. The extent of the pipe is 200 cm long. The pipe is broken in the center where the scattering chamber is located. The beam pipe is filled with perfect vacuum.

Scattering Chamber:

The scattering chamber is an aluminum box 30 cm x 30 cm x 10 cm (in z) with 5 mm thick walls.

Target:

The target is a carbon 3 cm long, 20 micro meters wide and 6 micro meters thick. This thickness is 240 times thicker than the 5 micro gram / cm^2 ribbon used for CE75. I made it thicker by accident at first, but soon realized this was necessary to increase statistics.

Detector (Annulus):

In order to again increase statistics, I created an annulus around the target where our detector would be located, essentiall integrating the background hits over phi. The annulus is at 10 cm radius and is 4 cm wide (in z). Particles that hit this annulus are the only ones stored in the output ntuple.

Pictures:

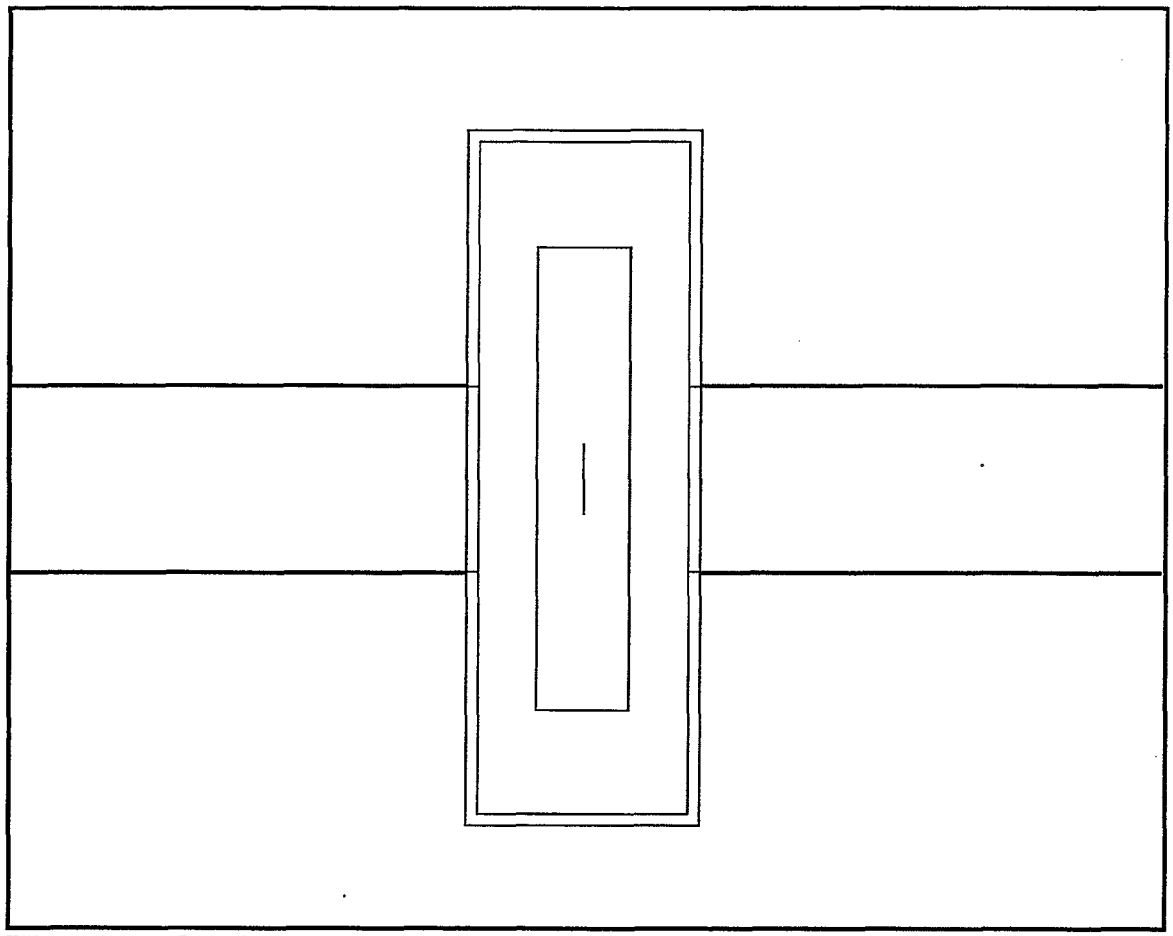

Side

View (y-z plane)

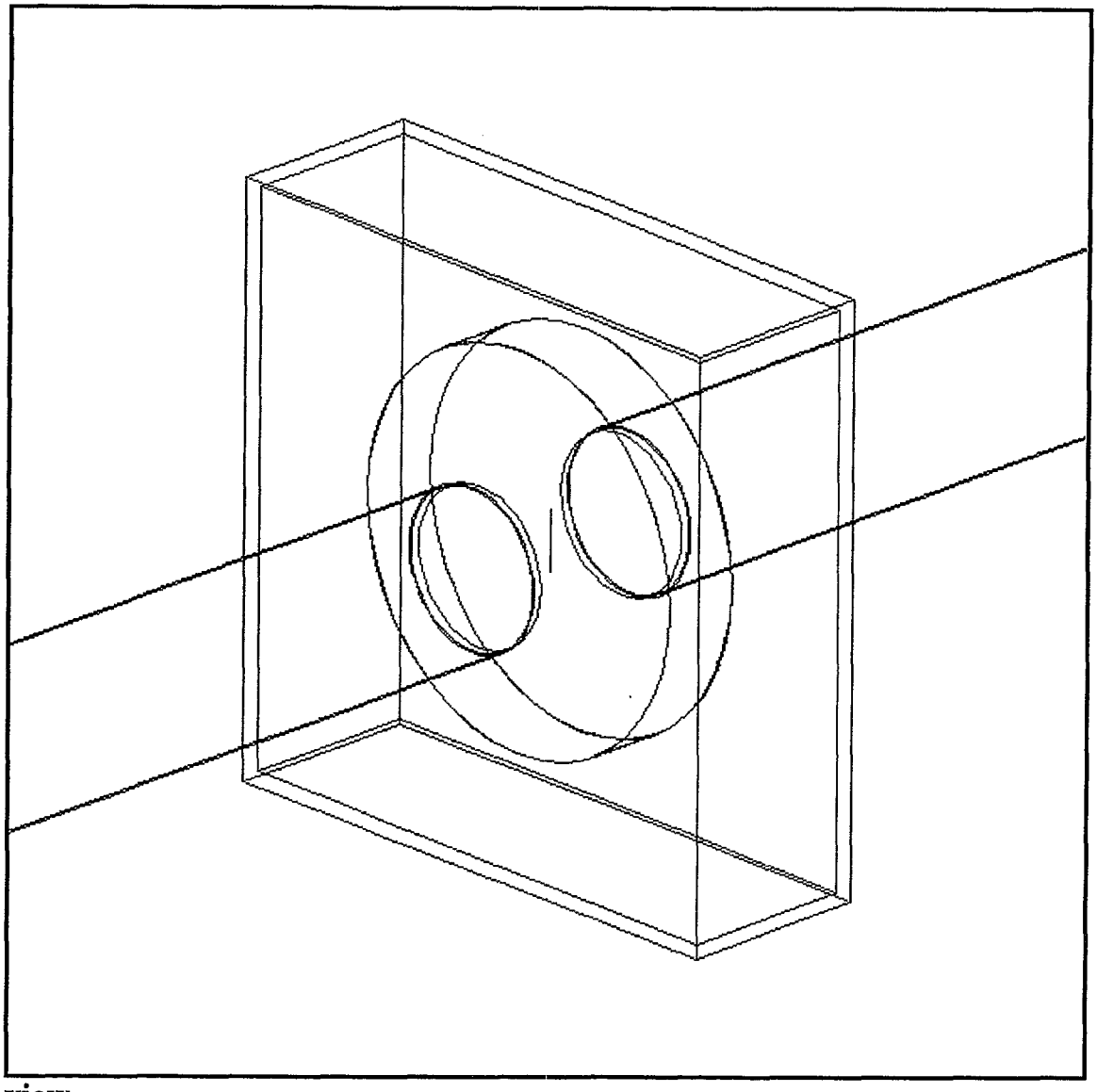

Objective view

Run Conditions

Events were generated by just throwing 250 GeV protons at the target at x = y = 0. I have left it to GEANT to have the correct cross sections for hadronic interactions. GEANT does NOT have included elastic scattering (???). For the analysis below, I threw 1 x 10^8 protons at the target. A typical interaction in the target is shown below.

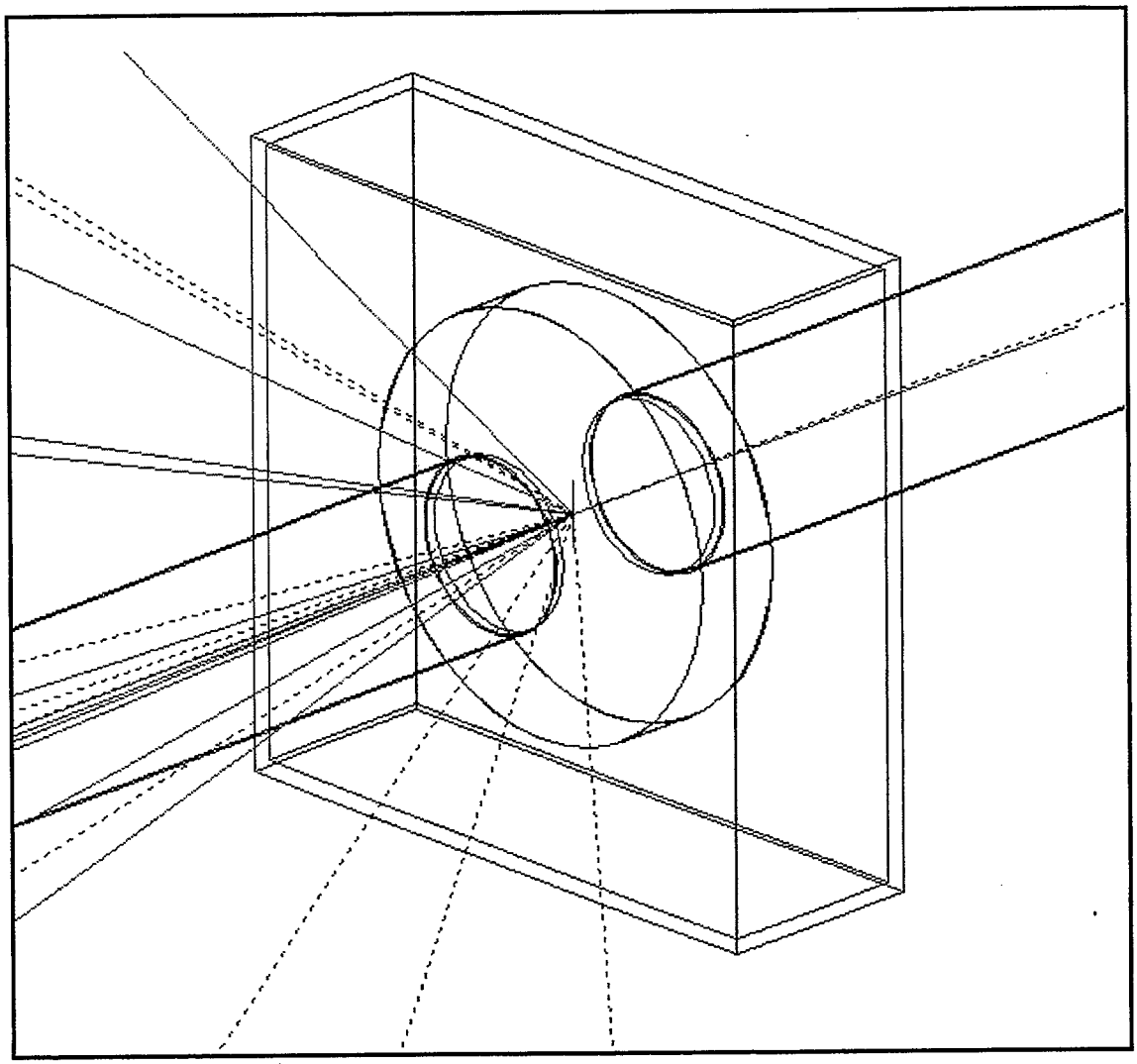

Single hadronic interaction

Analysis

Only secondaries that hit the annulus around the target were stored to an ntuple file. In order to determine how many would actually hit the real detector geometry, I can place a theta cut and then scale by the ratio of real phi coverage to the full 360 degree coverage of the simulation. We first look at the secondaries themselves to understand what their properties are:

Particle ID:

For those secondaries hitting the annulus, the figure below shows the GEANT ID distribution. For reference, ID=1 (gamma), ID=8,9 (charged pions), ID = 13,14 (neutrons, protons) and ID = 40's (deuterons, tritons, alpha's ...).

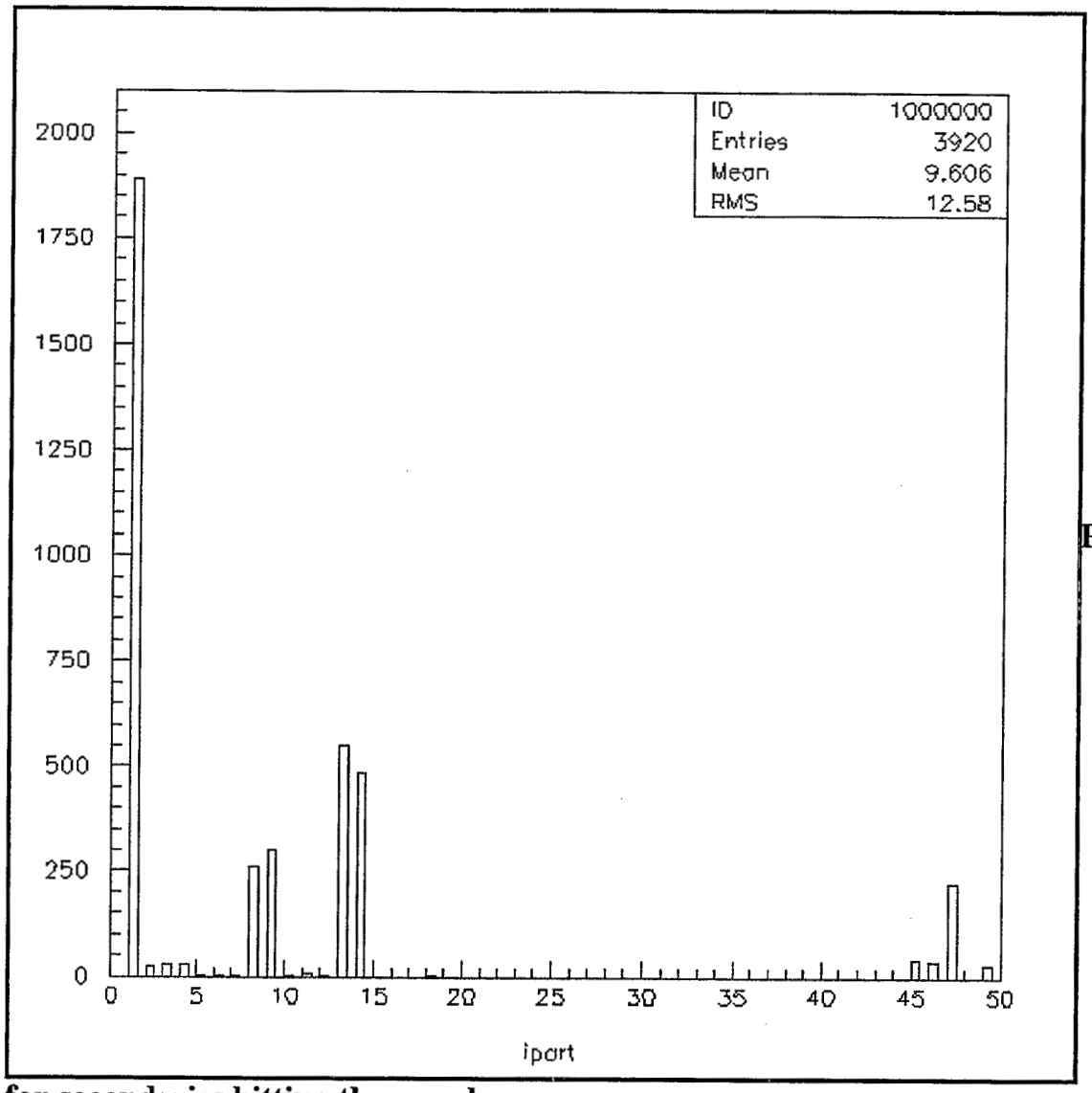

Particle ID for secondaries hitting the annulus

For the gammas (most of the spectrum), the momentum distribution looks like:

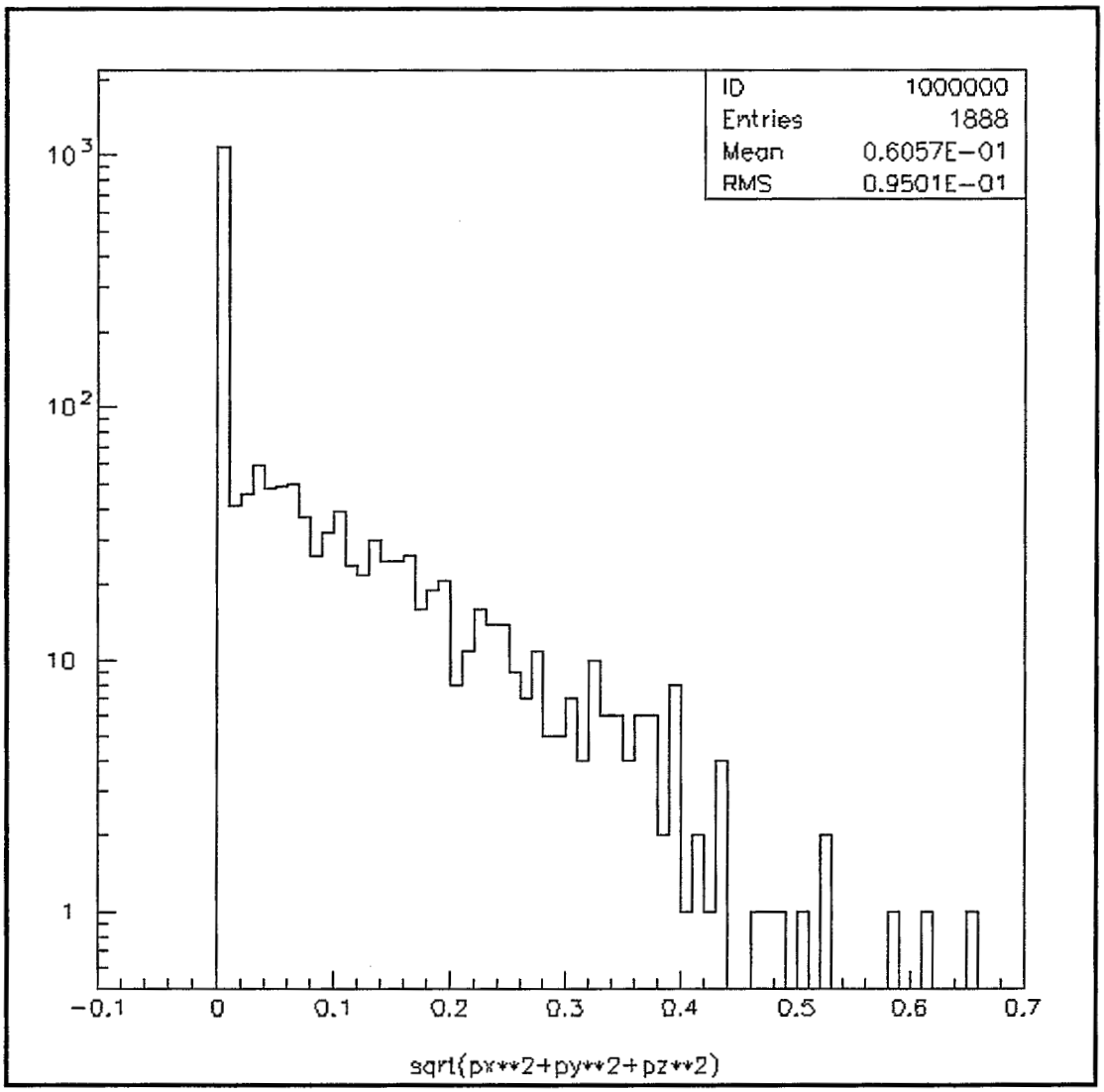

Momentum distribution of gammas

All of the gammas in the spectrum are above 1 MeV. The cross section at 1MeV on silicon is 3 barns/atom. For 300 micron thick silicon (density = 2.33 g/cm^3), then atoms/cm^2 = (2.33 g/cm^3)*(0.03 cm)/(28.086 g/mole)*(6.02 x 10^23 atoms/mole) = 1.498 x 10^21 atoms/cm^2.

So the interaction rate for these gammas are:

(3 x 10^-24 cm^2/atom)*(1.498*10^21 atoms/cm^2) = 0.0045

So, we can mostly ignore gammas. Of the rest, about 1/4th are neutrons and can also be ignored.

Rate Calculations

The number of protons in a single bunch is (2 x 10^11). Given the size of the beam (r = .24 cm) and the size of the target (10 microns), the ratio of protons in the beam to protons actually hitting the target is (0.85 x 10^-3). Then the number of protons in a bunch hitting the target is (2 x 10^11)x(0.85 x 10^-3) = 170 x 10^6. In the simulation, I ran 100 x 10^6 protons on a target which was 240 times too thick, so the number

of secondaries must be scaled by 1.7/240 = 7.1 x 10^-3. Restricting the theta angular range to the range of 88 - 89 degrees (one detector) gives 172 secondaries (all phi). Removing gammas and neutrons (see above) leaves 70 secondaries in 360 degrees of phi. Assume that the detector covers 6 degrees in phi (~1 cm), then the number of secondaries in one detector per crossing is:

70 * (7.1 x 10^-3) * (6/360) = **.008 secondaries per crossing**.

Now, for the calculation of the elastics rate I need to make a few assumptions. Let's take the total cros: section as scaled up from the p+p total cross section by A^2/3. The p+p total cross section is 40 mb in the range from 20 - 1000 GeV. So for p+C, take 40 mb x 12^2/3 = 210 mb [Gerry used 330 mb in his calculation. Was this from a reference?] A 5 microgram/cm^2 gives 2.5 x 10^17 carbon/cm^2. Taking the ratio of protons hitting the target gives a target thickness to beam T = 2.5 x 10^17 x .85 x 10^-3 = 2 x 10^14/cm^2. The luminosity per crossing is then:

L/crossing = N(protons) x T = 2 x 10^11 x 2 x 10^14/cm^2 = 4 x 10^25/cm^2.

The rate/crossing is then L/crossing x sigma = 210 x 10^-27 x 4 x 10^25 = **8.4 total interactions per crossing**

Now, again using the p+p data, the ration of total to elastic is about 6:1 which gives 1.4 elastics per crossing. Most of the elastics will give a carbon recoil in a two degree theta range, so we divide by two to give the elastics in one 1-degree theta detector = 0.7 elastics in 360 degrees of phi. Again scaling by the phi coverage, we get:

0.7 * (6/360) = **0.012 elastics per crossing**

for a total rate of **0.02 hits per detector per crossing.** Since the crossings are 100 ns apart, this gives a rate in the detector of

0.02/(100 x 10^-9) = **120,000 hits per second** or one hit every 8 microseconds.

Conclusions

The electronics that were used for the IUCF test run had a fall time of about 30 microseconds. In order to avoid pile-up then, the rate would have to be reduced by about a factor of 100 (which gives some safety margin).

MCP Test Experiment @ Kyoto

J. Tojo , K. Imai , M. Nakamura ,
Y. Kondo , J. Murata , R. Muramatsu , K. Yamamoto
Department of Physics , Kyoto University

* We need to detect low energy C below 1 MeV for pC CNI polarimeter .

* Possible detector : MCP

* Test experiment
  1. Mesurement of pC elastic scatt. using 10 MeV proton beam / C target .
  2. We tested 3 configuraations .
  3. Results

3 configurations of MCP we tested

A. MCP : direct detection of C

B. MCP + SSD (Au surface) : detection by secondary e from SSD

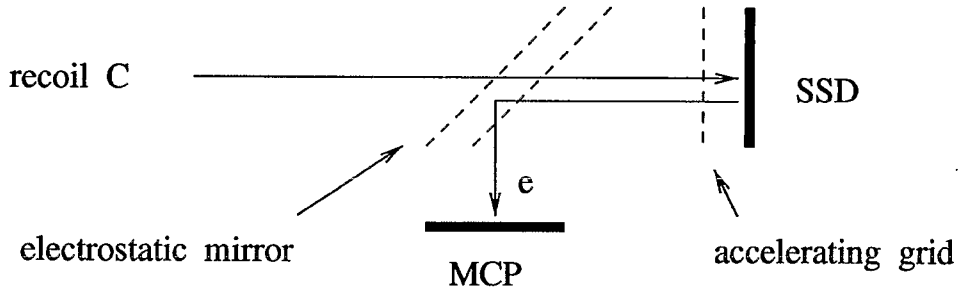

C. Two MCPs : detection by secondary e from C foil

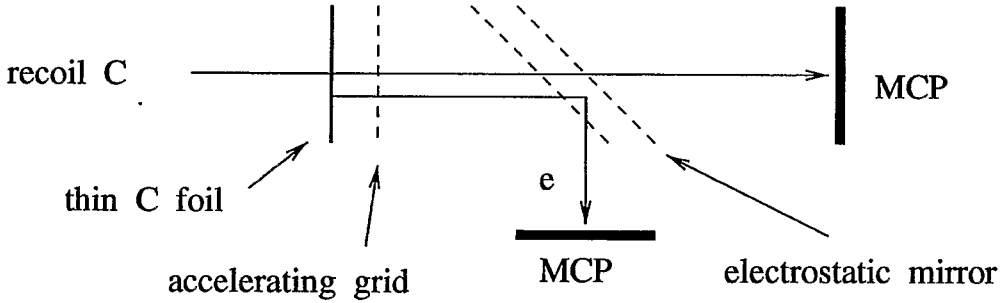

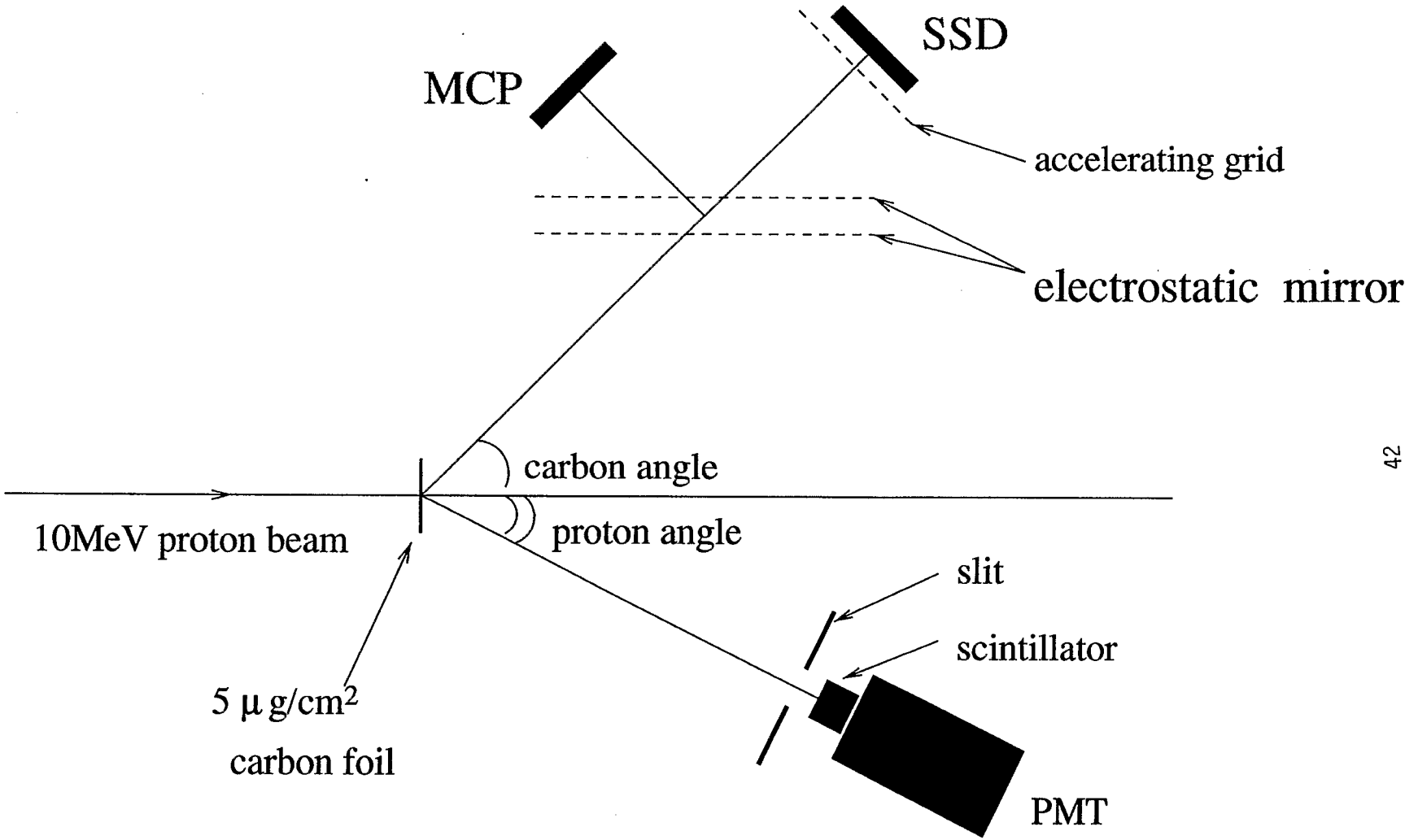

Experimental setup

TOF Resolution for 2 MCPs

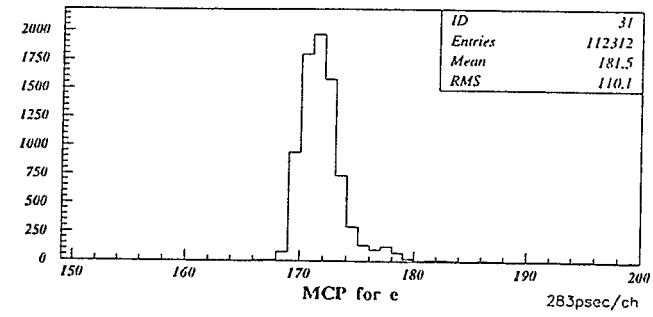

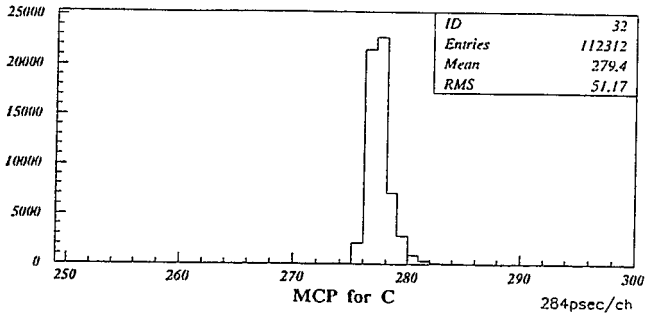

TOF Resolution

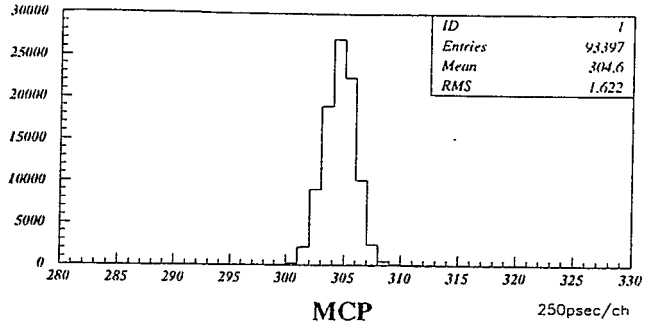

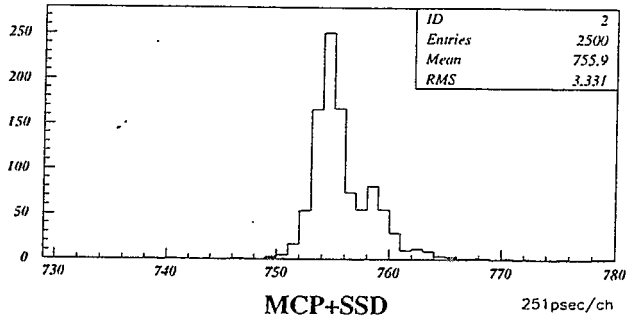

Energy Spectrum obtained from MCP

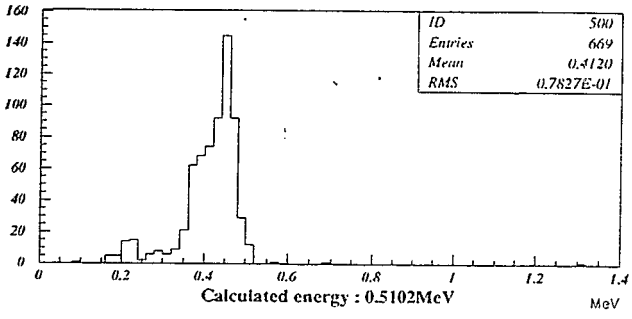

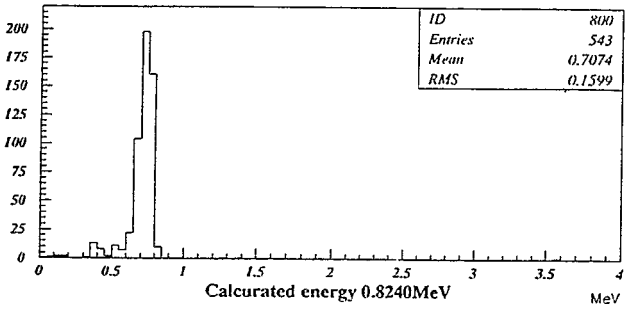

Energy Spectrum obtained from MCP

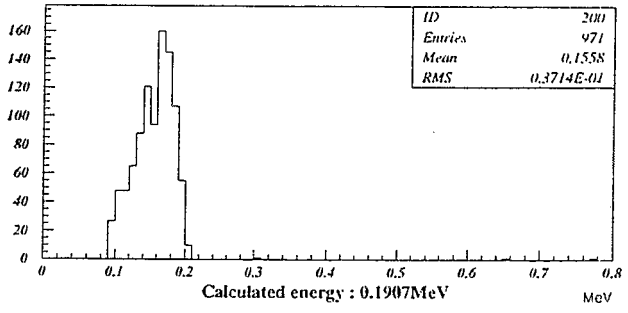

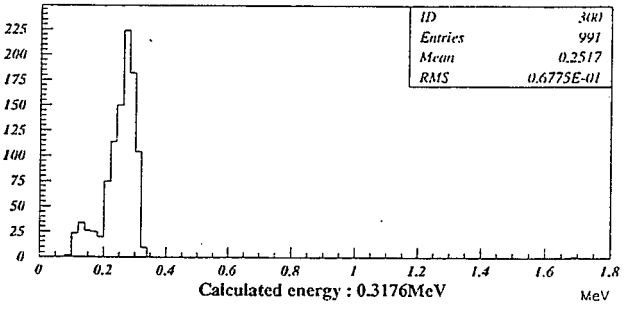

Energy Spectrum obtained from MCP+SSD

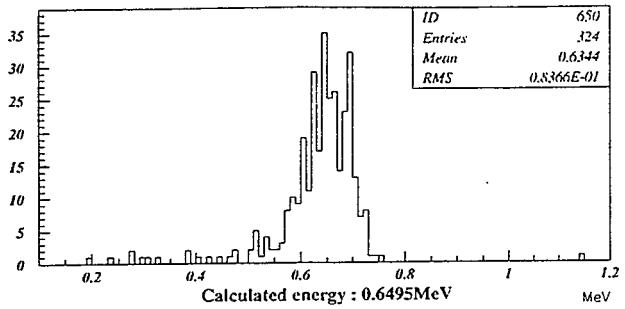

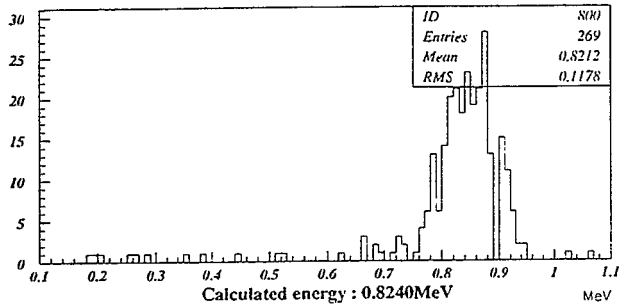

Energy Spectrum obtained from MCP+SSD

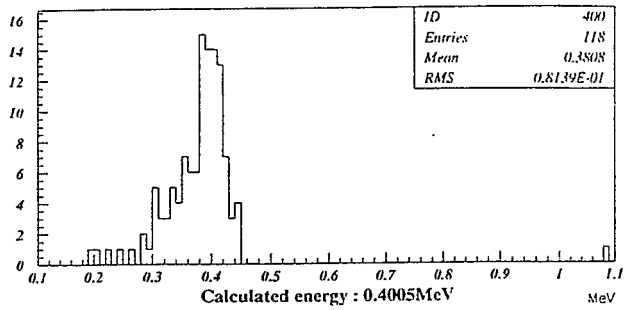

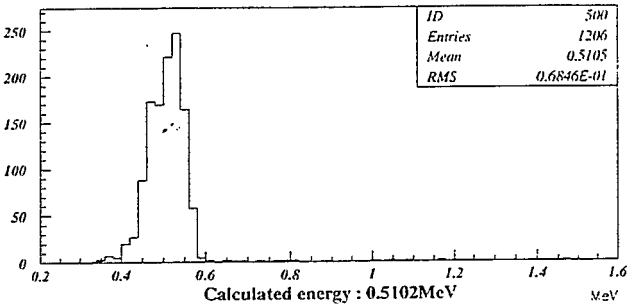

Efficiency

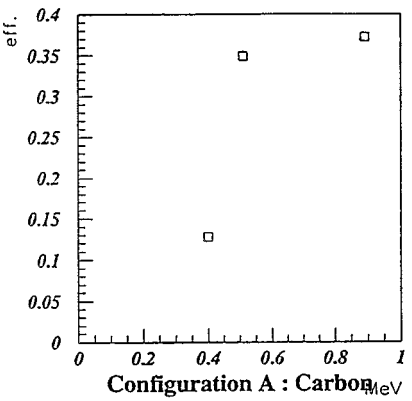

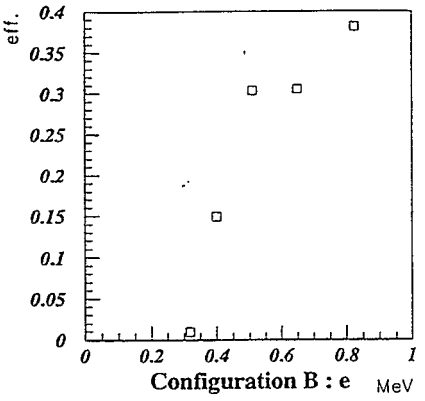

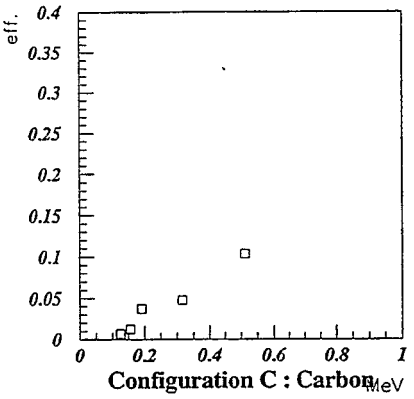

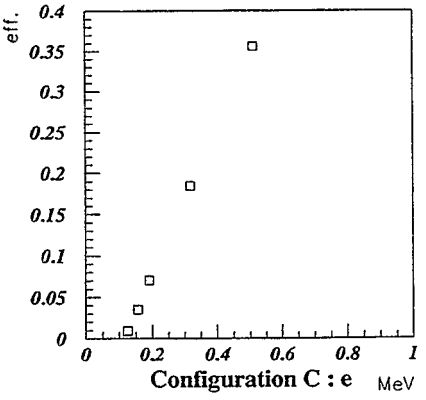

Summary

* We have carried out test experiments for pC CNI polarimeter.

* MCP was tesed as a possible detector using three configurations.

* Results

1. TOF resolution, energy spectrum, efficiency with each configuration were shown.

2. Carbon ions we need to detect were successfully detected with MCP.

3. From the data of the efficiency, the secondary electron method is effective for the polarimeter.

Toward RHIC CNI Polarimeter

Kenichi Imai, Kyoto University and Riken-BNL Research Center

The analyzing power of the p-C elastic scattering at Coulomb-nuclear interference region is expected to be around 4% and energy independent at high energy. It is expected to be useful as a polarimeter at RHIC. The difficulty is that one has to detect carbon ions to identify the elastic scattering and the energy of carbon ions ranges 100 to 500 keV. We have tested several methods to detect such low energy carbon ions by using the microchannel plate (MCP). The test results are presented by J.Tojo in this workshop. We found that the method to use carbon foil as the secondary electron emmitter for the MCP (carbon-foil-MCP detector) is the best way to detect low energy carbon ions. There can be several schemes as the RHIC p-C CNI polarimeter. Among several possible schemes, we propose to use both the carbon-foil-MCP detector and SSD for the AGS test run and RHIC. Two detectors provide energy and velocity information even without using the RF of the accelerator, which is important for the particle identification. One can add one more carbon-foil-MCP detector before the SSD just for redanduncy to reduce backgrounds, if necessary. One can make a test measurement with this proposed detector system at either IUCF or Kyoto before the AGS test run.

I also estimated the count rate for the AGS test run and RHIC, both day-1 and design beam intensity. I have used the beam parameters such as intensity and size given from the accelerator experts. I assume the target thickness can be from 1 to 5 $\mu g/cm^2$ and its width from 5 to 25 micron. Then, the count rates are calculated to be 3600 counts/sec at the AGS test run, 12000 c/sec at the RHIC day-1 and 2.5×10^5 c/sec at the RHIC design intensity. We can get 10% accuracy for the beam polarization within a reasonably short period of time with this polarimeter. At the RHIC design intensity, we have to study how to handle the very high event rate.

3. Toward AGS test and RHIC Polarimeter.

- Design RHIC polarimeter and
  Test it at AGS.

  (not enough time for the installation at summer (999).

Work. items.

- For all configurations
  - count rate ?
  - Trigger ?
  - S/N. ?
- Which configuration is the best ?
- How many θ bins ? 1 or 2
- t_{max} ?

Toward RHIC Polarimeter

Possible Setups

A. MCP + SSD

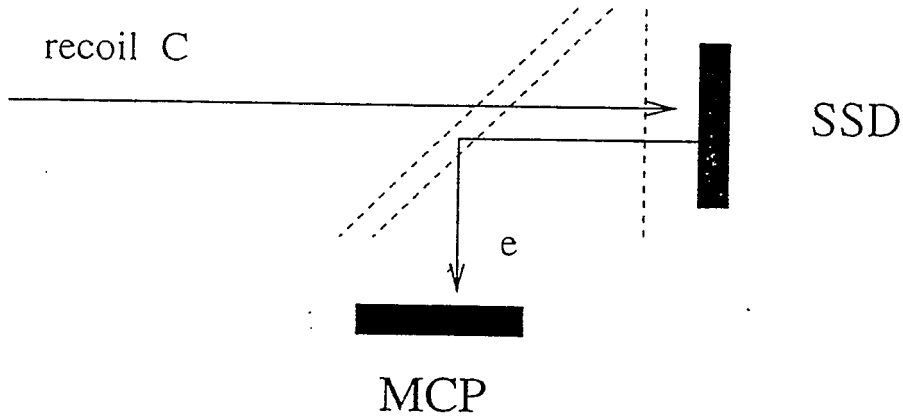

B. Two MCPs : secondary e + direct C

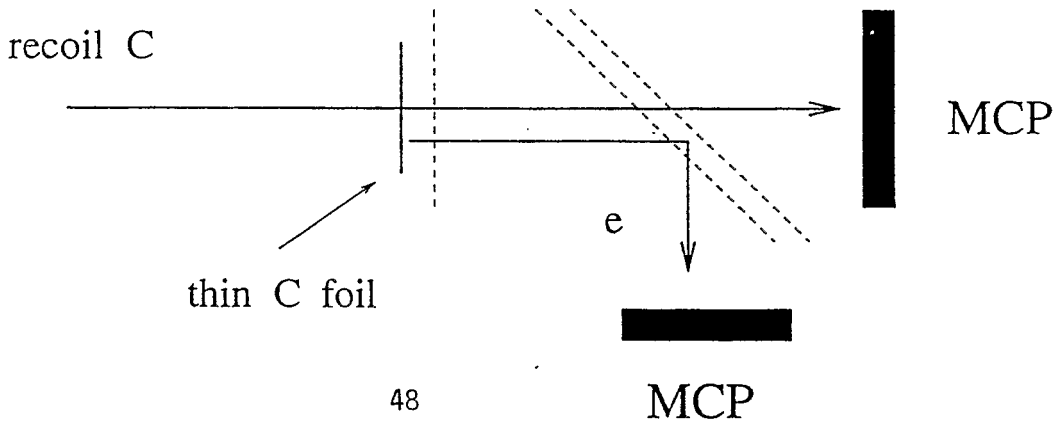

C. Two MCPs : secondary e only

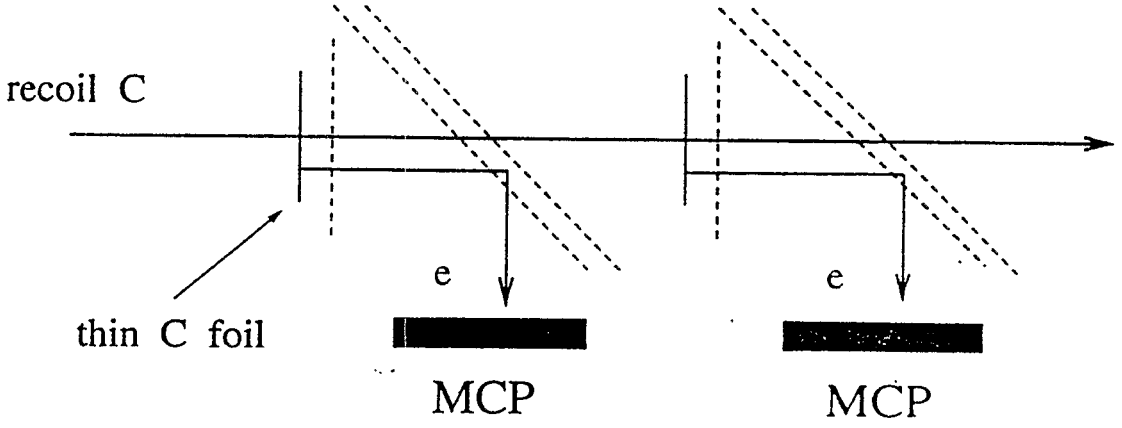

D. Two MCPs + SSD

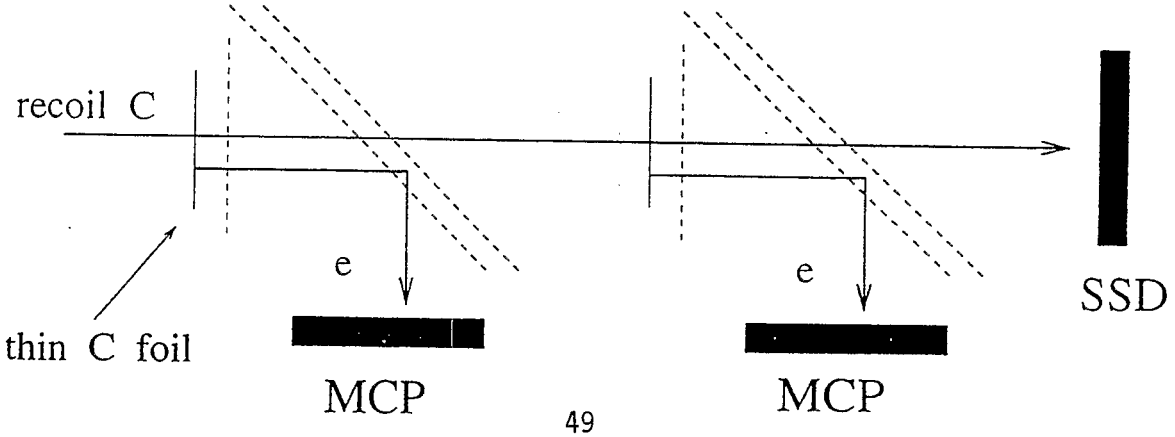

Count rate.

PC-CNI. $d\sigma/dt \simeq 2.8\times10^{-24}\ cm^2/(GeV/c)^2$ $\Delta t \simeq 1\times10^{-2}$.

$\Delta\phi \simeq \pm 3^\circ$.

$\sigma \simeq 5\times10^{-28}\ cm^2$.

① RHIC 1st year

$Y_b = 2.5\times10^{3}/b$ $Y = 1.2\times10^{4}/s$.

② RHIC Design.

$Y_b = 2.5\times10^{2}/b$ $Y = 2.5\times10^{5}/s$.

③ AGS.

$Y_b = 1.2\times10^{-3}/b$ $Y = 3.6\times10^{3}/s$.

assumption.

① RHIC 1st year.

2×10^{10} p/bunch 60 bunch ~ 200 nsec ~ 5×10^{6} b cross/sec.

1 mmϕ beam. target : 5 μm width. 1 μg/cm².

$$L = 2\times10^{10}\cdot 0.5\times10^{17}\cdot 5\times10^{-3}\cdot 5\times10^{6}$$
$$= \underline{5\times10^{24}/\mathrm{cm}^2\cdot\mathrm{b}}\cdot 5\times10^{6} = \underline{2.5\times10^{31}/\mathrm{cm}^2\cdot\mathrm{sec}}.$$

② RHIC Designed goal.

2×10^{11} p/b 120 bunch ~ 100 nsec ~ 10^{7} b cross/sec.

1 mmϕ. tgt : 5μm width. 1 μg/cm².

$$L = \underline{5\times10^{25}/\mathrm{cm}^2\cdot\mathrm{b}}\cdot 10^{7} = \underline{5\times10^{32}/\mathrm{cm}^2\cdot\mathrm{sec}}.$$

③ AGS (E880).

2×10^{9} 6 bunch ~ 350 nsec ~ 3×10^{6} b cross/s.

2 mmϕ tgt : 10 μm width. 5 μg/cm².

$$L = \underline{2.5\times10^{24}/\mathrm{cm}^2\cdot\mathrm{b}}\cdot 3\times10^{6} = \underline{7.5\times10^{30}/\mathrm{cm}^2\cdot\mathrm{sec}}$$

The polarimeter for RHIC based on the elastic (pe)-scattering.

D.M.NIKOLENKO, I.A.RACHEK, D.K.TOPORKOV, Yu.V.SHESTAKOV and V.F.DMITRIEV
Budker Institute for Nuclear Physics, 630090 Novosibirsk, Russia.
Yu.F.KRECHETOV
Scientific-Research Institute for Nuclear Physics, 634050 Tomsk, Russia.
S.B.NURUSHEV
Institute for High Energy Physics, 142284 Protvino, Russia.

Abstract

The polarimeter for RHIC based on the elastic (pe)-scattering is proposed. The polarimeter includes the internal hydrogen gas target in which atomic electrons are polarized, the detectors of the scattered protons and the recoil electrons. The proton beam polarization may be measured with a statistical accuracy $\approx 5\%$ during 500 sec, a hadron background may be rejected.

1 Introduction.

Elastic scattering of a polarized proton on a polarized electron can be used with the purpose to define the high energy proton beam polarization [1]. Indeed this process is very simple from theoretical point of view and this reaction provides a sufficiently large analyzing power. One of the possible way to obtain a polarized electron target is to use an internal gaseous target of polarized hydrogen atoms. We propose to apply a technique of polarized internal gas target with an atomic beam source (ABS) and an active storage cell [2] for polarized atoms for realization of the (pe)-polarimeter. Indeed the utilization of a storage cell in combination with a state-of-the-art ABS strongly increases the thickness of the polarized target [3], while the degree of polarization of the target electrons can be measured with high accuracy by the accessible methods [4].

2 Beam and target parameters and the statistical errors.

The proton beam has a transverse polarization at the straight section of the RHIC where the polarimeter may be placed, therefore A_{sl} component of the analyzing power will be considered.

The parameters of the beam and the target:

- The proton beam current is taken to be 100 mA.
- Such a degree of proton beam polarization is assumed that the product $P_p \cdot P_e = 0.5$, where P_e is a degree of the target electrons polarization.
- The thickness of the hydrogen target was taken to be $2 \cdot 10^{14} \frac{at}{cm^2}$. This thickness may be obtained by using an ABS similar to the Novosibirsk cryogenic ABS [5] and with a cooled ($120^o K$) storage cell having a diameter of 15 mm and a length 400 mm. Under the very first test of Novosibirsk ABS $6.4 \cdot 10^{16}$ polarized deuterium atoms per second were injected into the storage cell. For hydrogen atoms flux is expected to be about $1.0 \cdot 10^{17}$ per second with an electron polarization in the beam 0.99. The polarization of the target P_e expected to be about 0.8.

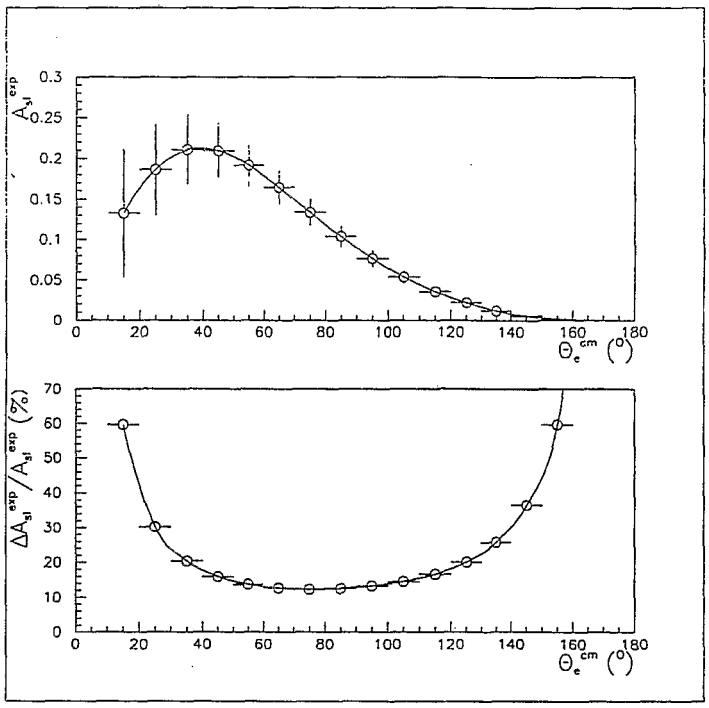

Figure 1: Calculated experimental asymmetry A_{sl}^{exp} (top panel) and the relative statistical errors of A_{sl}^{exp} (bottom panel) as a function of the recoil electron angle. Measuring time is 500 sec.

3 The proton and electron detectors.

Both particles – proton and electron are detected in coincidence.

The scattered protons may be detected after DX and D0 magnets where they are deflected from the proton beam orbit both in horizontal and vertical planes. The position measurements of the protons with accuracy 0.1-0.2 mm in two directions with a base between detectors 1 m should provide a possibility to reconstruct the proton energy with an accuracy $\delta E_p/E_p \approx 10\%$. The expected parameters of the electron detector are: energy range: 20–40 GeV, momentum resolution: $\Delta p/p \leq 10\%$, energy resolution in BGO calorimeter: $\Delta E/E \leq 3\%$.

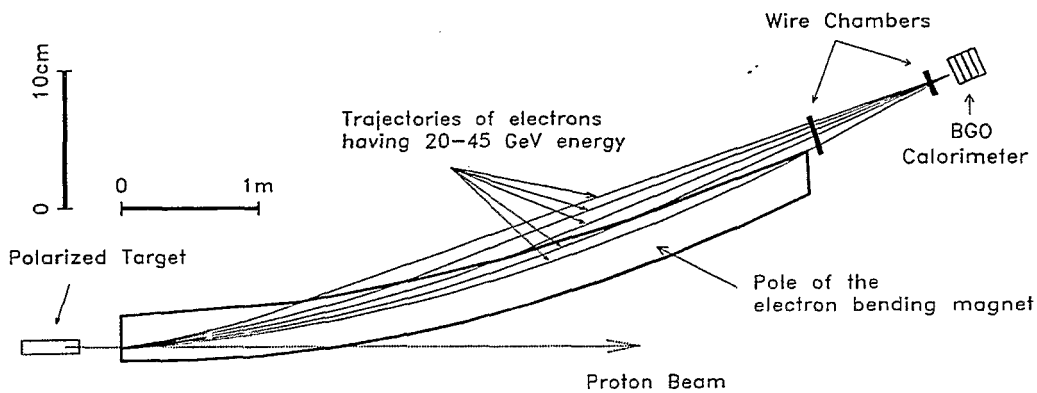

Figure 2: The sketch of the recoil electron detector, top view.

To decrease an influence of bending magnets on the proton beam orbit we suggest to set the opposite direction of the magnetic field in these magnets and additionally to apply two compensating magnets. One can see that such a magnetic system has small local perturbation of the proton beam orbits. Also this scheme has a vanishing influence on the proton beams spin dynamics.

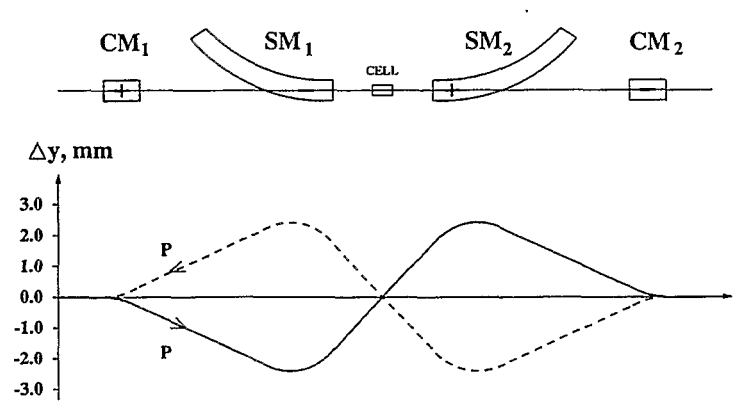

Figure 3: The schematic view of the polarimeter magnets (top panel) and its influence on the proton beam orbits (bottom panel). Here SM_1, SM_2 are the electron bending magnets, CM_1, CM_2 are the compensating magnets. We assume here that the length of magnetic field of SM_1 (as well as of SM_2) which acts on the proton beam equals to 1.5 m.

4 Energy deposition for electrons and pions in the calorimeter.

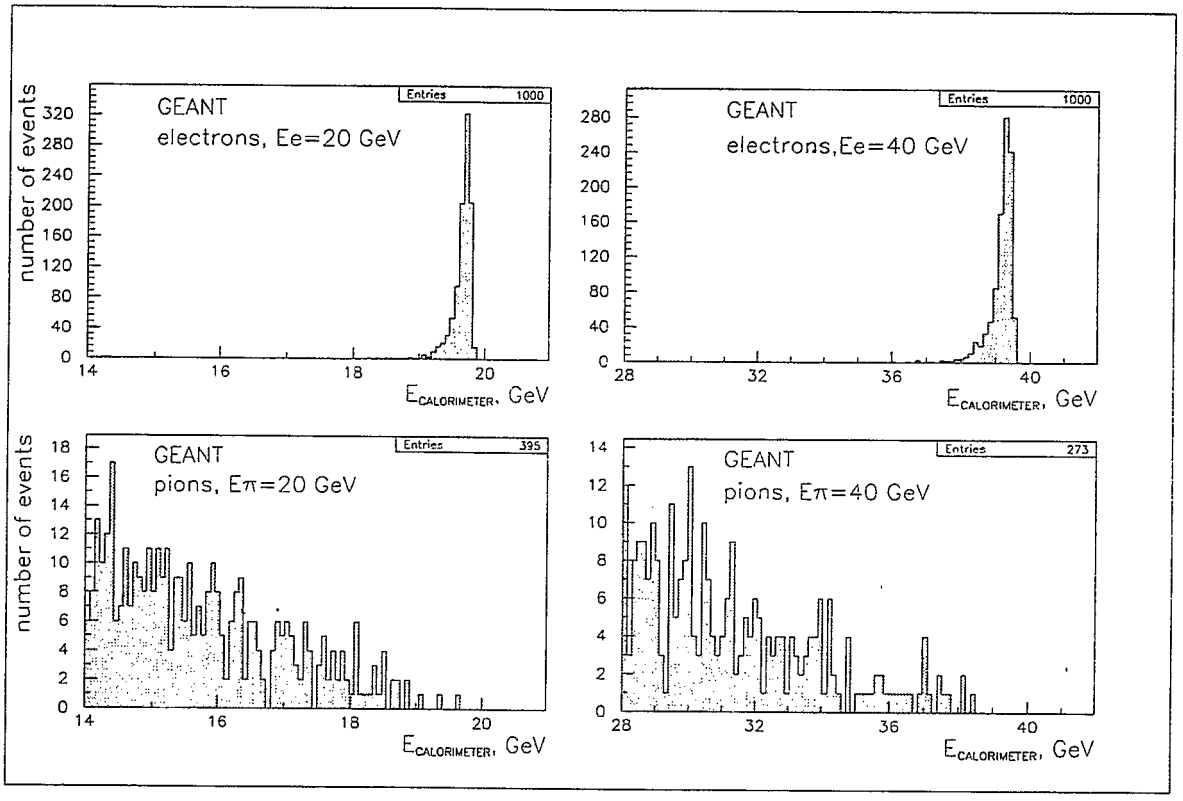

Figure 4: GEANT results for the BGO calorimeter response to electrons and pions. The calorimeter consists of 24cm–thick BGO crystal. Histograms show event distributions for energy deposition in the calorimeter. Simulation was done for 1000 electrons and 10000 pions for each energy point. It is clearly seen that nearly all electrons deposited $\geq$ 95% of their initial energy in the calorimeter (999 and 998 out of 1000 electrons for E=20 GeV and 40 GeV respectively), while only very few pions did the same (27 and 18 out of 10000 pions respectively). Comparing the energy deposited in the calorimeter and the one determined from the particle momentum, defined from particle trajectory in the magnet, one can effectively reject the pions, leaving the electrons untouched.

5 The background from hadron scattering.

The PYTHIA code was used to generate the events of (pp)-scattering. Most of the background particles which are hitting the electron detector are π^- mesons. However it was found that in a number of background events high-energy electrons are produced N^e_{pyth} in Tab. Such events survive the kinematical constraints and could not be rejected by the particle identification in the calorimeter. Fortunately the ratio of the rate of this background events and that of (pe)-elastic scattering R^e in Tab. is also small.

Table 1: The results of background estimation (RR is background-to-effect ratio).

$\theta_1 - \theta_2$	$E_1 - E_2$	E^+	N_{pyth}	N^e_{pyth}	$\frac{d\sigma_{bg}}{d\Omega}$	$\frac{d\sigma_{bg}}{d\Omega}^e$	$\frac{d\sigma_{pe}}{d\Omega}$	R	R^e	RR
mr	GeV	GeV			mb/str	mb/str	mb/str		%	%
0-1	53.6-56.6	174	101	0	126	< 1.3	12.2	10.3	< 11	2.1
1-2	46.4-53.6	177	620	0	258	< 0.42	16.8	15.4	< 3	3.1
2-3	37.8-46.4	183	973	0	243	< 0.25	24.4	10.0	< 1	2.0
3-4	30.0-37.8	193	863	1	154	0.18	33.0	4.7	0.5	0.9
4-5	23.8-30.0	198	834	1	116	0.14	40.9	2.8	0.3	0.6
5-6	18.9-23.8	204	613	4	69	0.45	48.0	1.4	0.1	0.3
6-7	15.2-18.9	208	391	5	38	0.48	53.0	0.7	0.1	0.1

References

[1] I.V.Glavanakov *et al.*, Nucl. Instr. and Meth. **A381**, 275 (1995).

I.V.Glavanakov *et al.*, Pis'ma Zh.Eksp. Teor. Fiz. **65**,No2,123-127 (25 January 1997)

[2] K. P. Coulter *et al.*, Nucl. Instr. and Meth. **A350**, 432 (1994).

[3] R. Gilman *et al.*, Nucl. Istr. and Meth. **A327**, 277 (1993).

[4] H.G.Gaul and E.Steffens, Nucl. Istr. and Meth. **A316**, 297 (1992).

B.Braun, Proc. of 12th Int.Symp. on High-Energy Spin Physics, Sept.10-14, 1996, Amsterdam, The Netherlands, p.241.

[5] L.G.Isaeva *et al.*, Proc. of 12th Int.Symp. on High-Energy Spin Physics, Sept.10-14, 1996, Amsterdam, The Netherlands, p.602.

Results from AGS-E925

Aki Yokosawa

UCLA, Los Angeles, Cal. USA

Abstract

The analyzing power in inclusive charged pion production has been measured using a $\sim$ 22 GeV/c polarized proton beam scattering off of a carbon target. An x_F dependence has been observed similar to what was found at 200 GeV/c by the FNAL E704 collaboration. A_N increases from 0 to .18 as x_F increases from .4 to .8 for $p_T \geq .7$ GeV/c. The analyzing power for inclusive proton production has also been measured and is consistent with zero.

PACS number(s): 13.85Ni,13.88+e

E-925 Inclusive $\pi^{\pm}$ Production at large x_F

Fermilab Expts (E-704) in inclusive meson production by polarized protons have shown significant asymmetries. There are some reasons to believe that the polarization in hyperon production is related to the asymmetry in meson production

In hyperon polarization – 10 GeV to 2000 GeV.
Slight decrease for heavier nuclei due to a rescattering effect.

Check earlier ZGS data

We measured $\vec{p}C \to \pi^+ X$ $\vec{p}C \to \pi^- X$ $\vec{p}C \to pX$

Beam polarization measurements with a target of CH_2
Forward arms, recoil arms
Analyzing power $A_N = 0.032$ at $t = -0.015$

ADC, TDC cuts π^+, contaminated by protons
increased π^+ asymmetry by a factor of 2

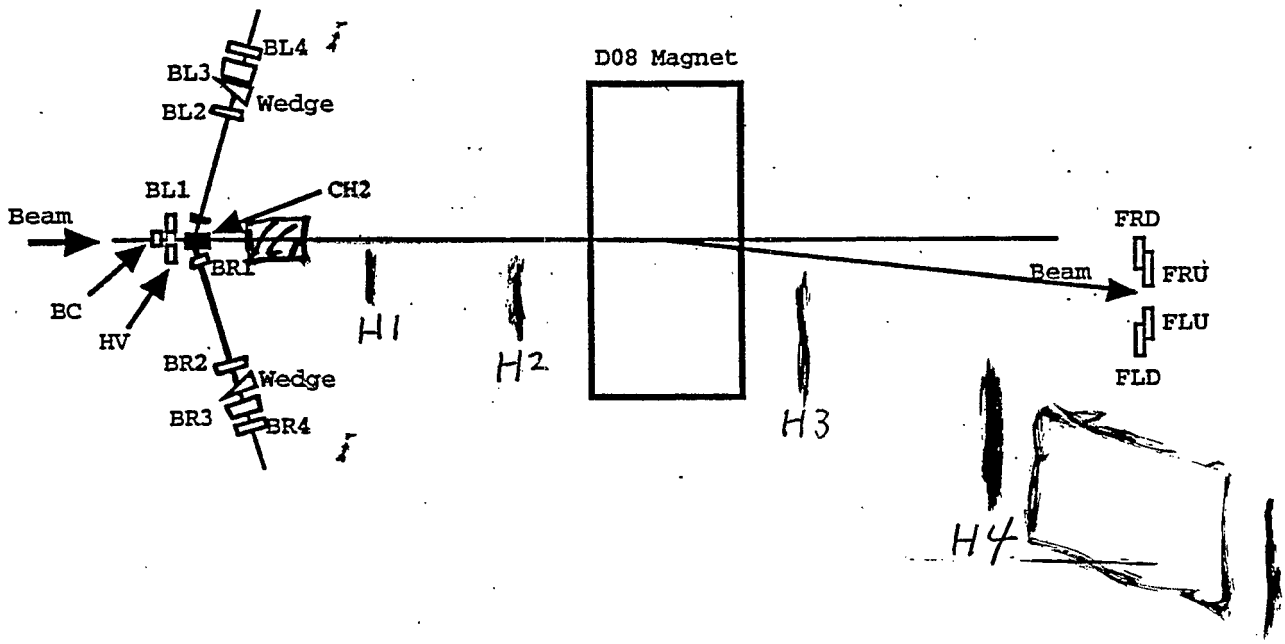
BL4
BL3
BL2
Wedge
BL1
CH2
Beam
BC
HV
BR1
BR2
Wedge
BR3
BR4
D08 Magnet
H1
H2
H3
H4
Beam
FRD
FRU
FLU
FLD

For inclusive pion production, H1 – H4, S1 – 3, and a $\tilde{C}$ counter were used.

4.0 – cm thick carbon target

The x – positions of charged particles from the target are measured by H1 (16 ctrs, 31 segments) and H2.
H3 (24 ctrs, 47 segments) and H4 (28 ctrs, 55 segments)
Each of these hodoscopes consist of 6 mm wide scintillators with 1/3 overlap.

Scintillators S1 – 3 were used – trigger counters

$\tilde{C}$, CO_2 at ~ 2 atomosphere

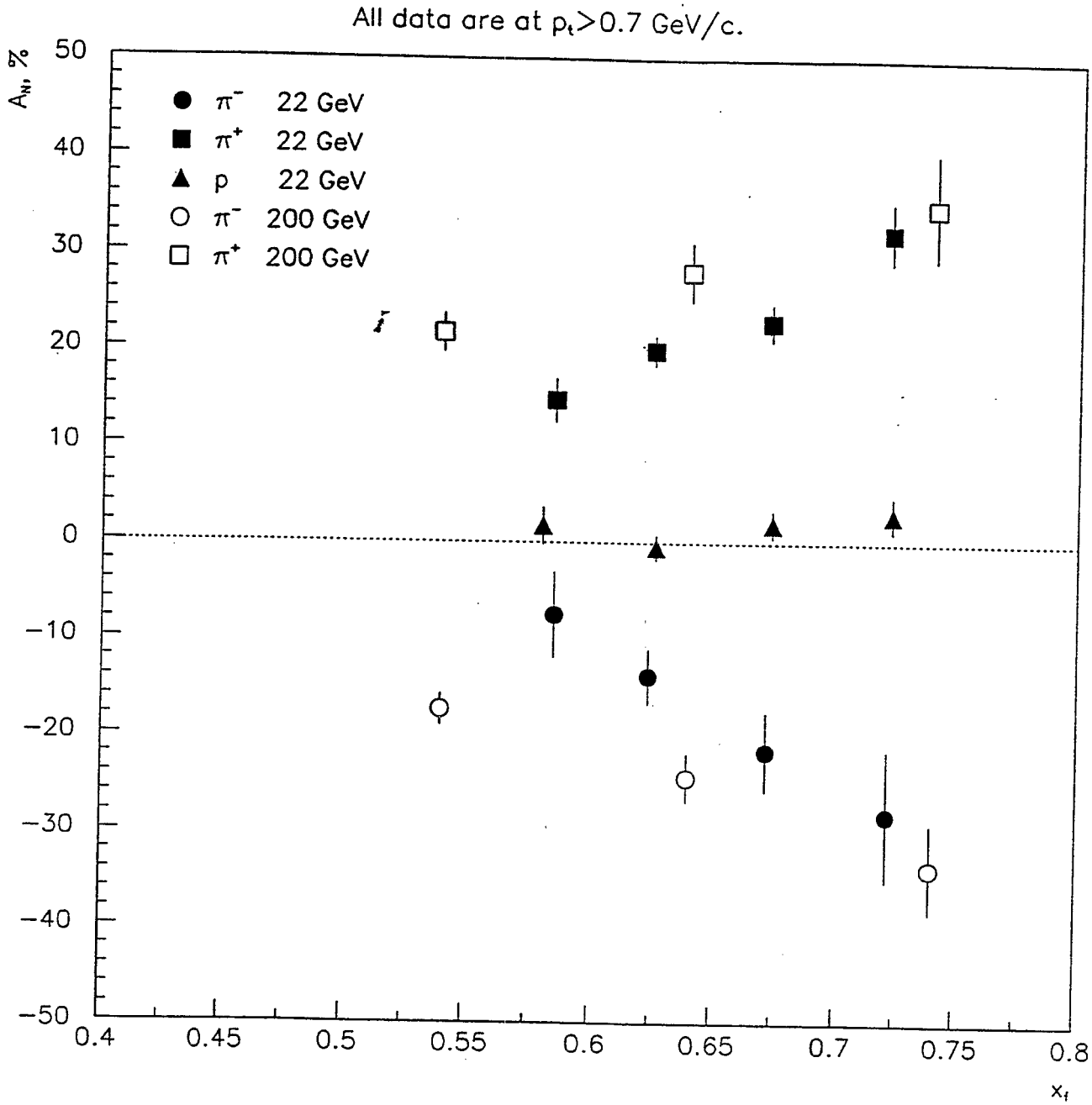
All data are at p_t>0.7 GeV/c.
A_N, %
50
40
30
20
10
0
−10
−20
−30
−40
−50
0.4
0.45
0.5
0.55
0.6
0.65
0.7
0.75
0.8
x_f
π^- 22 GeV
π^+ 22 GeV
p 22 GeV
π^- 200 GeV
π^+ 200 GeV

A model by Meng et al. explains the asymmetry due to a correlation between the spin of the proton and the orbital motion of the valence quarks. The u-valence quarks are more likely to be polarized in the same direction as the proton spin – the d-quark polarized in the opposite direction to the proton spin.

E-704 polarized antiproton beam

At the leading edge of the collision between a pol. proton and target proton A π^+ will form a valence u quark and a sea $\bar{d}$ quark and go to left (surface effect) when the polarization is up.

Test of the Coulomb-Nuclear-Interference-Polarimeter with the extracted polarized proton beam of AGS at 23 GeV/c

N. Akchurin[a], E.A. Andreeva[b], V.A. Kaplin[b], A.I. Karakash[b], Yu.F. Krechetov[c], S.B.Nurushev[b,d,1], A. Penzo[e], P. Potylitsin[c], M.F.Runtzo[b], M.N. Strikhanov[b]

[a] *University of Iowa, Iowa City, USA;*
[b] *MEPHI, Kashirskoe Avenue 31, 115409 Moscow, Russia;*
[c] *Tomsk Institute of Nuclear Physics, Tomsk, Russia;*
[d] *IHEP, 142284 Protvino, Russia;*
[e] *INFN and University of Trieste, Trieste, Italy.*

Abstract

We propose to make a precise measurement of t-dependence of the elastic pp-scattering analyzing power by using a slow extracted polarized proton beam of AGS. The measurement will be done in the Coulomb-Nuclear Interference (CNI) region at 23 GeV/c. The goal of this experiment is twofold. One part is to demonstrate that the CNI Polarimeter (CNIP) can measure the high energy beam polarization with an accuracy of less than 5 % which is essential for RHIC Spin Program. The other aim is to improve the A_N measurement with higher statistics in order to clarify the contribution of the spin flip amplitude to the analyzing power in the small momentum transfer region.

RHIC operation with polarized proton beam makes a polarimeter as an essential prerequisite for the success of the whole RHIC Spin Physics. We propose to use the CNIP for such task since it has the following advantages: 1. Its analyzing power weakly depends on the initial momentum. 2. It is an absolute polarimeter. 3. Its analyzing power is calculable with a good precision at any energy. 4. It may operate in nondestructive mode. 5. It may be used in both modes: in collider mode and in the fixed target mode. 6. If it is necessairy both particles (scattered and recoil) may be detected for clean separation of elastic scattering event.

The only measurement of the pp-elastic scattering analyzing power A_N in the CNI region was made by E704 Collaboration at 200 GeV/c [1] (see Fig.1a).

[1] *e-mail:nurushev@mx.ihep.su*

These data put a limit on the ratio of spin flip to spin nonflip amplitudes of order 10 % [2]. We suggest to improve such limit by several times making a special experiment at the AGS. We plan to use the same beam line and magnet as it was proposed in the recently approved experiment for pion polarimetry [3]. The acceptance of our apparatus permits to make a good measurement of pp-polarization at -t=0.1 (GeV/c)^2, which serves as a refering point [4].

The differential cross-section and the analyzing power of elastic pp-scattering are usually parametrized in the CNI region in the following way:

$$\frac{d\sigma}{dt} = \frac{4\pi\alpha^2(hc)^2}{|t|^2} + \frac{\sigma_{tot}^2}{16\pi(hc)^2} \cdot (1+\rho^2) \cdot e^{Bt} + \frac{\sigma_{tot} \cdot \alpha \cdot \rho}{|t|} \cdot e^{Bt/2}, \qquad (1)$$

and

$$A_N = (\sqrt{|t|}/m_p)([(\mu - 1) - 2I] \cdot \frac{z}{1+(\rho - z)^2} + \frac{2 \cdot (\rho \cdot I - R)}{1+(\rho - z)^2}). \qquad (2)$$

The parameters are: σ_{tot} - total cross-section, B - slope parameter, ρ - ratio of real to imaginary part of spin nonflip amplitude at $|t|$=0, μ - protons magnetic moment, $z = t_0/t$ with $t_0 = 8\pi\alpha(hc)^2/\sigma_{tot}$. I and R are the ratios of the imaginary and real parts of the spin flip amplitude to the spin non flip one, e.g. I=$(m_p/\sqrt{|t|})\cdot \mathrm{Im}f_{sp}/\mathrm{Im}f_{nf}$ and R=$(m_p/\sqrt{|t|}\cdot)\mathrm{Re}f_{sp}/\mathrm{Im}f_{nf}$. Some of these parameters are shown in Table 1 for 23 GeV/c, but two ones, I and R, are not yet measured at this energy. We aim to define them in this Proposal.
The experimental data from [5] at 18.9 GeV/c are used for the estimates of counting rates and expected statistical accuracy in A_N measurement. The analyzing power measured at 200 GeV/c by E704 Collaboration is presented in Fig.1a. The solid line corresponds to the prediction of the model without spin flip in hadron amplitude; the dashed line is a fit to these data by parametrization (2). The measured points are shown by the experimental error bars. Fig.1b corresponds to the analyzing power at 23 GeV/c calculated through the same way as for 200 GeV/c. above. The error bars correspond to the precisions expected after realization of this proposal. The possible precisions in parameters I and R after fulfilling such an experiment are shown in Table 1 too.
Further measurements with a well calibrated polarized target can clean up any theoretical speculation on this subject.

As it is seen from the Fig.1 the essential region for A_N measuring is $10^{-3} \leq |t| \leq 10^{-1}$ $(GeV/c)^2$. Accordingly the maximum and minimum laboratory angles subtended by detectors are defined through the relation $\vartheta = \sqrt{|t|}/p_0$, where p_0 is initial beam momentum. Therefore the accepted polar angle must be in the range 1.3 $mrad \leq \vartheta \leq 13$ $mrad$. The angle ϑ_{min} puts a limit on the beam divergence $\alpha_x = \alpha_y = \alpha_B \leq 1/3 \cdot \vartheta_{min} = 0.4$ $mrad$. Another restriction on the beam divergence comes from the desirable resolution in $|t|_{min} = 10^{-3}$ $(GeV/c)^2$. Let us take $\Delta|t|/|t| = 0.3$. Then the beam divergence must be less than $\alpha_B \leq 0.2$ $mrad$

beam momentum (GeV/c)	σ_{TOT} (mb)	slope B ($[GeV/c]^{-2}$)	ρ	Δ I	Δ R
23	39	$10.33 \pm .08$	$-.232 \pm .003$	0.03	0.009

Table 1: pp-elastic scattering parameters at 23 GeV/c.

(sigma). This value (smaller than 0.64 mrad in [3]) is taken as a basic number in following discussions. It means that the thicknesses of total materials in the incident beam and on the path of scattered particle must give a multiple scattering angle less then this number. If we don't like to put detectors in the direct beam the size of the beam, ϕ, must be limited by the following condition: $\phi = 1/3 \cdot l \cdot (\vartheta_{min} - \alpha_B)$, where l is a distance from a target to the detectors (downstream of target). For example $l = 3\ m$ for FH3 (see Fig.2), then $\phi = 1.4\ mm$ or beam size in FWHN=$1.4 \cdot 2.35 = 3.3\ mm$ instead of 10 mm, as it is now in E925 experiment [3]. The third requirement to the beam is related to its momentum dispersion. Since we would like to avoid a particle identification system and rely only on the momentum measurement of the scattered particles by magnetic spectrometer we impose the following condition on the momentum dispersion $\Delta p/p \sim m_\pi/p \sim 0.14/23 = 0.7$ %. Finally for the CNI polarimeter we like to get a beam with the following parameters: $\phi = 3.3\ mm\ (FWHM), \alpha_B = 0.47\ mrad\ (FWHM)$ and a beam dispersion $\Delta p/p = 0.6$ %. Then we use the detectors only downstream of beam, with holes for beam and detectors will not be overloaded by the beam flux. That is, we can tolerate a flux of order $2 \cdot 10^7$ pp/spill. If for some reason our requirements for the beam parameters would not be acceptable we will operate at the lower beam intensity ($I \sim 5 \cdot 10^6$ pp/spill).

As alternative scenario, we take the following layout for apparatus compatable with E925 setup (see Fig.2).

- The beam hodoscopes BH1, BH2 (x, y plane each), the scintillating counters BS1, BS2, BS3 and veto counters HV.
- The liquid hydrogen target LH 25 cm of lengths.
- The forward hodoscopes FH1, FH2, FH3 and FH4.
- The magnet (B=2 T, L=1.5 m, aperture: 30'x16').

The gross sizes of the beam hodoscopes are defined by the beam parameters and that for the forward hodoscopes are determined additionally by the useful angular

intervals: $\phi = 2 \cdot \pi$, $\vartheta = [1.3 - 13]$ $mrad$ and taken into account the multiple scattering angles. These dimensions are shown in Table 2.

parameters	beam hodoscopes		forward ho doscopes				comments
	BH1	BH2	FH1	FH2	FH3	FH4	
Location (in m from target)	-5	-1	1.5	4	6.5	11.5	
gross sizes (mm)	10	10	50	117	183	316	
pitch (mm)	1	1	1	1	2	2	
number of channels	10	10	50	117	92	158	
number of chann. after coder	4	4	6	7	7	8	

Table 2: The hodoscopes parameters for X-plane.

In order to get a resolution in $\Delta|t|_{min}/|t|_{min} = 0.3$. one needs an angular resolution of order 0.2mrad. For a distance 3 m between BH1 and BH2 it leads to the σ_x and $\sigma_y \sim 0.6$ mm or to the pitch of order of 1 mm. The $|t|$ resolution does become bigger with scattering angle and one can also vary a pitch, but this is not a practical thing at moment, later we may look at different pitches estimating the yields of particles. In order to estimate the pitches for FH3 and FH4 we require that the momentum of scattered particles must be determined with a precision $\Delta p/p \sim \Delta\psi/\psi \leq 0.7$ %. Taking into account the positions of FH3 and FH4 and the momentum kick in magnet of 0.8 GeV/c one gets a pitch of 2 mm(Table 2). More accurate results of the MC calculations support those results in Table 2, respectively, for precisions in the scattering angle and the momentum reconstruction.

The pp-elastic differential cross-section in the CNI region was taken from [5] at 18.9 GeV/c (closest to 23 GeV/c). The minimum angular band is defined by a pitch of FH2 and it is $\Delta\vartheta \sim 1$ $mm/4$ $m \sim 0.25$ $mrad$. The corresponding minimum band in $|t|$ is $\Delta|t| = |t|_{max} - |t|_{min} = p^2 \cdot (\vartheta^2_{max} - \vartheta^2_{min}) = 2 \cdot p^2 \cdot \vartheta \cdot \Delta\vartheta$. Here ϑ is a mean scattering angle. It is seen that $\Delta|t|$ depends on the mean scattering angle. The counting rate for each bin is defined through relation $N_i = \kappa \cdot I_B \cdot d\sigma/d|t| \cdot \Delta|t| \cdot \Delta\phi/2\pi \cdot n$, where $I_B = 5 \cdot 10^6$ pp/spill, $n = 8.4 \cdot 10^{23} g/cm^2$, κ is a safety factor taken as 1/3. Putting $\Delta\sigma_i = d\sigma/d|t|_i \cdot \Delta|t|_i$, we got an expected counting rate for bin i: $N_i = 1.26 \cdot 10^3 \cdot \Delta\sigma_i$ (mb). The integrated counting rates is of order 7 KHz. To estimate a running time we look at two distinct points:

1. The measurements in exact CNI region taken as $[10^{-3}, 2 \cdot 10^{-2}]$ $(GeV/c)^2$. The average analyzing power is $\overline{A_N} \simeq 2$ %; the average differential cross

section is 100 mb, so one gets a counting rate $2.39 \cdot 10^3$ events/spill. Assuming 1,000 spills/hour we can accumulate 2.39 Mevents/hour. In order to reach a precision in A_N measurement of 10^{-3} one needs $T \simeq 2$ hours measurement. Taking the efficiency of each plane of hodoscope as 0.9 and requiring the coincidences of all planes one gets a final efficiency of 0.28. Therefore the running time will be of order 6 hours.

2. We would like to measure the analyzing power at one reper point $|t| = 0.1\ GeV/c^2$, where the polarization was measured to be (3.6 ± 3) % [10]. At this point we like to reach a precision $\Delta A_N/A_N$=5 %. Taking $d\sigma/d|t| = 28\ mb$ and $\Delta|t|$=0.0073 (the upper limit of our geometry) we get 258 events/spill. Taking into account an efficiency 0.28 we expect to have 72 events/spill. Therefore the running time will be $T \simeq 17\ hours$.

We identify two types of backgrounds: $p+p \rightarrow \pi+X$ and $p+p \rightarrow p+X$. They influence on the angular and on the momentum trigger by different ways due to the sweeping magnet. Therefore we made two types of calculations: for the estimation of backgrounds on the hodoscopes FH1 and FH2 and for hodoscope FH3 and FH4. The background is negligible in the higher $|t|$ range (after sweeping magnet), but may be essential for trigger.

We plan to use the scintillating fiber hodoscopes equipped with multianode photomultipliers as a basic element of our detectors. The scintillating counters BS1, BS2, BS3 and BS4 define the beam, veto counters HV should suppress the events from beam halo. In general these counters initiate a start signal for detectors. The average time between beam particles is of order 200 ns and if the beam structure is flat one can expect a good condition for counters. If we take a resolution time as 10 ns for two coincidence signal one can expect an accidental counting rates of order 2 %. The same is true for the downstream hodoscopes staying directly in the beam (that is for part of hodoscopes). For rest of hodoscopes (out of beam region) the counting rate is less than 100 KHz including the backgrounds, so the accidental counting rates will be much lower. Beside the 0 level trigger defined by the scintillating counters the additional triggers (online) are foreseen:

1. The level "1" trigger is organized by requiring one and only one particle in each hodoscope plane (x and y). This should take a time of order 1/3 of 200 nsec, that is 60 nsec.

2. The level "2" trigger is organized by requiring that the scattered angle must be more than 1 mrad. Assuming the upper limit for counting rate as 100 KHz the decision time must be of order 1/3 of 100 KHz, that is 3 μsec. As an experience of experiment [9] showed such trigger must suppress the unscattered beam particles by factor of 200 at least.

3. The level "3" trigger requires that the beam momentum of scattered particle defined by hodoscopes FH1-FH4 (x planes only) must be in a selected region (for example 10 % around the beam momentum).

After keeping events only with signals"1" one can code the output signals and decrease the number of output channels from 437 to 36 channels giving a large gains in electronics and making faster the data analyzis which was demonstrated by experiment [9].

The following requirements must be imposed on the detector parameters:

1. The beam of big angular divergence ($\simeq$1.5 mrad) and size (FWVM$\approx$10 mm) is not suitable for making CNI experiment. So we need to put in the beam the hodoscopes BH1 and BH2 selecting the protons with high angular resolution.

2. Due to a small scattering angle of proton on the target all downstreams hodoscopes (FH1$\div$FH4) are placed also directly in the beam . Since the hodoscopes are not tolerating a high beam intensity of order $2 \cdot 10^7$ p/spill (as it was accepted in E925) one needs to decrease this intensity to level of $5 \cdot 10^6$ p/spill.

3. In oder to select the elastic scattering event one needs to cut the scattering angle and momentum of secondary particle. Therefore the pulses from hodoscopes will be used for the decision making system working in on-line regime.

The scintillating hodoscopes on the base of optical fibres and multianode photomultipliers which are manufactured by industry are most suitable for our purposes. In order to increase the efficiency of particle detection we intend to use a 2 mm (along particle direction) thick scintillator keeping a 1×1 mm^2 (cross section) fiber. By allowing the signals from adjacent counters, one can gain also in efficiency of particle detection.
As a zero level trigger the signals from counters BS1 and BS2 vetoed by pulses from veto counters will be used (see Fig.2) Pulses from each anode feed the fast amplifiers-discriminators (the number of channels are indicated in Table 2) and then the shaped signals are accepted by coders, which select only one signal from each X and Y plane corresponding to a passage of only one particle and transform the input information to a binary code. For suppression the accident rates the coders are strobed by external pulses with minimum delay. This goal is reached by using output signals from scintillation counters BS1$\div$BS4 on the fast photomultiplyers. Each coder(s) is strobed by signals from nearby scintillating counters.

Output pulses from coders(X and Y planes including), corresponding to a passage of only one particle, are used to build a 1-level trigger T1. The trigger configuration might be programmed and changed depending on an efficiency and a possible particle load, on the data acquisition speed. The same scheme produces the information for visual observations and storage in memory.

The binary information from codes are used by coordinate processors for calculation the scattering angles θ_x, θ_y and momentum p. If these angles $\theta_x = \theta_y \geq$ 1.3 mrad and the momentum difference $|P_beam - P_mean| \leq 10$ % then the Trigger 2 will be produced allowing to memorize the information on the intermediate memory which in pause between spill can be written to the main storage system.

The running plan looks like as following:

- Run with hydrogen target: two runs with 20 hours each.
- Run with scintillating targets: two runs also with 20 hours each.
- Run with carbon target (thin): two runs with 20 hours each and with one heavy huclear target: one run of order 24 hours.
- Apparatus debugging time in parasitic mode: 3 weeks.
- Final tuning of apparatus: 1 week in own beam (in real condition).

References

[1] N. Akchurin et al., Phys. Lett.B29(1989)2999 and Phys. Rev.D48(1993)3026

[2] N. Akchurin et al., Phys. Rev. D51(1995)3944.

[3] Experiment E925 at AGS, BNL.

[4] D. Dekkers et al. Phys. Rev.B137(1964)962

[5] G.G. Beznogikh et al. Nucl. Phys. B54(1973)78

[6] W.F. Baker et al., Phys.Rev.Lett 7(1961)101

[7] G. Cocconi et al., Nucl. Phys. B28(1971)341

[8] W.Guryn et al., Experiment pp2pp at RHIC, BNL.

[9] A.A. Derevschikov et al., Nucl.Instr. and Meth.108(19730381

[10] D.G. Crabb et al., Nucl. Phys.B121(1977)231

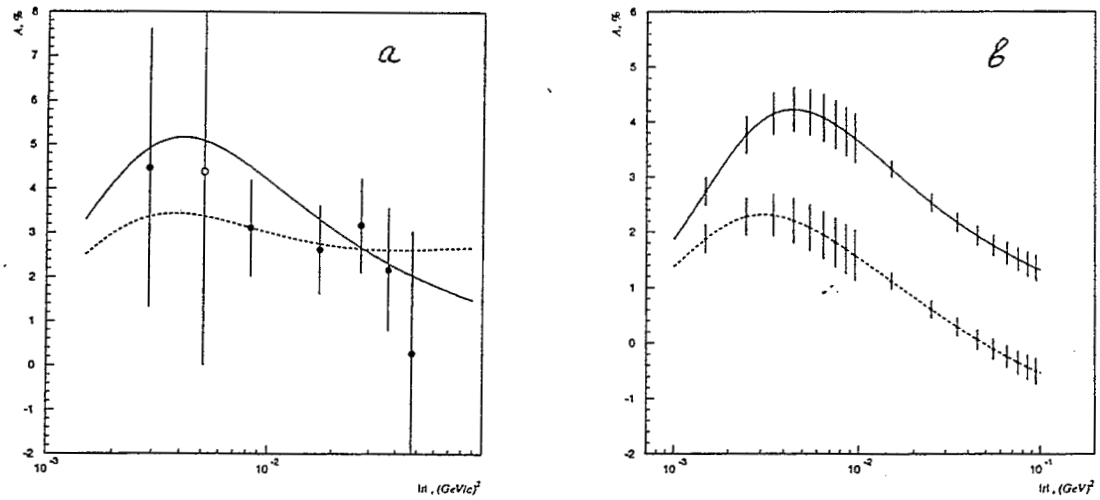

Fig.1: a) The analyzing power A_N for pp-elastic scattering at 200 GeV/c(E704 data). Solid line is a theoretical prediction with no hadronic spin-flip, dotted with spin-flip: I=0.295, R=0.044; b) predictions for 23 GeV/c for two above cases. Error bars are the expected accuracy at AGS.

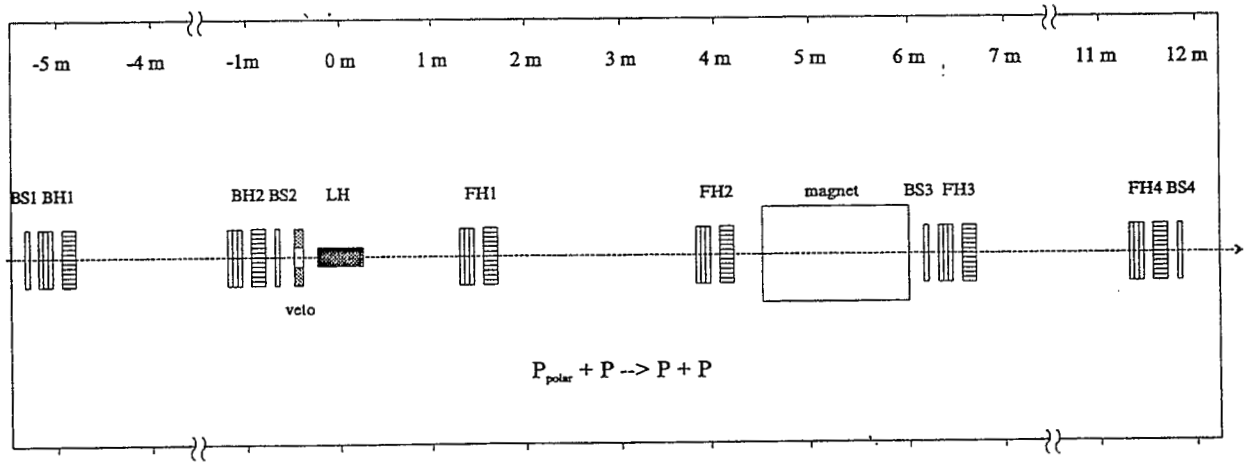

Fig.2: The experimental setup for A_N measurements at AGS at 23 GeV/c.

13 $\pi^{\pm}$ INTO 2CM X 2CM AT 10 C.M, 90°
PER 10^4 INT

Note on Calculation of Pion Production from Carbon Target

D. Underwood

Aug 3, 1998

This table comes partially just from cross section calculations using Carbon dimensions, and partially from a revised version of the pion Monte-Carlo that was used to study the pion polarimeter.

For this case, I looked at pions in 2 cm x 2 cm silicon at 10 cm to the side of the interaction point.

The beam size in RHIC vs energy, the overlap with the target etc is included.

Energy	200	200	23	200	23
Luminosity	high	high	high	low	low
(part / bunch)	2.E11	2.E11	2.E11	2.E10	2.E10
Target	5u dia.	5ug/20u	5ugx20u	5ugx20u	5ugx20u
Interactions / RHIC bunch	10^4	10^2	30	10	3
pions per interaction/NUCLEON?	6.5	6.5	4.	6.5	4.
pions per bunch crossing	65000	650	120	65	12
pions into Silicon /bunch	13.	0.13	0.024	0.013	0.0024
rate into Silicon detector	*	10^6/s	2x10^5/s	10^5/s	2x10^4/s

ABOVE DONE WITH FWHM = 500 μ
SHOULD BE 1 σ = 500 μ

CNI MULT SCATT

RMS ANGLE IN DEG

MG TRAVERSED	x .001	.002	.005	.01	.015
1	8.5	4.3	1.7	.8	.6
2	12.1	6.0	2.4	~~1.2~~	.8
3	14.8	7.4	2.9	1.5	1.0
4	17.1	8.5	3.4	1.7	1.1
5	19.1	9.6	3.8	1.9	1.3

$$\theta_{RMS} = \frac{13.6\ MeV}{p\ \beta}\ Z \sqrt{\frac{x}{X_0}}$$

$$X_{0_C} = 43\ gm/cm^2$$

RHIC proton beam polarimeter based on Primakoff effect

S.B.Nurushev (IHEP, Protvino)

I.V.Glavanakov, Yu.F.Krechetov, A.P.Potylitsin, G.M.Radutsky
(INP, Tomsk)

The Primakoff-effect polarimeter gives the beam polarization by measuring the asymmetry in coherent Coulomb dissociation [1], in which an incident proton is converted to a $p\pi^0$ system in the Coulomb field of a high-Z nuclear target. This reaction, when produced at high energy, is related to the low energy photoproduction of a π^0 from a proton [2]. The beam polarization can then be determined from the low energy data and the measured asymmetry.

The differential cross section of the process is [2]

$$\frac{d\sigma_{pA}}{dk^2 ds_1 d\varphi^* dt} = \frac{Z^2\alpha}{\pi} \left|F_A\left(k^2\right)\right|^2 \frac{1}{k^4} \frac{d\sigma_{\gamma\pi}}{d\varphi^* dt} \frac{\Delta^2}{\lambda^{\frac{1}{2}}\left(s_1, k^2, m_N^2\right)},$$

where $F_A(k^2)$ is the charge form factor of a nucleus A, t is a momentum transfer squared between the incident and scattered protons, φ^* is the azimutal angle of the pion in the c.m.s. of $p\pi^0$, k is the photon four momentum, s_1 is the invariant mass of the $p\pi^0$ system, Δ is the transverse momentum of the photon.

The asymmetry of the process has been measured for the first time with the use of the 185 GeV/c FNAL polarized-proton beam and the large asymmetry was observed in the region of Δ^2 <0.001 (GeV/c)^2 and $1.36 < s_1 < 1.52$ (GeV/c)^2 [3]. It was consistent with the analysing power of the π^0 production process deduced from the existing low energy $\gamma p \rightarrow \pi^0 p$ data.

Target asymmetry of π^0 photoproduction has been measured in the second πN−resonance region ($\sqrt{s_1}$ =1.36÷1.54 GeV/c^2) and runs in 90%. In the first πN resonance region ($\sqrt{s_1}$< 1.36 GeV/c^2) practically there are no experimental data on target asymmetry but it can be calculated by multipole analysis results. It is worth to note yet that there are discrepancies between analyses which are reflected in their predictions for unmeasured experimental observables, especially in the polarization and asymmetries. In Fig.1 target asymmetry is displayed given by BDW multipole analysis [4] as function of pion c.m. angle for three values of s_1. Little accuracy of the sparse experimental data (σ >10%) on target asymmetry of the pion photoproduction process without additional efforts to improve the situation make one to doubt of possibility to measure the absolute polarization with the needed (5%) accuracy.

In this report we consider a possibility to build the Primakoff-polarimeter for RHIC using process

$$p + Au \rightarrow \pi^0 + p + Au$$

that takes away the problem of the target design.

In first of the above mentioned range of s_1 the products of the Primakoff process are distributed in a narrow cone about the direction of the primary proton beam. Thus the significant part of scattered protons falls in an entrance window of the dipole magnet DX. We have studied an opportunity of use of the dipole magnets, located around the interaction region, as magnetic analyzers of the scattered protons momenta. This would allow essentially to lower their cost.

The calculations were executed by Monte-Carlo method. It was assumed, that the position-sensitive proton detectors are located between the magnets DX and $D0$. The azimutal acceptance of the scattered proton detector equals π. Fine segmented electromagnetic calorimeter, that measures energy and X and Y coordinates of two photons from neutral pion decay, is located between the intersection point (IP) and the magnet DX near to the last.

We consider that the event can be registered, if

a) scattered proton passes through a beampipe inside the magnet DX and deviates from the beam axis on a distance more than 20 times the root-mean-square radius of the beam size at the position of the detector;

b) the pion scattering angles are those, that the symmetrical decay photons cross an entrance calorimeter window on a distance from the beampipe external surface, that exceeds a size of a crystal (2cm).

As a result borders of kinematical area of events, that would be registered by the described above equipment, were determined in the (E_γ, θ_π) plane.

The calculations were performed for the RHIC mode of operations, at which the primary proton beam forms an angle 3.85 mrad with the magnet DXaxis. At such mode the measurement of the proton polarization by this method is possible in a greater range of proton energy.

In Fig.2 the dependence of geometrical detection efficiency from the proton energy is displayed. The reduction of the detection efficiency in the low energy region is connected to increase of a scattered proton trajectory curvature in the magnet, therefore protons can not pass the magnet. At large proton energy the detection efficiency decreases because of reduction of a pion scattering angle and corresponding reduction of the detection efficiency of decay photons. For an example, in Fig.3 the shaded regions show the disposition of the scattered protons and pions tracks relatively DX and $D0$ magnets for the initial proton energy 250 GeV.

The comparative study of the E-704 Primakoff Polarimeter tested at the Fermilab Polarized Beam Facility and the planned Primakoff Polarimeter for Polarized RHIC is presented below:

	E-704	RHIC
1. Beam mode	fixed target	colliding beams
2. Proton energy range, GeV	200	24-250
3. Heavy ion energy range, GeV/u	0.0	7-100
4. Detector acceptance :		
inv. mass of (pi0+p) system, GeV	1.36-1.52	1.36-1.52
pi0 angle in (pi0+p) system, degr.	60-120	60-120
inv. mom. transfer to proton, GeV**2	0.2-0.4	0.2-0.4
pi0 energy region in Lab. syst., GeV	25-75	35-110
proton energy reg. in Lab. syst., GeV	110-160	140-215
5. Detector resolution in Lab. syst.:		
proton angular resolution, mic.rad,	50	45
proton momentum resolution, %	2	2
pion angular resolution, mic.rad,	200	200
pion energy res.(at lowest energy), %	3	3
6. Proton beam polarization, %	~35	~70
7. Luminosity, 1/mb	1	~100
8. Polarized target asymmetry, %	65(+,-)4	65(+,-)4
9. Dilution factor, f	0.55(+,-)0.20(measured)	0.55(+,-)0.05(exp.)
10. Raw asymmetry, %	14(+,-)3(meas.)	28(+,-)3(exp.)
11. Run time for [Delta(PsubB)/PsubB]=10%, min	?	20

Due to the higher polarization and luminosity of RHIC one hopes to get a better precision than in E-704 experiment, if the systematic errors will not put the trouble. We plan to study this point in details later basing on the facts that combinations of polarized and unpolarized beams, as well as tne energy variations, switching on and off each of both beams, using different heavy ions will offer the good tools for revealing the sources of the systematic errors.

From very preliminary studies we can conclude that the Primakoff Polarimeter might be suitable for RHIC absolute and fast polarimeter. We plan to look at details of RHIC environments in order to decide should we pursue this direction of polarimetry at polarized RHIC.
We wish to thank G. Bunce, K. Imai, Y. Makdisi, N. Saito and D. Underwood for useful discussions and comments.
One of us(S.B. Nurushev) wants to thank BNL/RIKEN Center for invitation to participate in this Workshop and for financial support of such visit.

REFERENCES

[1] H. Primakoff, Phys. Rev. 152(1951)899.
[2] Yu.P. Nikitin, I.Ya. Pomeranchuk and I.M. Schmuschkevitch, Sov.Phys. JETP 41(1961)963.
[3] D.C. Carey et al., Phys. Rev. Lett. 64(1990)357.
[4] F.A. Berends, A. Donachie, and D.L. Weaver, Nucl. Phys. B4(1967)54.

FIGURE CAPTIONS:

Fig.1. Polarized target asymmetry for pi0 photoproduction process.
Fig.2. The geometrical efficiency of Primakoff detector for secondary protons taking into account DX aperture.
Fiog.3. A sketch of Primakoff Polarimeter at RHIC. V.C.-veto cnts, EMC-electromagnetic calorimeter, TD1 and TD2-tracking detectors, S1, S2, S3- scintillation cnts.

Figure 1:

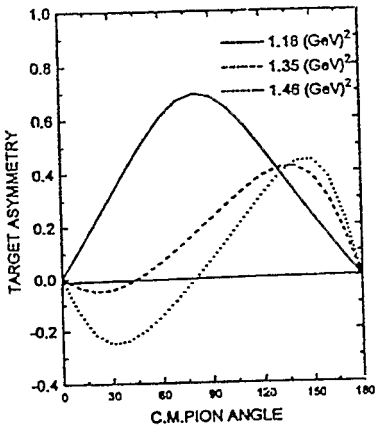

Figure 2:

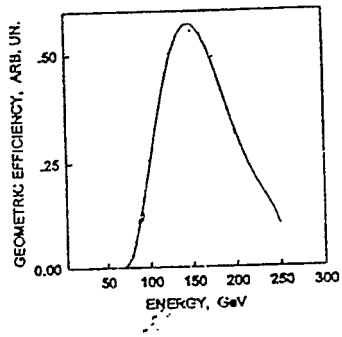

Figure 3:

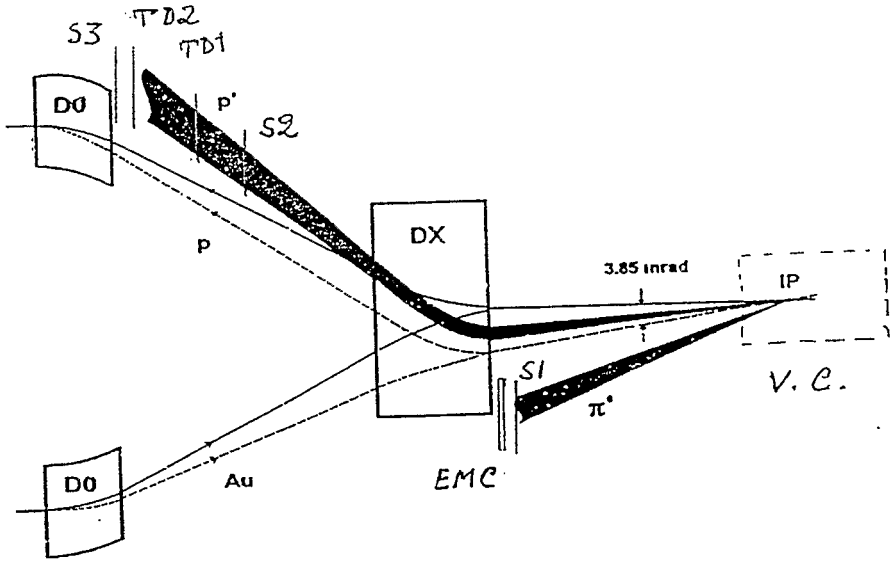

The Inclusive Neutral Pion Polarimeter for High Energy Accelerators/Colliders

A.A. Bogdanov[a], V.A. Korotkov[b], S.B. Nurushev[b], V.A. Okorokov[a], K.E. Shestermanov[b], M.N. Strikhanov[a], A.N. Vasiliev[b]

[a] - Moscow Engineering Physics Institute, 115409, Moscow, Russia.
[b] - Institute for High Energy Physics, 142284 Protvino, Russia.

Abstract

The inclusive π^o polarimeter is proposed for the oncoming polarized RHIC collider. The attractive features of such a polarimeter are - a high counting rate, a high analyzing power, a complete azimuthal coverage. It fits to the requirements to be applicable over the large energy region as well as to be readjustable for fixed target and collider modes of operations.

The inclusive charged pion polarimeter (ICPP) has been recently proposed [1]. This proposal bases on the high analyzing power, $A_N^{(\pm)}$, discovered by E-704 Collaboration at Fermilab [2]. In the current paper we propose, basing on the A_N^0 measurement by the same Collaboration [3], to apply the inclusive neutral pion polarimeter (INPP) to the RHIC environment. We argue that a high analyzing power and a large cross-section are very attractive features of such a polarimeter. Some additional advantageous are full azimuthal coverage, easy fit to the accelerator/collider environments, the background suppression by selecting the high energy threshold for the photon detection.

The results of the E704 measurement of analyzing power for the inclusive π^o production in pp-collisions at 200 GeV/c are well known [3]. The analysing power in the kinematical region

$$0.4 < x_F < 0.8;\ 0.6 < p_T(GeV/c) < 2.0, \tag{1}$$

appears to be higher than 5%. There are no additional experimental data on analyzing power A_N for inclusive π^0 in pp - collisions in the kinematical region of interest. Therefore we assume that A_N does not depend on an initial

energy and it is the same as measured by E704 [3] for the same kinematical domain (1).

The scheme of the proposed detectors is shown in Fig.1. The detectors are supposed to be installed in 2 o'clock straight section of RHIC. It is preferable to install the INPP at the RHIC Interaction Point (IP). In this case in the Fixed Target (FT) mode one can calibrate either *beam1* or *beam2* by using two symmetrically placed INPP around the IP. As an internal target we plan to use the hydrogen gas target with density about $3 \cdot 10^{13}$ $atoms/cm^2$. During the main RHIC run (colliding beam (CB) mode) one can continuously monitor beam polarizations by both INPP. There is a limitation $\pm 7m$ in free space around IP which may influence on the detector's position. The INPP consists of two Electro-Magnetic Calorimeters EMC1 and EMC2. EMC1 has a hole of diameter $D_1 = 60$ mm defined by a vacuum pipe (V.P.). EMC2 is placed either in front or in rear part of the DX magnet and aims to cover a hole in EMC1 completely. DX magnet presents one of the bending magnet belonging to accelerator/collider and placed just at the end of straight section. In such a way the EMC1 and the EMC2 together present one integrated EMC covering whole azimuthal angle and subtending with high efficiency the useful kinematical interval (4). The central part of EMC, that is EMC2, can be removed from the beam and put behind DX magnet. Therefore it is not radiated by the direct beam and one may hope that the charged secondary particles will not reach it due to a strong magnetic field of DX. The combination of two calorimeters offers some flexibility for an on-line scheme of the INPP as we can see later.

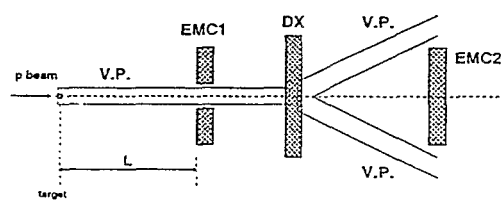

Figure 1: Possible layout of the inclusive neutral pion polarimeter.

For separation photon shower from charged particle shower each EMC1 and EMC2 are supplied by scintillating hodoscopes installed in front of them (they are not shown in Fig.1).

The experimentally measured asymmetry, ϵ, depends on the beam polarization, P_B, the analyzing power of the reaction, A_N, and the purity of selected π^o sample, $d = S/(S+B)$, where S means the number of π^o mesons produced in region (1) and B presents the backgound contribution, in the

following way:

$$\epsilon = A_N \cdot P_B \cdot d. \tag{2}$$

From this relation one can extract the magnitude of P_B and estimate its dispersion

$$\sigma^2(P_B) = \frac{1}{(A_N \cdot d)^2 \cdot \sigma_s \cdot \mathcal{L}}. \tag{3}$$

Here, σ_s is the inclusive π^o cross section integrated over region (1), $\mathcal{L} = L \cdot T$ is an integrated luminosity, L is a machine luminosity and T is a running time. As it is seen from the above relation to reach a minimum dispersion one needs get a maximum value of the factor of merit

$$M = (A_N \cdot d)^2 \cdot \sigma_s. \tag{4}$$

In further discussion we limit ourself to the case when each of the two photons is detected by the different calorimeters. Such combination is very important, since it may result in building an on-line INPP. The reason is that we can make a coincidence of signal S1 from EMC1 and S2 from EMC2. The optimization of the INPP parameters was made by looking for the maximum of the factor of merit, M, as a function of two variables: a) a distance L from IP to EMC1 and b) photon detection threshold E_γ^{min}. In the latter case both detector thresholds were put the same for simplicity. The diameter of the EMC1 hole was taken as $D_1 = 6cm$. The inclusive π^o production in the reaction $p + p \rightarrow \pi^o + X$ for the energy region of interest was studied using Monte-Carlo program FRITIOF-7.02 [4].

Fig.2 presents the results of the optimization calculations for different scenarios of the RHIC polarimetry: FT and SB modes at top (250 GeV) and injection (23 GeV) energies. One can see that in all cases there is a clear maximum in M versus L and the shape of the curves resembles a gaussian. The curve falls down on the left side of the maximum due to a decreasing analyzing power, while on the right side of the maximum it drastically drops because of a sharp decrease of the useful cross section, σ_s. The magnitude of M strongly depends on the threshold photon energy. The position of maximum weakly depends on this cut. The maximum threshold energy was taken in accordance with the condition (1) in order to avoid a cut of the useful events. Comparison of the FT with the CB modes shows that the maximum position practically does not depend on the mode of RHIC running.

Table 1: **The Inclusive Neutral Pion Polarimeters Parameters.**

E, GeV	250	250 + 250	23	23 + 23
L, m	5.6	5.5	0.5	0.5
S/S+B	0.90	0.90	0.90	0.90
σ_s, μ b	12	10	15	13
n, counts/sec	156	200	195	260
A_N, %	10	10	10	10
$N_{5\%}(10^4)$	9	10	10	10
$T_{5\%}$, min	10	10	9	7
D_{out} EMC1,mm	360	360	300	300
D_{out} EMC2,mm	300	300	800	800

In passing from the top energy to the injection energy, $E_{inj} = 23$ GeV, one sees a change in the optimum position of EMC1. The change is roughly proportional to the energy variation and this fact is understandable through the kinematics of the production and decay of π^0 mesons. The shape of the figure is not changing almost. Therefore we may conclude that the INPP can be effectively used in the FT and the CB modes of RHIC, as well as at top and injection energies. Fig.2 present also dependences of some other useful observables on the distance L: the ratio of signal S to signal plus background (S+B), the useful cross section for accepted cuts σ_s, and the expected analyzing power. If we want to reach of 5% precision in the beam polarization measurement we can calculate now all parameters by using numbers from Fig. 2. The results of the calculations are presented in Table 1. The last two rows of the Table 1 present the expected outer diameters of calorimeters which permit to accept 99% of photons from π^0 decay. As it is seen from Table 1 the INPP parameters in the CB mode are close to that in the FT mode, but the time of the polarization measurement is much shorter due to the higher luminosity of the colliding beams. The gross sizes of the calorimeters are practically the same as in the FT mode. The main parameters of the INPP at the injection energy of 23 GeV are practically the same as at the colliding mode but two changes are obvious: one must put the EMC1 very close to the IP and make bigger the gross size of the EMC2. It is obvious

that the INPP can measure the beam polarization at RHIC in the whole range of the beam energy and in both modes of operation.

As a conclusion, we propose to use the INPP at RHIC for the following reasons: i) its high analyzing power, A_N; ii) its large production cross section, σ_s. As a result the INPP has a high factor of merit, M $= (A_N)^2 \cdot \sigma_s$; iii) it fits well to the RHIC environment and it can be easily used in FT as well as in CB modes; iv) it serves as a local polarimeter; v) it is a "transparent" polarimeter allowing to make a continuous control of beam polarization; vi) it may be used as on-line polarimeter; vii) it is less sensitive to the background due to the high energy threshold for photons; viii) the technique (electromagnetic calorimeters) is robust and reliable.

One can stress the following advantageous of INPP over ICPP: i) full azimuthal coverage. This allows to measure any transverse component of beam polarization in the same run; ii) practically full coverage of useful x_F range; iii) practically full coverage of useful p_T range; iv) due to use of the electromagnetic calorimeter the INPP becomes more preferable with growth of energy than the ICPP; v) no necessity for a magnetic spectrometer and extra particle identification. EMC fulfils all these functions itself.

There are two open problems which must be solved in order to make the INPP as a real polarimeter: a) an absence of the precise experimental data on $A_N(\pi^0)$ in the energy range of interest, and b) necessity to demonstrate in experiment that an INPP can be operated as an on-line polarimeter.

References

[1] Mariam F.G. et al.- In: Proc.of 12th Intern. Symp. on High-Energy Spin Physics, September 10-14, 1996, Amsterdam, The Netherlands, p.797.

[2] Adams D.L. et al., Phys.Lett., B264, 462(1991).

[3] Adams D.L. et al., Z.Physik C, 56, 181(1992).

[4] Hong Pi, *Comp. Phys. Comm. 71, 173(1992).*

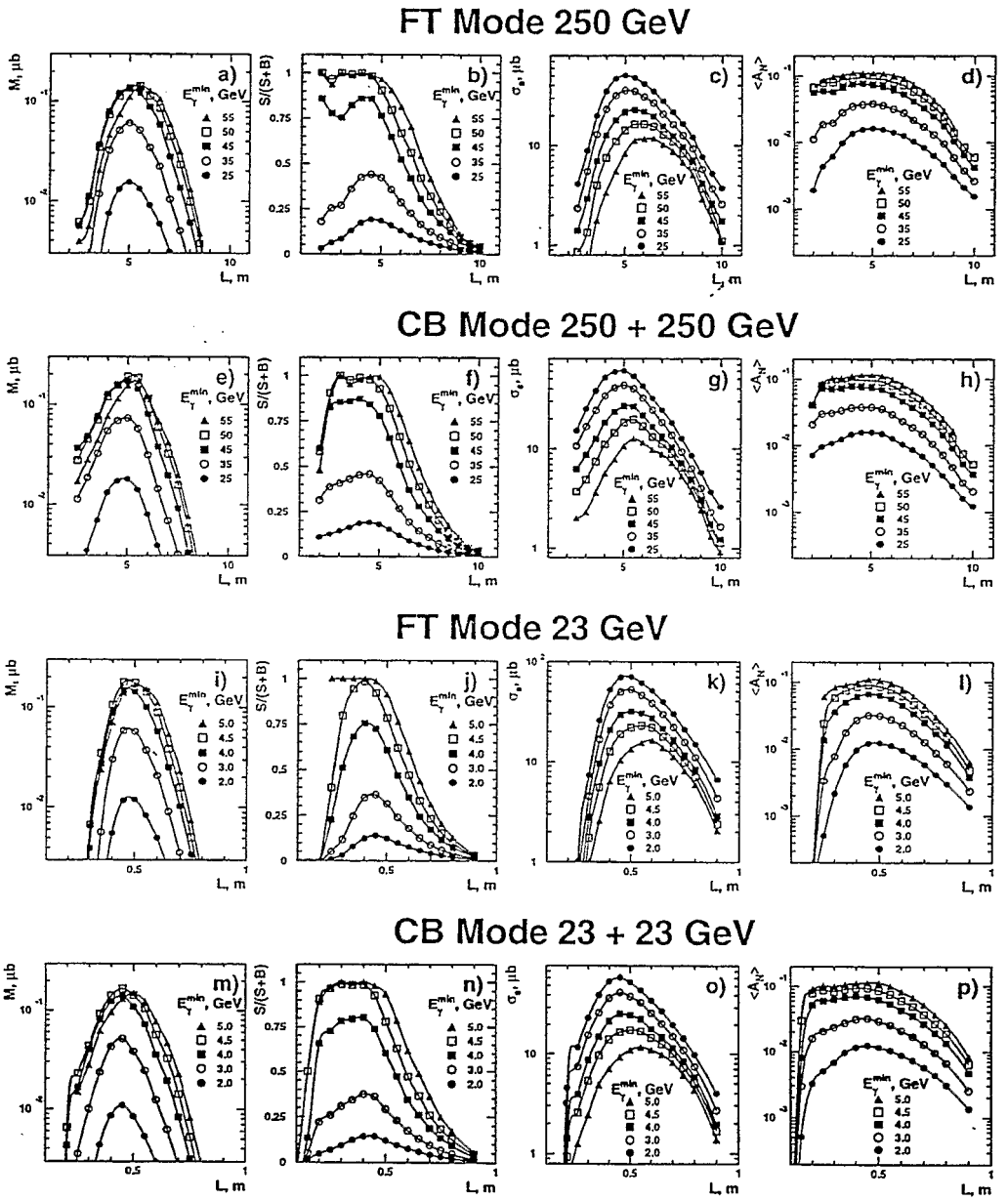

Figure 2: Shown as a function of EMC1 position, L, are: a,e,i,m) figure of merit, b,f,j,n) the signal significance, c,g,k,o) the integrated useful cross section for inclusive π^0 production, d,h,l,p) the average analyzing power. The curves are labeled by threshold energy, E_γ^{min}, for detection of decay photons in EMC1 and EMC2.

Summary of Working Group on
PP2PP and RHIC Polarimetry

M. Conte
Dipartimento di Fisica and Sezione INFN di Genova,
Via Dodecanneso 33, I-16146 Genova - Italy

W. Guryn
RHIC Project, Brookhaven National Laboratory,
Upton, NY 11973 - USA

A. Penzo
Sezione INFN and Dipartimento di Fisica di Trieste,
Via A. Valerio 2, I-34127 Trieste -Italy

Abstract

Considering recent conceptual progress on polarimetry at RHIC we have developed a scheme to use PP2PP for the absolute measurement of beam polarization in RHIC. This scheme involves a jet target and a recoil detector in addition to the equipment proper to PP2PP for detection of scattered protons. Three regions of four-momentum transfer $-t$, where the analyzing power A_N in pp elastic scattering is appreciably different from zero, are considered here: the CNI region [$10^{-3} < |t| < 2\ 10^{-2}$ (GeV/c)^2] and the regions of small - $|t|$ [$0.1 < |t| < 0.4$ (GeV/c)^2] and medium - $|t|$ [$0.8 < |t| < 1.4$ (GeV/c)^2]. The jet target and the apparatus for the measurement of recoil protons are described, including a recoil polarimeter. The rates and attainable precisions for the beam polarization absolute calibration are discussed.

Main goals of polarimetry at RHIC

Polarimeters at RHIC have to accomplish two fundamental tasks for the polarized collider project:

a) - during the commissioning of polarized beams in the momentum range 25 - 250 GeV/c, the beam polarization P_B has to be measured with 10-15% relative (statistical) error in few minutes,

b) - absolute calibration measurements of the beam polarization should be performed at top momentum 250 GeV/c (and other relevant energies) with an absolute polarimeter at a level better than 5% of precision;

In the first case a (relative) high-rate polarimeter would be sufficient, provided it has sizable analyzing power throughout the full momentum range, even if not known at the desired 5%. Ideally the absolute polarimeter should be capable of providing the beam polarization with the required precision in a typical time of 10 hours, corresponding to one machine fill of stored protons, in such a way of providing the beam polarization for each physics run.

Self- calibration method

Elastic pp scattering is by far the process whose asymmetry A_N has been measured most extensively between 25 and 300 GeV/c (28, 45, 50, 75, 100, 150, 200 and 300 GeV/c). At small |t|-values [$0.1 < |t| < 0.4$ $(GeV/c)^2$] the asymmetry is positive and, although decreasing with increasing energy, it maintains positive values of some percent up to the highest measured energies; in the CNI region [$10^{-3} < |t| < 2\ 10^{-2}$ $(GeV/c)^2$] the asymmetry is estimated (and measured by E-704) to reach +5%, almost independent of energy. At momenta larger than 40 GeV/c and larger |t|-values [$0.8 < |t| < 1.4$ $(GeV/c)^2$] it shows negative asymmetries close to - 10%. Three kinematical regions of pp elastic scattering can be considered:

- CNI [$10^{-3} < |t| < 2\ 10^{-2}$ $(GeV/c)^2$]
- Small-|t| (ST) [$0.1 < |t| < 0.4$ $(GeV/c)^2$]
- Large-|t| (LT) [$0.8 < |t| < 1.4$ $(GeV/c)^2$]

PP2PP experiment at RHIC has access to all these elastic scattering regions in collider mode (and for the forward scattered protons in fixed target mode). A jet target in the PP2PP intersection (with a recoil detector) would allow measurements in the last mode also.

The simple kinematical configuration of the elastic process in the CNI region is well suited for a real-time selection of the events by means of fast on-line processors.

Present uncertainties on contributions by hadronic spin-flip amplitudes amount to 8-10% of the CNI analyzing power. To reach a 5% (absolute) precision in beam polarization the analyzing power of the polarimeter has to be calibrated to better than this level. This can be achieved with measurements off a polarized jet target (P_T _ 95±3%).

In the CNI region the polarization is expected to reach about 5% and measurements with a polarized jet will fix the degree of uncertainty on the spin flip amplitude to 3-5% of the analyzing power in less than 1 day per energy, using the same apparatus described for the CNI measurements.

Rate estimates

In this section an outline of the recoil detector kinematical coverage and resolutions is given, as well as estimates of the rates and statistical precision for pp elastic scattering in the three regions listed above for the FT measurements with a jet target.

CNI region

The kinematical parameters for the CNI region [$10^{-3} < |t| < 5\ 10^{-2}$ (GeV/c)^2] are listed in Table 3.

Table 3: Kinematical parameters for pp elastic CNI			
$\|t\|$ (GeV/c)^2	T_R (MeV)	Θ_R (mrad)	ToF (0.5 m) (nsec)
0.001	0.53	17.4	50
0.005	2.66	34.8	25
0.01	5.33	52.3	15
0.05	26.6	113.4	7

Θ_R is measured from the axis perpendicular to the beam line through the jet. The range of protons in Si is 30 μm at 1 MeV and 250 μm at 5 MeV. The estimated resolutions with Si drift detectors are respectively:

$$\Delta T_R = \pm [0.04 + 0.004\ T_R^2]^{1/2}\ \text{(MeV)}$$
$$\Delta\Theta_R = \pm 6\ \text{mrad}\ [= (\sigma_{jet} / l) = 3\ \text{mm} / 500\ \text{mm}]$$
$$\Delta\text{ToF} = \pm 0.8\ \text{nsec}$$

The rate is estimated: $dN/dT = L \times \langle\sigma\rangle \times \alpha = 3\ 10^{32} \times 3\ 10^{-27} \times 0.1 = 8\ 10^4$ /sec and attainable precisions are listed in Table 4.

Table 4: Estimates of precision and rates in the CNI region				
$\Delta P_B/P_B$ (*)	$\Delta A_N/A_N$ (*)	$\Delta\varepsilon/\varepsilon$	$N_{ev.}$	T(sec)
0.05	0.04	0.03	$2.5\ 10^6$	31 (125)
0.1	0.08	0.06	$6.3\ 10^5$	8 (32)
0.15	0.1	0.11	$1.9\ 10^5$	2.5 (10)

(*) Target value for $\Delta P_B/P_B$ and assumed value for $\Delta A_N/A_N$.

Rates are sufficiently high to meet the following conditions:

- less luminosity by a factor 10-100 (either lower beam intensity or jet density) still compatible with measurement times of few (2-5) minutes;
- smaller beam polarization $P_B = 0.4 - 0.2$;

- bunch-to-bunch polarization monitoring.

A polarized jet of 10^{12} atoms/cm^2 would give about 600 events/sec, thus taking about 1.5 hours for a 5% calibration at full beam intensity.

Small - | t | region

Kinematical parameters for small-|t| [$0.1 < |t| < 0.4$ (GeV/c)^2] are listed in Table 5.

Table 5 : Kinematical parameters for the small- | t | region				
| t | (GeV/c)^2	T_R (MeV)	p_R (MeV/c)	Θ_R (degrees)	ToF (1.5 m) (nsec)
0.1	50	320	9.5	15.5
0.3	150	570	16	9
0.5	250	750	21	7

Θ_R is measured from the axis perpendicular to the beam line through the jet. A dE/dx scintillation counter precedes the setup consisting of the polarimeter MWPCs and hodoscope counters for time-of-flight. The expected resolutions are:

$\Delta T_R = \pm 0.08\ T_R$ (MeV) [from dE/dx]

$\Delta\Theta_R = \pm 2$ mrad [$= (\sigma_{MWPC} / l)$ _ 1mm/ 500 mm]

ΔToF = ± 0.5 nsec

Rates are given by $dN/dT = L \times \langle\sigma\rangle \times \alpha = 3\ 10^{32} \times 2\ 10^{-27} \times 0.2 = 1.1\ 10^5$ /sec.

Table 6: A_N precision and rates for small- | t | region				
$\Delta P_B/P_B$ (*)	$\Delta A_N/A_N$ (*)	$\Delta\varepsilon/\varepsilon$	N	T(sec)
0.05	0.04	0.03	$5.6\ 10^6$	50 (275)
0.1	0.08	0.06	$1.4\ 10^6$	13 (65)
0.15	0.1	0.11	$4.2\ 10^5$	4 (21)

(*) Target value for $\Delta P_B/P_B$ and assumed value for $\Delta A_N/A_N$.

Medium - | t | region

Kinematical parameters for medium-|t| [$0.8 < |t| < 1.4$ (GeV/c)^2] are listed in Table 8.

Table 8 : Kinematical parameters for the large- | t | region				
| t | (GeV/c)^2	T_R (MeV)	p_R (GeV/c)	Θ_R (degrees)	ToF (1.5 m) (nsec)
1.	500	1.12	31	4.5
1.2	600	1.25	33	" "
1.4	700	1.37	34.5	" "

The rate is estimated : $dN/dT = L \times \langle\sigma\rangle \times \alpha = 3\ 10^{32} \times 0.3\ 10^{-30} \times 0.2 = 17$ /sec and attainable accuracies are listed in Table 9. Here the rate limitation does not come not from DAQ, but from the pp yield itself.

Table 9 : Estimates of rates and precision for the large-|t| region				
$\Delta P_B/P_B$ (*)	$\Delta A_N/A_N$ (*)	$\Delta\varepsilon/\varepsilon$	N	T(min)
0.05	0.03	0.04	$2\ 10^5$	200
0.05	0.04	0.03	$3.5\ 10^5$	340
0.1	0.04	0.1	$3.2\ 10^4$	30
0.1	0.08	0.06	$8.9\ 10^4$	90
0.15	0.04	0.14	$1.6\ 10^4$	15
0.15	0.1	0.11	$2.6\ 10^4$	25

(*) Target value for $\Delta P_B/P_B$ and assumed value for $\Delta A_N/A_N$.

In this case a polarized jet of 10^{12} atoms/cm^2 would give about 0.1 event/sec, thus taking about 300 hours for a 5% calibration at full beam intensity.

Measurement and calibration strategy

The results of this analysis can be summarized as follows:

- in CB mode PP2PP will measure the CNI region with L _ 10^{31} cm^{-2} sec^{-1} [standard (β^*= 10 m) optics] with coarse |t| resolution. In these conditions statistics sufficient for $\Delta P_B/P_B$ = 10-15% will be obtained in about 5 minutes. This accuracy matches uncertainties on theoretical value of CNI asymmetry. *Certainly a viable and cost effective option for day-one relative polarimeter.*

- FT measurements with unpolarized jet and L= 3 10^{32} cm^{-2} sec^{-1} will allow initial RHIC beam polarization measurements with a statistical precision of $\Delta P_B/P_B$ = 10-15% in times less then 1 min. This level of statistical accuracy can be achieved in short runs also with luminosities lower by an order of magnitude and/or beam polarization as low as 20%.
  MC jet available: also a low-impact option for day-one relative polarimeter.

- In the second case the analyzing power can be absolutely calibrated with a polarized jet (just few hours for replacing the MC head with the PAB source in the jet assembly) and the same apparatus; with L _ 2 10^{30} cm^{-2} sec^{-1} the calibration will take about 1.5 hours per energy for a 5% accuracy.

The jet polarimeter comes for free and with its own built-in calibration.

The polarized atomic beam source is well on its way in development and construction, the main practical problem being the full integration in the existing unpolarized jet assembly. Another calibration procedure has however been devised in reserve and for cross-check, that uses only an unpolarized jet and a recoil polarimeter. For larger |t| values this method will provide a 5% calibration in about one week per energy; at low |t| values the necessary time would be less then 1 hour, but with small analyzing power.

Upgraded Setup for PP2PP

The forward scattered particle detection at large angles is limited by the DX magnet acceptance, that transmits up to |t| _ 1.4 $(GeV/c)^2$ for 250 GeV/c beam momentum, but cuts drastically the acceptance for lower beam momenta at an angle close to 5.4 mrad. The luminosity $L = 10^{31}$ cm^{-2} sec^{-1} ($\beta^* = 10$ m) for a 4.3 10^6 sec run (100 days at 50% efficiency) would provide a 1% error on a double-spin asymmetry in a bin $\Delta t = 0.2$ $(GeV/c)^2$ for a cross-section of 10^{-33} $cm^2/(GeV/c)^2$, corresponding to |t| _ 4.5 $(GeV/c)^2$ in the energy range of RHIC. With a jet target (FT mode) the luminosity $L = 3\ 10^{32}$ cm^{-2} sec^{-1} would give access, in the same conditions, to cross-sections close to 3 10^{-34} $cm^2/(GeV/c)^2$, corresponding to |t| _ 7 $(GeV/c)^2$ at 200 GeV/c momentum.

Conclusions

This conceptual and feasibility study shows that the challenge of measuring the polarization of the RHIC polarized proton beams with an absolute accuracy better than 5% can be fulfilled in principle by exploiting the basic symmetry properties of the pp elastic scattering process, providing a self-calibration of the analyzing power A_N of this process at any desired momentum in the RHIC range of operation, by specific measurements with a (polarized) jet target and/or recoil polarization analysis.

The project described here builds upon extensive R&D work of the INFN groups (Genova /Trieste) on (polarized) jet technology and real estate from previous experiments, experience with high energy (WA6, E-704) and low energy (Saturne, SIN, LEAR) polarimetry, and integration with the PP2PP scattering apparatus.

The price-tag on a brand-new jet target system being close to 800 k$ (or higher), the solution outlined here represents a cash saving of at least about 500÷ 600 k$. It also makes an expeditious installation plan possible, with a reliable schedule (target year 2000) or earlier.

The luminosity is given by: $L = N_B \times n_B \times n_T \times l_T \times q \times f_o$

Typical MC J-T parameters	
Total gas input (@ 1 bar)	20 mbar . l/s
Nozzle diameter	0.07 mm
Nozzle temperature	28 K
Distance nozzle - beam	25 cm
Jet density (n_T)	$3\ 10^{14}$ atoms/cm^3 (_ $5\ 10^{-10}$ g/cm^3)
Jet sectional area ($w \times l_T$)	Ø _ 5.4 mm
B -T overlap factor (q)	typically _ 1
Target thickness (t_T)	$1.5\ 10^{14}$ atoms/cm^2
Background gas (n_b)	< $2\ 10^9$ atoms/cm^3
Residual pressure bump	$8\ 10^{-8}$ mbar (_ 5 m)

$L = 2\ 10^{11} \times 120 \times 1.6\ 10^{14} \times 79\ 10^3 = 3\ 10^{32}\ cm^{-2}\ s^{-1}$

For a polarized atomic beam jet (assuming a target thickness of $1\ 10^{12}$ atoms / cm^2):
$L = 2\ 10^{11} \times 120 \times 1\ 10^{12} \times 79\ 10^3 = 1.9\ 10^{30}\ cm^{-2}\ s^{-1}$

Components and cost estimate

Stage/ Element	Type/ Manufacturer (*)	Element Value	Stage Cost k$	Existing parts	Net new cost k$
Source stage:			168.		
Upper chamber	AISI316L steel (CSC)	13.		13.	
Nozzle/Skimmers + frame	CERN, CSC, Beam Dynamics Inc.	6.		6.	
Cold head	RG20	8.		8.	
Refrigerator	RG 1240	12.		12.	
Turbo pumps	1 Turbovac 1000 2 Turbovac 360	85.		60.	25.
Primary pumps	2 Trivac-B D25B 1 Ruvac WSU500 1Trivac-B D40B	28.		10.	18.
Vacuum gauges	3 ionization IE 220 1 Pirani TR205	16.		16.	
Target Stage:			109.		

Scattering chamber	AISI316L steel (CSC)	9.		9.	
Fast Valves	VAT Ø 25 mm	14.		14.	
Turbo pumps:	2 Turbovac 1000	60.		30.	30.
Primary pumps	2 Trivac-B D25B	14.		14.	
Vacuum gauges:	4 IE220	12.		12.	
Sink Stage:			140.		
Dump chamber	AISI316L steel (CSC)	12.		12.	
Cold head+compr.	RG20	14.		14.	
Turbo pumps:	1 Turbovac 1000 2 Turbovac 360	85		60.	25.
Primary pumps	3 Trivac-B D25B	20.		20.	
Vacuum gauges	3 IE220	9.		9.	
Infrastructure			71.		
Accessories	Conflact flanges, etc.	14.		14.	
Flowmeters	2 Teledyne-Hastings 3 Bronkhorst F211C	6.		6.	
Vacuum gauges	3 Pirani TR205	6.		6.	
Electropneumatic valves	6 DN25KF	5.		---	5.
Cables, pipes		12.		4.	8.
Support structure		8.		8.	
Controls	PMC(ORSI)	20.		20.	
Total			488.		111.

(*) All UHV components are manufactured by Leybold-Heraeus (L-H), unless specified.

The additional parts and relative costs for integrating the polarized atomic beam source into the system are listed in the next Table.

Main parts for the polarized atomic beam source and costs						
Stage/ Element	Status			Element Value	Existing parts	Net new cost
	R&D	Design	Construction			
Dissociator	X	X	in progress	14	60%	6
Sextupoles	X	X	done	36	100%	---
Extra pumps	to be purchased			80	40%	48.
RF transitions	X	X	in progress	20	50%	10.
Total for PABS				150		64.

The total new investment is 175 k$ for a 663 k$ worth of equipment (overheads, manpower and contingency not included).

RHIC POLARIMETRY AND PP2PP

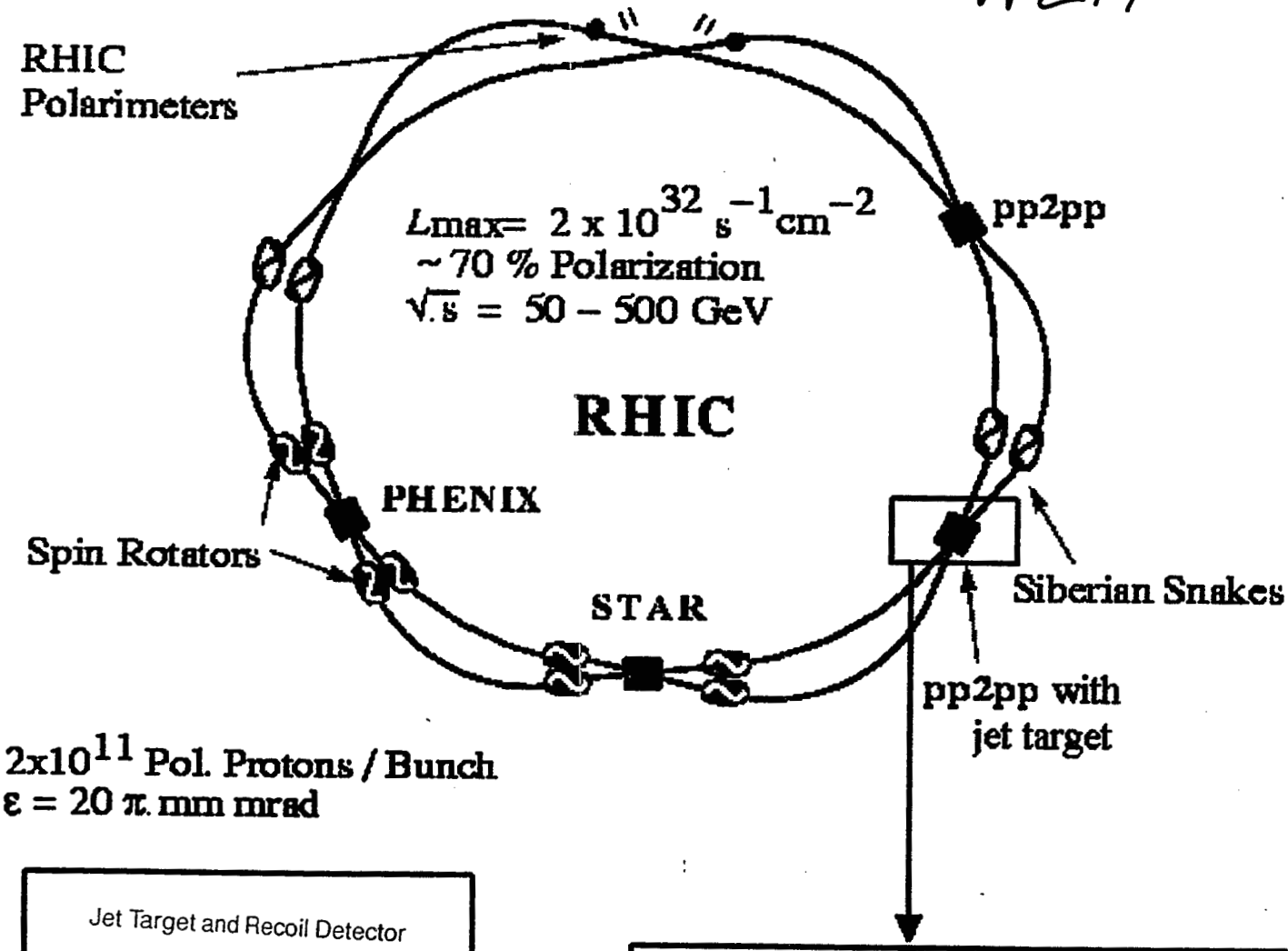

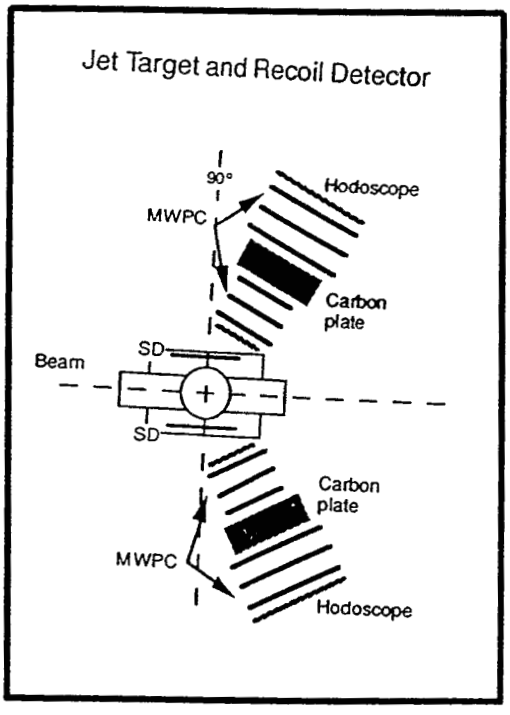

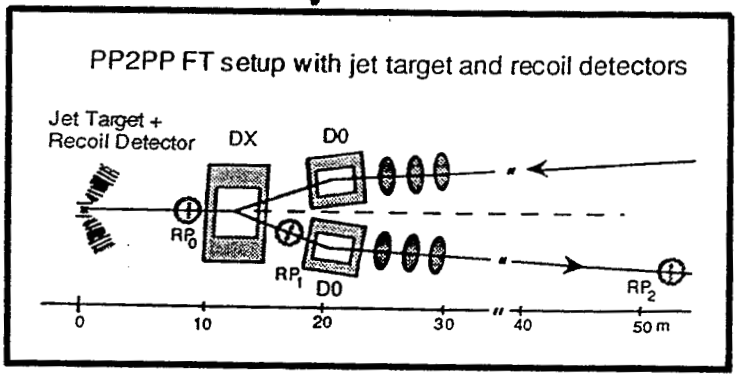

Current Design of Polarimeter Area

Haixin Huang

Brookhaven National Lab

Abstract

This presentation summarizes the current design of the year-one pion polarimeter which utilizes five C-magnets and four existing hodoscopes used in E925. This polarimeter measures beam polarization by measuring the asymmetry of π^- inclusive production. It will cover the year-one commissioning energy range 23-100GeV. The first three magnets will be movable transversely to cover the energy range. The measuring time is about 1 minute at the injection energy for the year-one intensity and the emittance growth is about 5%. The target is a 5μ m/cm^2, 10μ m wide carbon ribbon and will be shared with CNI polarimeter. This kind of target has been used at IUCF in the CE75 experiment. With the separation of angle (given by the position at hodo1) and momentum (given by the difference between positions at hodo3 and hodo4), the matrix logic can be used as a clean trigger to eliminate the low analyzing power. A LeCroy 2367 with 3MByte memory, and internal logic to trigger with lower x_F and p_T cut would allow 0.5 million events to be stored by using two units.

Components of the Pion Inclusive

Polarimeter

- Carbon Ribbon Target.
  5 - 10 μgm/cm^2 0.01 mm wide
  plus a thin window in the vacuum box for pions to exit

- Five Dipole Magnets.
  first three are movable, others are fixed

- Four Scintillator Hodoscopes.
  modified from BNL E925 and FNAL E704
  6 mm wide scintillators and 2 mm wide segments

#1	X plane	8-10 cm $\times$ 4 cm
#2	X planes	3-4 cm $\times$ 5 cm
#3	X,Y planes	3-4 cm $\times$ 7 cm
#4	X,Y planes	10 cm $\times$ 10 cm

- Three Trigger Scintillators Near Hodoscopes #2-4.

- Optional Cerenkov Counter.
  to identify pions from kaons and protons

- Hadron Calorimeter. (Probably from E814)
  (borrow existing modules?)

- Luminosity Monitor Telescopes.
  (three small scintillation counters per telescope, mounted above and below the beam looking at the carbon ribbon target)

- Cables, HVPS, Electronics.

- Data Acquisition Hardware.
  including computer and associated software

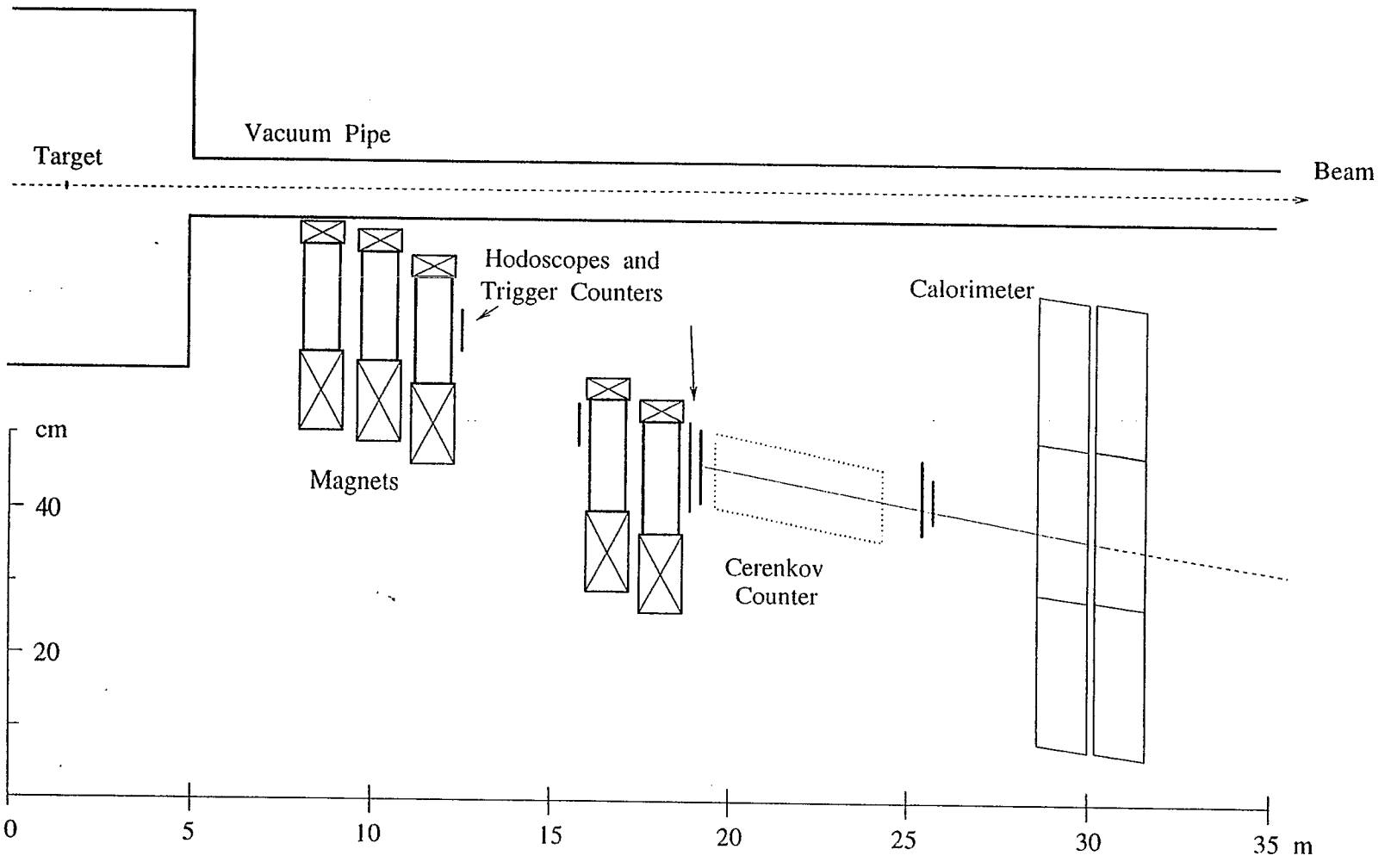
Vacuum Pipe
Target
Beam
Hodoscopes and
Trigger Counters
Calorimeter
cm
40
20
Magnets
Cerenkov
Counter
0
5
10
15
20
25
30
35 m

Parameter Table of Year-one pion Polarimeter

	Trgt	M1	M2	M3	M4	M5
Longitudinal Positions (m)	1.5	8.5	9.75	11.0	16.0	17.25
Length (m)		1	1	1	1	1
Full Gap (cm)		3.7	4.3	4.9	7.8	7.8
Current (A)		920	1070	1230	1950	1950
Power (kW)		41	56	74	185	185
Transverse Positions (cm):						
23 GeV/c		31	32	35	29	33
50 GeV/c		16	17	20	29	33
75 GeV/c		11	12	15	29	33
100 GeV/c		8	9	12	29	33
Settings:						
23 GeV/c		1	1	.15	−1	−1
50 GeV/c		0.36	0	0	−1	−1
75 GeV/c		−0.15	−0.2	−1	−1	−1
100 GeV/c		−1	−1	−1	−1	−1

Table 1.1: Parameters for the polarimeter gaps and transverse positions. The transverse positions of the dipoles are with respect to the beam pipe center. The longitudinal positions of the dipoles are with respect to the end of Q4. The magnet settings are in fractions of the TOSCA design fields in Fig. 1.5.

	p_π (GeV/c)	$\delta\Omega$ (μster)	$\delta\sigma$ (nb)	T_{meas} (sec)	$\Delta\epsilon_x$ ($\Delta\epsilon_y$) (π mm mrad)
@100 GeV →	60	6.4	231	1.9	0.0028 (0.0032)
@23 GeV →	13.8	26.1	49.7	~ 18	0.22 (0.33)

Table 1.2: Acceptance and rate estimates for the pion polarimeter. Also includes expected emittance dilution due to multiple scattering for collecting 10^4 pions. The following parameters were assumed: $\epsilon_N = 20\pi$ mm mrad, protons/fill = 120 bunches at 2×10^{11} protons/bunch, $d_f = 2.5 \times 10^{-8}$m, $p_T = 0.8$ GeV/c, $\delta p/p = 0.1$

Schedule

The short-term schedule is:

- Feb. 1999 E925 run with liquid hydrogen
- Mar., April 1999 install some polarimeter hardware
- Mar.–Aug. 1999 modify E925 hodoscopes
- Aug., Sept. 1999 install additional polarimeter hardware
- after Oct. 1999 first polarized runs in one beam

After the first polarized runs, the polarimeter performance will need to be evaluated and perhaps changes or improvements made. A polarimeter in the other beam will need to be constructed before the first data taking with both beams polarized.

E880 Status

Mei Bai

Indiana University

To accelerate polarized protons in the AGS to the RHIC injection energy (about 25GeV), about 41 imperfection spin resonances and 7 intrinsic spin resonances will be encountered. The current scheme is to use a 5% solenoid partial Siberian snake to correct all the imperfection resonances and use an RF dipole with horizontally oriented magnetic field to overcome the 4 strong intrinsic resonances while the other three are weak ones and would not cause significant polarization loss under the normal AGS acceleration rate. In the latest polarized proton acceleration experiment (E880), we achieved about 0.51polarization at $G\gamma = 41.5$ and about 0.37 polarization at $G\gamma = 45.5$. To improve the beam polarization in the AGS, the polarization loss due to the coupling effect caused by the solenoid field has to be eliminated. In the experiment, we also observed a new type of spin resonance which is associated with both the vertical betatron oscillation and the horizontal closed orbit distortion. It can be corrected by using harmonic correctors to eliminate the 9th component of the horizontal closed orbit distortion. The Future plan for the AGS includes a new polarized ion source and a helical partial snake which reduces the coupling effect. Furthermore, we can also use energy jump method to reduce polarization loss when crossing weak intrinsic resonances like $48-\nu$.

Polarized Proton Experiments in the AGS with a Partial Siberian Snake (E880)

(ANL,BNL,INDIANA,TRIUMF,KEK,RIKEN,IHEP)

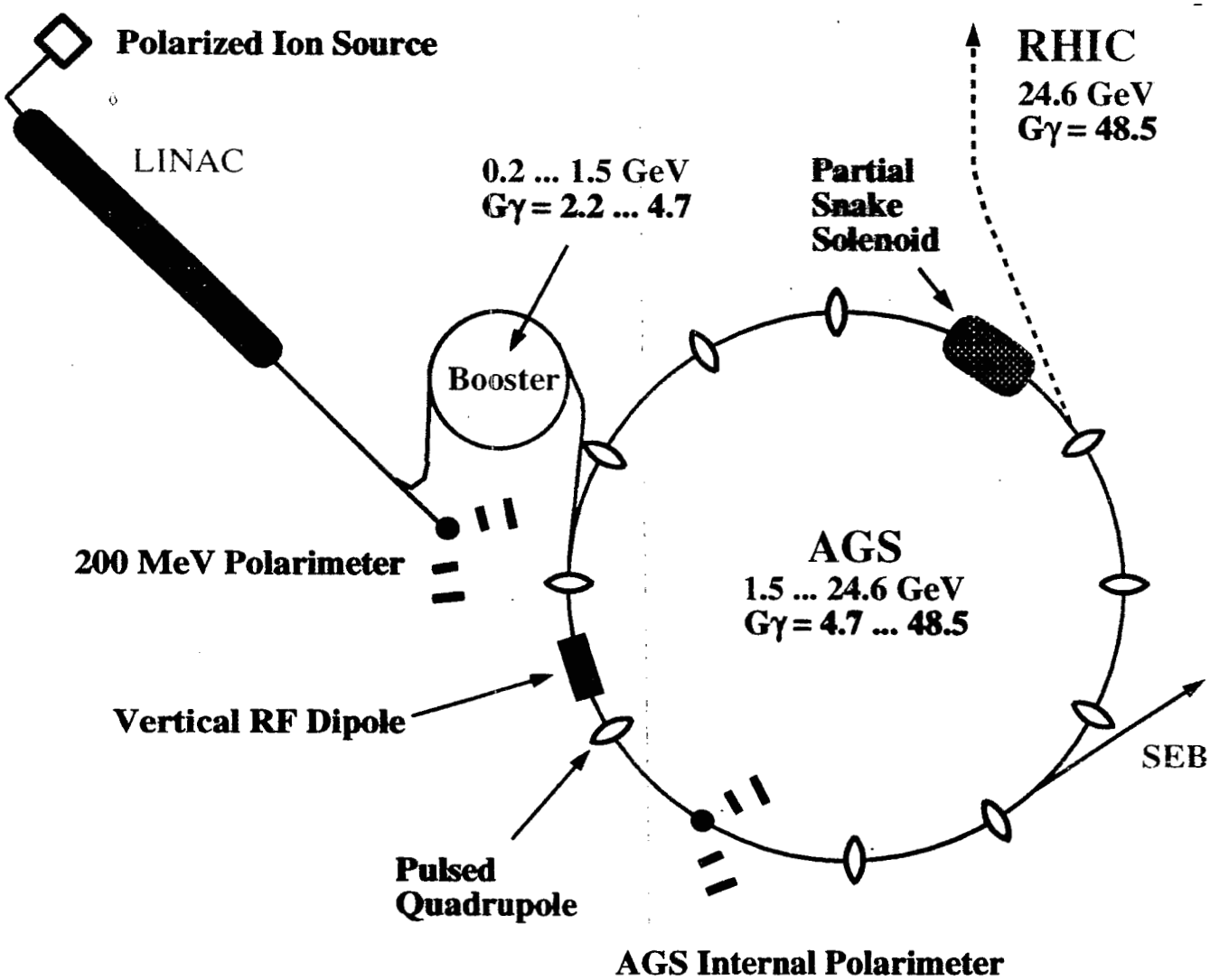

For AGS, the nominal acceleration rate $\alpha = 4.8\text{x}10^{-5}$, P_f/P_i is calculated as well as the required acceleration rate for a 99% spin flip:

$G\gamma$	ε	For $\alpha =$ $4.8\text{x}10^{-5}$	P_f/P_i	For $P_f/P_i =$ -0.99	α [$\text{x}10^{-5}$]
$0+\nu_z$ *	0.00750		-0.57 *		0.0888
$24-\nu_z$	0.00030		0.99		0.000142
$12+\nu_z$ *	0.00290		0.29 *		0.0133
$36-\nu_z$ *	0.00620		-0.43 *		0.0607
$24+\nu_z$	0.00050		0.97		0.000395
$48-\nu_z$	0.00077		0.93		0.000936
$36+\nu_z$ *	0.01340		-0.84 *		0.2083

Note: This is calculated for the beam with 15π normalized 95% emittance.

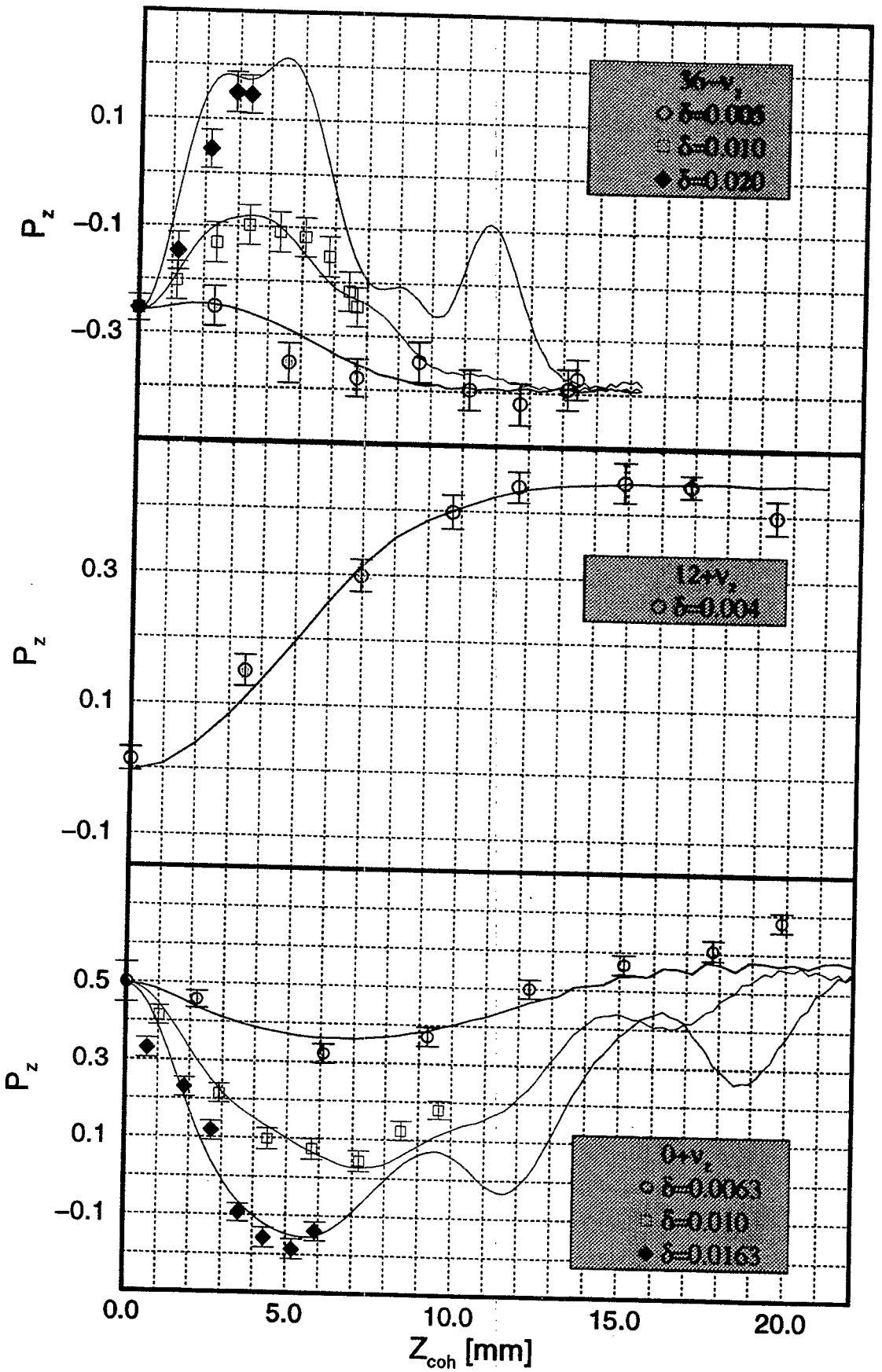
36-ν_z
δ=0.005
δ=0.010
δ=0.020
12+ν_z
δ=0.004
0+ν_z
δ=0.0063
δ=0.010
δ=0.0163
P_z
0.1
-0.1
-0.3
0.3
0.5
0.0
5.0
10.0
15.0
20.0
Z_coh [mm]

AGS Polarization

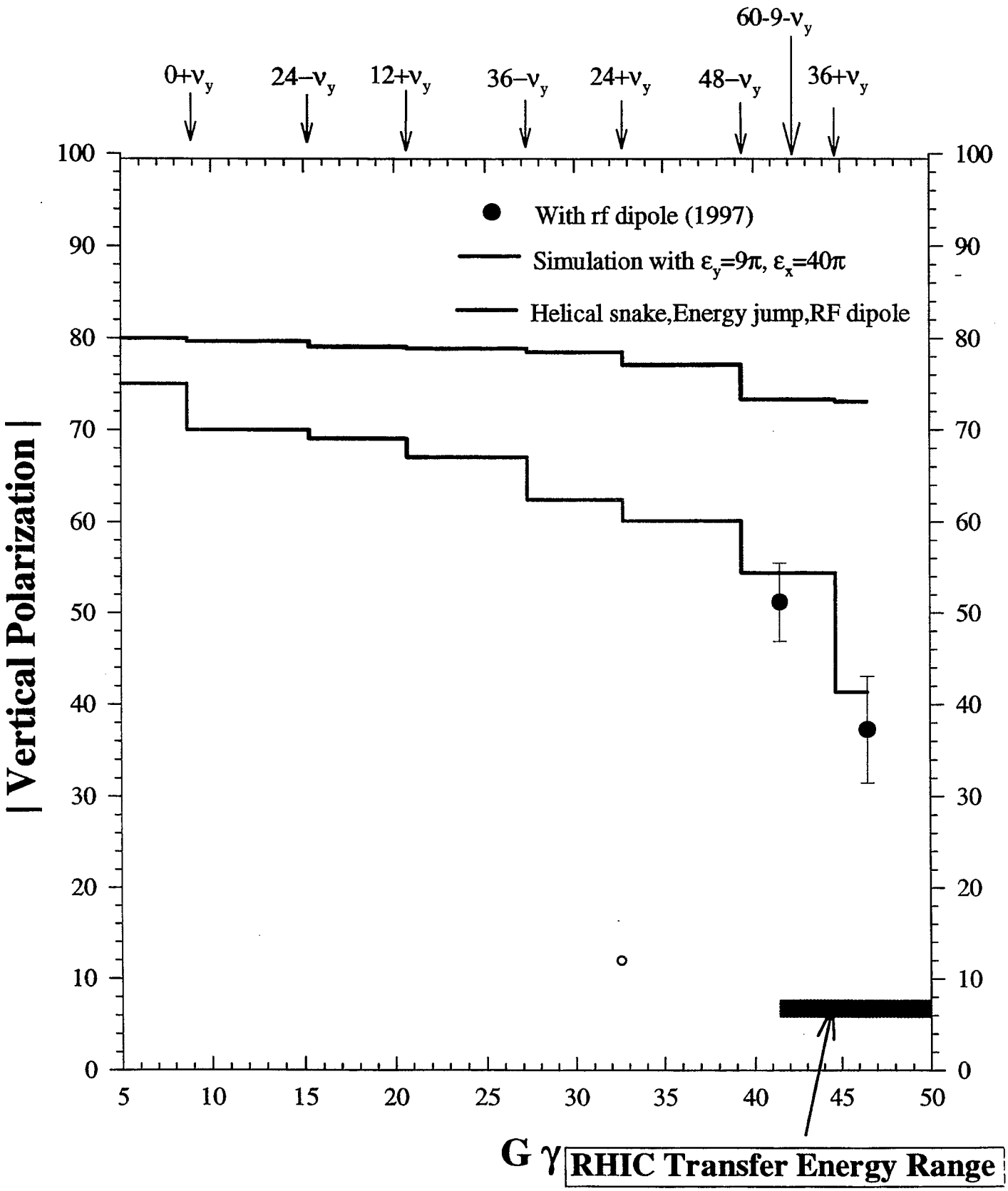

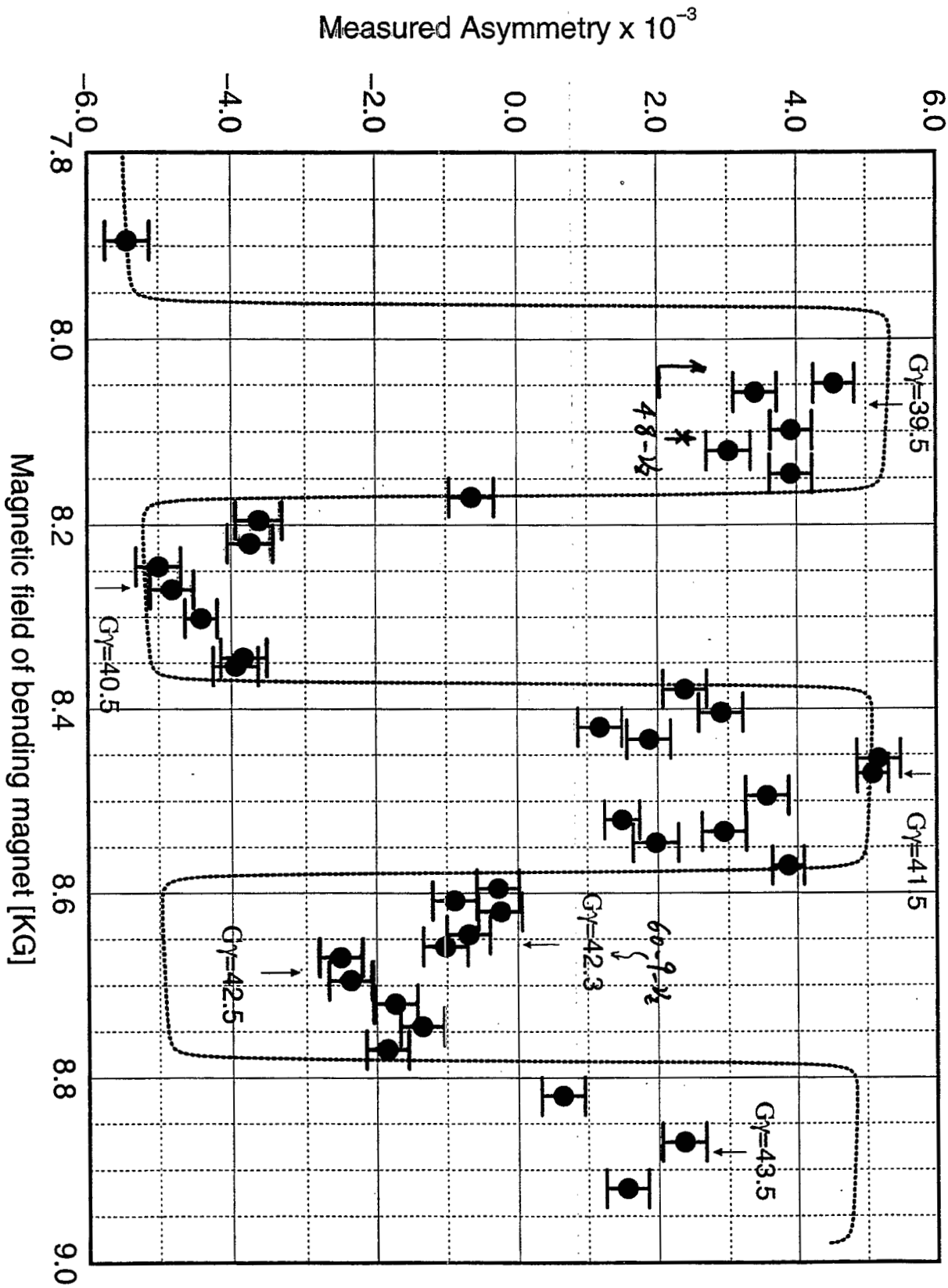
Measured Asymmetry x 10^-3
6.0
4.0
2.0
0.0
-2.0
-4.0
-6.0
7.8
8.0
8.2
8.4
8.6
8.8
9.0
Magnetic field of bending magnet [KG]
Gγ=39.5
Gγ=40.5
Gγ=41.5
Gγ=42.3
Gγ=42.5
Gγ=43.5
48-1/2
60-1/2

Future plan

- New polarized ion source.
- Helical partial snake: reduce the coupling effect to eliminate the coupling spin resonances.
- Use harmonic correctors to eliminate the 9th harmonic component of horizontal closed orbit distortion to correct the spin resonance at $G\gamma = 42.3$.
- Use energy jump method to cross weak resonances like $48-\nu$.

5% helical partial snake

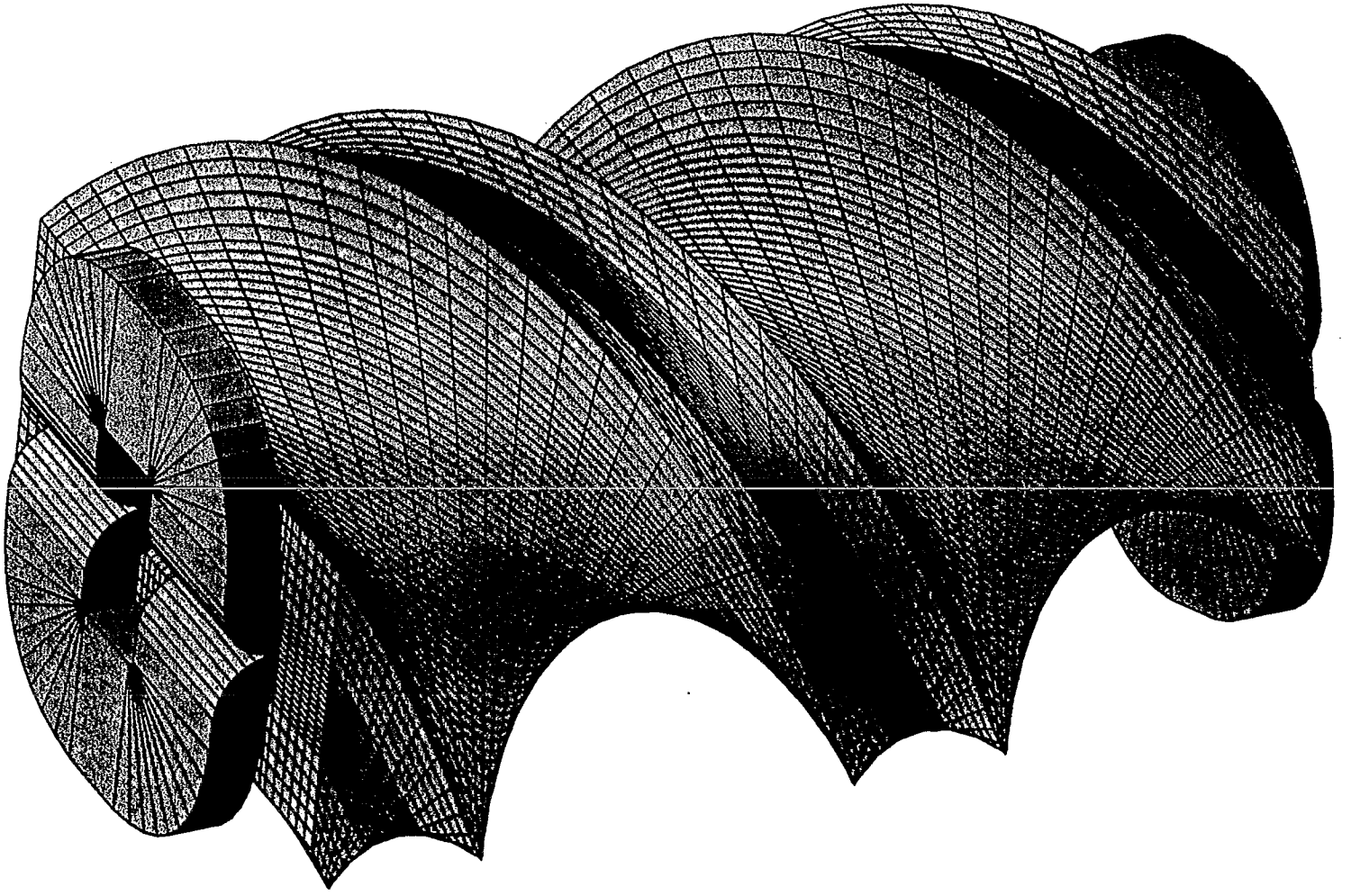

Energy jump

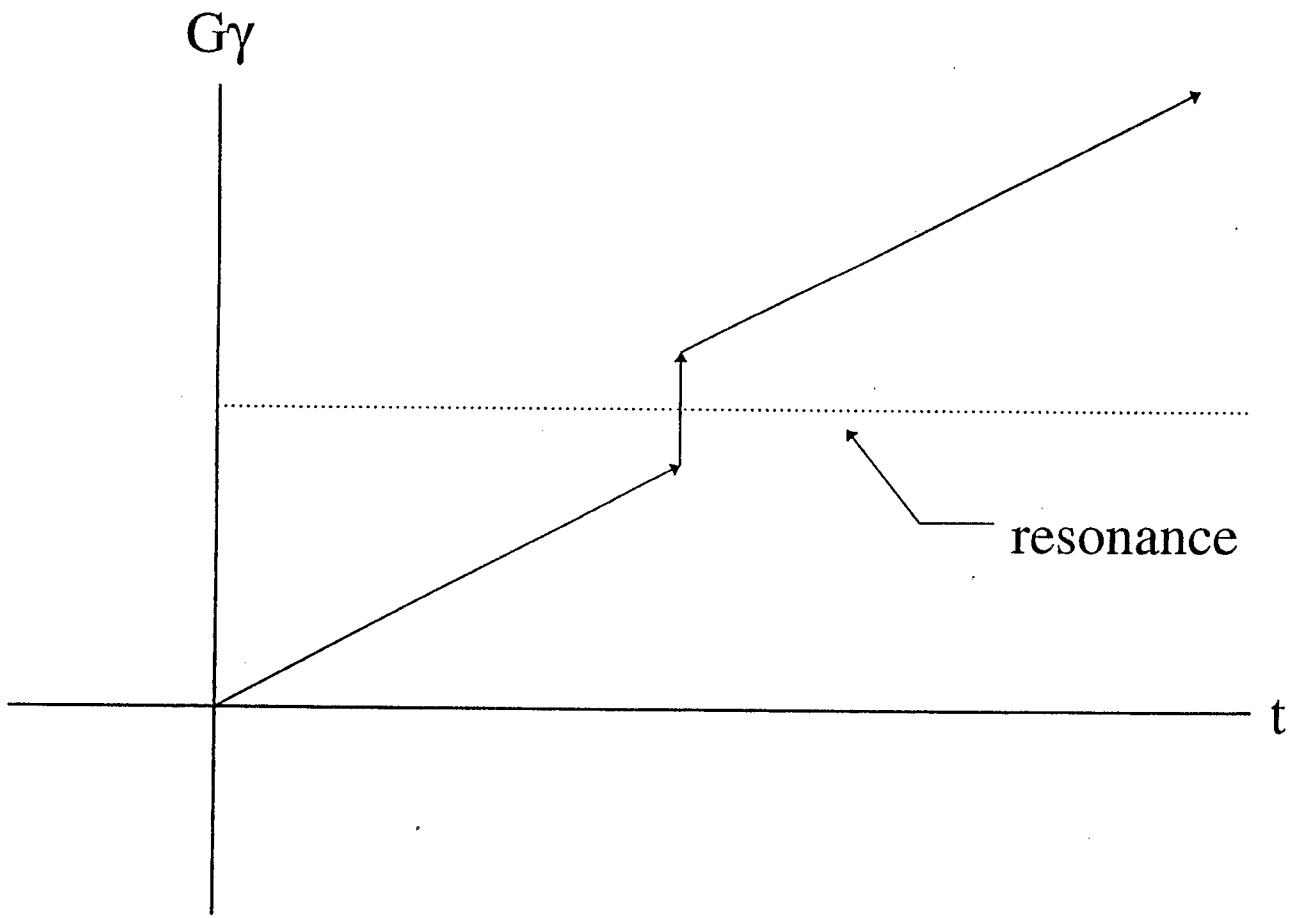

SUMMARY OF THE WORKSHOP

The RBRC Workshop on Physics of Polarimetry at RHIC was held from Aug 4 to 7, 1998 at BNL. The primary motive of the workshop is 1) to discuss the RHIC polarimeter using the elastic proton-carbon scattering at Coulomb-nuclear interference region (p-C CNI polarimeter) in detail and write a proposal for the test experiment at the AGS, 2) to discuss the related physics, 3) and to discuss other options for the RHIC polarimetry.

About twenty people have participated the workshop and discussed above items and worked for the proposal. The idea of the p-C CNI polarimeter was proposed last year as a simple, inexpensive and efficient polarimeter for RHIC. In order to establish this polarimeter, we have decided to carry out a test experiment by using a polarized beam at the AGS. We have made a draft of the proposal during the workshop. For the p-C CNI polarimeter, a telescope detector using both the micro-channel plate (MCP) and the SSD was proposed to detect low energy recoil carbon ions, based on the test measurements at IUCF and Kyoto, where the carbon ions as low as 200 keV were succesfully detected. The kinetic energy of carbon ion is measured with the SSD, and the velocity is measured by TOF between the two detectors and between the accelerator rf pulse and the two detectors. Counting rates for the background and true events were estimated. With the proposed polarimeter, one can expect to measure the beam polarization at the AGS and RHIC at an accuracy of 10% within a reasonable time period. We will test this detector system at Kyoto as soon as possible and install it in the AGS ring for the test measurement of A_N during E880 which is scheduled early in the next year.

It was also pointed out that the proposed p-C CNI polarimeter will have a possible difficulty at the designed maximum luminosity ($2x10^{32}$) of the RHIC because very high counting rate is expected for the detectors and the carbon foil target is heated to very high temperature. Therefore, the conclusion of the discussion in the workshop is to recommend the following scenario for the RHIC polarimetry.

1) If the p-C CNI polarimeter is proved by the AGS test experiment, the p-C CNI polarimeter on both arms should be installed by September 1999 to be ready for the commissioning of the polarized beam acceleration at RHIC.

2) The hydrogen gas jet target is an ideal choice to overcome the rate and heating problems and makes the p-p CNI measurement possible. The pp2pp detectors can be also useful for this polarimetry. We hope the hydrogen gas target is installed

until the spin physics runs.
3) The polarized gas target should be installed in a reasonable time scale to measure the analyzing powers of the reactions used for the polarimetry at RHIC energy and calibrate the polarimeter with an accuracy of 5%.

Besides the planned CNI and charged pion polarimeter, several ideas using other reactions such as the polarized electron-proton elastic scattering, Primakoff process and pizero production at large X_F, were proposed by S. Nurushev and discussed in the workshop. Among them, the pizero polarimeter is, in particular, attractive in order to measure the direction of the beam polarization at RHIC. Since the detector can easily have 2π coverage, one can measure the transverse component of the polarization at the colliding points and confirm the longitudinally polarized beam. Further study is very much encouraged.

(1998.8.7 Ken'ichi Imai)

WORKSHOP ON PHYSICS OF POLARIMETRY AT RHIC
AUGUST 4-7, 1998
ORGANIZERS: KEN'ICHI IMAI AND DOUG FIELDS (NAOHITO SAITO)

LIST OF PARTICIPANTS

NAME	AFFILIATION	E-MAIL ADDRESS
Mei Bai	ANL/Indiana University	bai@bnldag.ags.bnl.gov
Gerry Bunce	BNL/RBRC	bunce@bnldag.ags.bnl.gov
Doug Fields	University of New Mexico	fields@lanl.gov
Wlodek Guryn	BNL	guryn@mail.rhic.bnl.gov
Naoki Hayashi	RIKEN	hayashi@bnl.gov
Haixin Huang	BNL	huang@bnldag.ags.bnl.gov
Ken Imai	Kyoto University/RBRC	imai@ne.scphys.kyoto-u.ac.jp
Kazu Kurita	RIKEN, Japan	kurita@riksg01.rhic.bnl.gov
Yousef Makdisi	BNL	makdisi@bnldag.ags.bnl.gov
Sergei Nurushev	IHEP, Protovino	nurushev@mx.ihep.su
Naohito Saito	RIKEN/RBRC	saito@riksg01.rhic.bnl.gov
Mike Syphers	BNL	syphers@bnldag.ags.bnl.gov
Junji Tojo	Kyoto University/RBRC	tojo@nehp1.scphys.kyoto-u.ac.jp
Larry Trueman	BNL	trueman@sun2.bnl.gov
Dave Underwood	ANL	dgu@axp0.hep.anl.gov
David Wolfe	University of New Mexico	dwolfe@panda.phys.unm.edu
Aki Yokosawa	ANL	ay@axp0.hep.anl.gov

Riken-BNL Center Workshop on Polarimetry

1998.8.4-7 at BNL

Agenda

Aug. 4

10:00–10:30 RHIC polarimeter issue - G. Bunce

10:30–11:00 Polarimeter option overview - Y. Makdisi

11:00–11:30 Recent status of accelerator progress - M. Syphers

Lunch

01:30–02:00 CNI theoretical issue - L. Trueman

Break for Riken-BNL round table meeting and colloquium by M. Goldhaber

04:30–05:15 Results from CE75 test runs and GEANT MC - D. Fields

05:15–05:45 Test measurement of CNI with MCP - J. Tojo

05:45–06:15 Possible design of detector for pC CNI - K. Imai

06:15–07:00 Discussion

Aug. 5

09:00–09:30 $p + e$ polarimeter - S. Nurushev

09:30–10:00 Results from AGS-E925 - A. Yokosawa

10:00–10:30 Proposal of CNI test measurement at AGS - S. Nurushev

10:30–11:00 Pion production from carbon and multiple scattering carbon - D. Underwood

11:00–12:00 Discussion and first draft of AGS proposal on p-C CNI

Lunch

01:30–03:00 Working session

03:30–04:30 Discussion

04:30– Working on the proposal

Aug. 6

09:00–12:00 Presentation and discussion of the draft of proposal

Lunch

01:30–02:00 Primakoff polarimeter - S. Nurushev

02:00–02:30 Inclusive pizero polarimeter - S. Nurushev

02:30–03:30 Polarized gas jet target and pp2pp - W. Guryn

03:30–04:00 Discussion

Break

04:30–05:00 Current design of the pion polarimeter - H. Huang

05:00–05:30 E880 status and floor plan - Mel Bai

05:30–06:00 Discussion

09:00–12:00 Presentation and discussion of the final AGS proposal

RIKEN BNL Center Workshops

Title:	**Event Generator for RHIC Spin Physics**
Organizers:	N. Saito/A. Schaefer
Dates:	Sept. 21–23, 1998
Title:	**Quarkonium Production in Relativistic Nuclear Collisions**
Organizer:	D. Kharzeev
Dates:	Sept. 28–Oct. 2, 1998
Title:	**Workshop on Physics of the 1 Teraflop**
Organizer:	Robert Mawhinney
Dates:	October 16, 1998
Title:	**Quantum Fields In & Out of Equilibrium**
Organizers:	D. Boyanovsky/H. deVega/R.D. Pisarski
Dates:	Oct. 26–30, 1998
Title:	**QCD Phase Transitions**
Organizers:	T. Schaefer/E. Shuryak
Dates:	Nov. 4–7, 1998
Title:	**Hard Parton Physics in High-Energy Nuclear Collisions**
Organizers:	J. Carroll/R. Venugopalan/C. Gale/M. Tannenbaum
Dates:	Mar. 1–5, 1999

For information please contact:

Ms. Pamela Esposito
RIKEN BNL Research Center
Building 510A, Brookhaven National Laboratory
Upton, NY 11973, USA
Phone: (516)344-3097 Fax: (516)344-4067
E-Mail: rikenbnl@bnl.gov
Homepage: http://penguin.phy.bnl.gov/www/riken.html

RIKEN BNL RESEARCH CENTER

WORKSHOP ON PHYSICS OF POLARIMETRY AT RHIC

AUGUST 4–7, 1998

Li Keran

Copyright©CCASTA

Nuclei as heavy as bulls
Through collision
Generate new states of matter.
T. D. Lee

Speakers:

M. Bai
W. Guryn
Y. Makdisi
J. Tojo
A. Yokosawa
G. Bunce
H. Huang
S. Nurushev
L. Trueman
D. Fields
K. Imai
M. Syphers
D. Underwood

Organizers: K. Imai and D. Fields